

**ISTANBUL TECHNICAL UNIVERSITY ★ EARTHQUAKE ENGINEERING AND DISASTER  
MANAGEMENT INSTITUTE**

**THE INFLUENCE OF SITE HETEROGENEITY ON THE SEISMIC  
RESPONSE OF  
NUCLEAR POWER PLANT STRUCTURES**



**M.Sc. THESIS**

**Berke SAYIN**

**Earthquake Engineering and Disaster Management Institute**

**Earthquake Engineering Program**

**JULY 2019**



**ISTANBUL TECHNICAL UNIVERSITY ★ EARTHQUAKE ENGINEERING AND DISASTER  
MANAGEMENT INSTITUTE**

**THE INFLUENCE OF SITE HETEROGENEITY ON THE SEISMIC  
RESPONSE OF  
NUCLEAR POWER PLANT STRUCTURES**

**M.Sc. THESIS**

**Berke SAYIN  
(501101241)**

**Earthquake Engineering and Disaster Management Institute**

**Earthquake Engineering Program**

**Thesis Advisor: Dr. Öğr. Üyesi Ece BAYAT  
Thesis Co-Advisor: Dr. Yalçın BULUT**

**JULY 2019**



**İSTANBUL TEKNİK ÜNİVERSİTESİ ★ DEPREM MÜHENDİSLİĞİ VE AFET  
YÖNETİMİ ENSTİTÜSÜ**

**TEMEL ZEMİNİN HETEROJENİTESİNİN NÜKLEER GÜÇ SANTRALİ  
YAPILARININ SİSMİK DAVRANIŞINA ETKİSİ**

**YÜKSEK LİSANS TEZİ**

**Berke SAYIN  
(501101241)**

**Deprem Mühendisliği Anabilim Dalı**

**Deprem Mühendisliği Programı**

**Tez Danışmanı: Dr. Öğr. Üyesi Ece BAYAT  
Eş Danışman: Dr. Yalçın BULUT**

**JULY 2019**



Berke SAYIN, a M.Sc. student of ITU Earthquake Engineering and Disaster Management Institute student ID 501101241, successfully defended the thesis entitled “THE INFLUENCE OF SITE HETEROGENEITY ON THE SEISMIC RESPONSE OF NUCLEAR POWER PLANT STRUCTURES”, which he prepared after fulfilling the requirements specified in the associated legislations, before the jury whose signatures are below.

**Thesis Advisor :**      **Dr. Öğr. Üyesi Ece BAYAT** .....  
Istanbul Technical University

**Co-advisor :**            **Dr. Yalçın BULUT** .....  
Matriseb Engineering Co.

**Jury Members :**        **Prof. Dr. Recep İYİSAN** .....  
Istanbul Technical University

**Prof. Dr. Mehmet BERİLGİN** .....  
Yıldız Technical University

**Doç. Dr. Ufuk YAZGAN** .....  
Istanbul Technical University

**Date of Submission : 3 May 2019**

**Date of Defense : 4 July 2019**







*To my spouse and my family,*



## **FOREWORD**

First and foremost, I would like to express my deep gratitudes to my advisors Dr. Ece Bayat and Dr. Yalçın Bulut, not only for their support and guidance in the course of this research work, but also for presenting me with the opportunity to work on this study.

I wish to express my gratefulness to my wife Eylem Sayın for her optimism and support, and also my parents for their endless encouragements and moral support.

I gratefully acknowledge Ali Akgöz for his assistance and patience throughout my studies. Similarly, I would like to thank Burak Uçak and Batuhan İşcan and all my workmates for their motivation and tolerance.

July 2019

Berke SAYIN  
(Civil Engineer)



## TABLE OF CONTENTS

	<u>Page</u>
<b>FOREWORD</b> .....	<b>ix</b>
<b>TABLE OF CONTENTS</b> .....	<b>xi</b>
<b>ABBREVIATIONS</b> .....	<b>xiii</b>
<b>SYMBOLS</b> .....	<b>xv</b>
<b>LIST OF TABLES</b> .....	<b>xvii</b>
<b>LIST OF FIGURES</b> .....	<b>xix</b>
<b>SUMMARY</b> .....	<b>xxiii</b>
<b>ÖZET</b> .....	<b>25</b>
<b>1. INTRODUCTION</b> .....	<b>29</b>
1.1 A Brief History of Nuclear Power Plants Construction.....	33
1.2 Safety Considerations of NPPs .....	35
1.3 Objective and Scope .....	40
<b>2. LITERATURE REVIEW</b> .....	<b>43</b>
2.1 Site Response .....	43
2.1.1 Equivalent linear site response analysis.....	46
2.1.2 Nonlinear site response analysis .....	48
2.2 Dynamic Soil-Structure Interaction .....	50
2.2.1 Solution methods .....	53
2.2.2 Direct method .....	54
2.2.3 Substructuring method .....	55
2.3 SSI Analysis of NPPs Within Standards and Requirements.....	58
2.3.1 IAEA safety guides.....	58
2.3.2 U.S. standards and guides .....	60
<b>3. MODELLING OF SOIL MEDIUM</b> .....	<b>65</b>
3.1 Soil Parameters and Their Variations .....	69
3.2 Strain Dependent Modulus Degradation and Damping Curves.....	73
<b>4. SITE RESPONSE ANALYSIS PROCEDURE AND SEISMIC INPUT MOTION</b> .....	<b>75</b>
4.1 Seismic Hazards and Input Time Histories.....	76
4.2 Site Response Analyses for Different Soil Profiles .....	83
4.3 One-Dimensional Equivalent Linear Analysis Results.....	90
<b>5. INFLUENCE OF INCLINED LAYERS ON SITE RESPONSE ANALYSIS</b>	<b>99</b>
5.1 1D Equivalent Linear Analysis of Soil Profiles.....	99
5.2 Comparison With Plaxis 2D Analysis .....	100
<b>6. IMPLEMENTATION OF DYNAMIC SOIL-STRUCTURE INTERACTION ON A GENERIC NUCLEAR FACILITY DESIGN</b> .....	<b>109</b>
6.1 Model of a Generic Nuclear Facility .....	111
6.1.1 Facility description .....	112
6.1.2 Structural model and its dynamic properties .....	113
6.2 Soil Model.....	119
6.3 Input Ground Motion .....	135

6.4 Transfer Functions and In-Structure Response Spectra.....	139
<b>7. RESULTS AND DISCUSSIONS.....</b>	<b>145</b>
7.1 Effects of Soil Geometry .....	145
7.2 Effects of Soil Parameters Variation.....	146
7.3 Comparison of In-Structure Response Spectra .....	147
7.4 Future Recommendations .....	147
<b>8. SUMMARY AND CONCLUSIONS .....</b>	<b>149</b>
<b>REFERENCES.....</b>	<b>151</b>
<b>CURRICULUM VITAE.....</b>	<b>155</b>



## **ABBREVIATIONS**

<b>1D</b>	: One-dimensional
<b>2D</b>	: Two-dimensional
<b>3D</b>	: Three-dimensional
<b>ASCE</b>	: American Society of Civil Engineers
<b>BWR</b>	: Boiling Water Reactor
<b>CANDU</b>	: CANada Deuterium Uranium
<b>CLASSI</b>	: Continuum Linear Analysis of Soil-Structure Interaction
<b>EPR</b>	: European Pressurized Water Reactor
<b>IAEA</b>	: International Atomic Energy Agency
<b>INSAG</b>	: International Nuclear Safety Advisory Group
<b>ISRS</b>	: In-Structure Response Spectra
<b>MIT</b>	: Massachusetts Institute of Technology
<b>MWe</b>	: Megawatts Electric
<b>NPP</b>	: Nuclear Power Plant
<b>NUREG</b>	: U.S. Nuclear Regulatory Commission Regulation
<b>PEER</b>	: Pacific Earthquake Engineering Research
<b>PGA</b>	: Peak Ground Acceleration
<b>PSA</b>	: Peak Spectral Acceleration
<b>PSHA</b>	: Probabilistic Seismic Hazard Analysis
<b>PWR</b>	: Pressurized Water Reactor
<b>RBMK</b>	: Reaktor Bolshoy Moshchnosti Kanalnyy
<b>SASSI</b>	: A System for Analysis of Soil-Structure Interaction
<b>SL-1</b>	: Seismic Level – 1
<b>SL-2</b>	: Seismic Level – 2
<b>SRP</b>	: Standard Review Plan

**SSE** : Safe Shutdown Earthquake  
**SSI** : Soil–Structure Interaction  
**U. S.** : United States of America  
**U.S. NRC** : United States Nuclear Regulatory Commission  
**VVER** : Vodo-Vodyanoi Energetichesky Reaktor





## **SYMBOLS**

<b><math>C_v</math></b>	: Coefficient of variation
<b><math>G</math></b>	: Dynamic shear modulus
<b><math>m</math></b>	: Metre
<b><math>t</math></b>	: Time
<b><math>V_p</math></b>	: Pressure wave velocity
<b><math>V_s</math></b>	: Shear wave velocity
<b><math>\gamma</math></b>	: Shear strain
<b><math>\zeta</math></b>	: Damping ratio
<b><math>\tau</math></b>	: Shear stress
<b><math>\mu</math></b>	: Mean value
<b><math>\rho</math></b>	: Density
<b><math>\sigma</math></b>	: Standard deviation



## LIST OF TABLES

	<u>Page</u>
<b>Table 1.1:</b> Levels of Defense in Depth .....	39
<b>Table 2.1:</b> Suggested frequency intervals for response spectra calculation (U.S. NRC, 2007b) .....	61
<b>Table 3.1:</b> Properties of undersurface foundation material.....	68
<b>Table 4.1:</b> PGA and PSA values of surface and rock motions obtained from deconvolution analyses of BE soil profile for five earthquakes .....	78
<b>Table 4.2:</b> PGA and PSA values of surface and rock motions obtained from deconvolution analyses of LB soil profile for five earthquakes .....	79
<b>Table 4.3:</b> PGA and PSA values of surface and rock motions obtained from deconvolution analyses of LB soil profile for five earthquakes .....	81
<b>Table 4.4:</b> The chosen input ground motion .....	83
<b>Table 4.5:</b> Predominant periods, PSA and PGA values of input rock and surface motions obtained in site response analyses of each soil profile.....	96
<b>Table 5.1:</b> Soil parameters used in dynamic analyses of the inclined Plaxis 2D model .....	103
<b>Table 5.2:</b> Predominant periods, PSA and PGA values of input rock and surface motions obtained in site response analyses of each soil profile.....	107
<b>Table 6.1:</b> Effective stiffness of reinforced concrete members (ASCE, 2005).....	118
<b>Table 6.2:</b> Specified damping values for dynamic analysis (ASCE, 2005).....	118
<b>Table 6.3:</b> Calculated ISRS Locations .....	140



## LIST OF FIGURES

	<u>Page</u>
<b>Figure 1.1:</b> Schematic view of a typical pressurized water reactor .....	29
<b>Figure 1.2:</b> Schematic view of a typical boiling water reactor .....	30
<b>Figure 1.3:</b> Number of operational reactors by countries in the world.....	31
<b>Figure 1.4:</b> Number of under construction reactors by countries in the world.....	32
<b>Figure 1.5:</b> The first nuclear power plant, Obninsk NPP (“Url-3,” n.d.).....	33
<b>Figure 1.6:</b> Structure of the IAEA Safety Standards Series.....	37
<b>Figure 2.1:</b> Wave propagation process to the ground surface (Kramer, 1996).....	44
<b>Figure 2.2:</b> First-cycle stress-strain curve (Vucetic & Dobry, 1991) .....	47
<b>Figure 2.3:</b> Strain-dependent shear modulus degradation and damping ratio curves (Vucetic & Dobry, 1991) .....	47
<b>Figure 2.4:</b> Extended Masing rules: (a) variation of shear stress with time; (b) resulting stress-strain behaviour (backbone curve indicated by dashed line) (Kramer, 1996) .....	49
<b>Figure 2.5:</b> The lumped mass and finite element approaches in nonlinear site response analysis (Bolisetti, et al., 2014).....	50
<b>Figure 2.6:</b> Soil-structure modelling in direct method (Bolisetti, 2015) .....	54
<b>Figure 2.7:</b> Substructuring in soil-structure interaction analysis (adapted from (Lysmer F. Ostandan, and C.C. Chin., 1999)) .....	56
<b>Figure 2.8:</b> Types of substructuring methods (Ostandan, 2006).....	57
<b>Figure 3.1:</b> Borehole layout .....	66
<b>Figure 3.2:</b> Schematic representation of the studied site with inclined layers.....	66
<b>Figure 3.3:</b> Schematic representation of the soil under the foundation .....	67
<b>Figure 3.4:</b> Locations of the 7 1D soil columns.....	68
<b>Figure 3.5:</b> $V_s$ values of the soil profiles .....	70
<b>Figure 3.6:</b> $V_p$ values of the soil profiles .....	71

<b>Figure 3.7:</b> $C_v$ values change in depth .....	72
<b>Figure 3.8:</b> Shear modulus degradation with shear strain.....	73
<b>Figure 3.9:</b> Damping variation with shear strain .....	74
<b>Figure 4.1:</b> Deconvolution procedure .....	77
<b>Figure 4.2:</b> The response spectra obtained in deconvolution analyses for BE small-strain $V_s$ profile.....	78
<b>Figure 4.3:</b> The response spectra obtained in deconvolution analyses for LB small-strain $V_s$ profile.....	79
<b>Figure 4.4:</b> The response spectra obtained in deconvolution analyses for UB small-strain $V_s$ profile.....	80
<b>Figure 4.5:</b> Target spectra .....	82
<b>Figure 4.6:</b> Deconvoluted input ground motion time history .....	82
<b>Figure 4.7:</b> Material properties interface of DEEPSOIL software .....	84
<b>Figure 4.8:</b> Best-estimate (BE) soil profile and its soil properties.....	85
<b>Figure 4.9:</b> Lower-bound (LB) soil profile and its soil properties.....	85
<b>Figure 4.10:</b> Upper-bound (UB) soil profile and its soil properties.....	86
<b>Figure 4.11:</b> Column A soil profile and its soil properties .....	86
<b>Figure 4.12:</b> Column B soil profile and its soil properties.....	87
<b>Figure 4.13:</b> Column C soil profile and its soil properties.....	87
<b>Figure 4.14:</b> Column D soil profile and its soil properties .....	88
<b>Figure 4.15:</b> Column E soil profile and its soil properties.....	88
<b>Figure 4.16:</b> Column F soil profile and its soil properties .....	89
<b>Figure 4.17:</b> Column G soil profile and its soil properties .....	89
<b>Figure 4.18:</b> The comparison of maximum strain values of Col. A – Col. G with BE, LB and UB profiles.....	92
<b>Figure 4.19:</b> The response spectra at the surface and the top of rock.....	93
<b>Figure 4.20:</b> Comparison of the response of each column with BE-LB-UB results	95
<b>Figure 5.1:</b> $V_s$ profiles chosen for the comparison purposes with 2D results.....	100
<b>Figure 5.2:</b> Schematic foundation soil representation including surface points to compare.....	101

<b>Figure 5.3:</b> Comparisons of 1D and 2D site response analyses for the corresponding soil columns in 1D and surface points counterparts in 2D analyses.....	104
<b>Figure 5.4:</b> Comparison of the response of Column A with Plaxis 2D results at the same location .....	104
<b>Figure 5.5:</b> Comparison of the response of Column C with Plaxis 2D results at the same location .....	105
<b>Figure 5.6:</b> Comparison of the response of Column E with Plaxis 2D results at the same location .....	105
<b>Figure 5.7:</b> Comparison of the response of Column G with Plaxis 2D results at the same location .....	106
<b>Figure 6.1:</b> Soil layer plot interface in ACS SASSI .....	110
<b>Figure 6.2:</b> Analysis options interface in ACS SASSI .....	111
<b>Figure 6.3:</b> Schematic view of a VVER design (adapted from (Asmolov et al., 2017)) .....	112
<b>Figure 6.4:</b> Element section type and thickness interface in SAP 2000 .....	115
<b>Figure 6.5:</b> 3D model of the reactor building .....	116
<b>Figure 6.6:</b> 3D view of reactor building with the inner and outer containment structure .....	117
<b>Figure 6.7:</b> (a) The variation of strain-compatible $G/G_{max}$ , (b) damping ratio with depth for BE, LB and UB profiles .....	120
<b>Figure 6.8:</b> The comparison of strain-compatible $G/G_{max}$ of Col. A – Col. G with BE, LB and UB profiles.....	122
<b>Figure 6.9:</b> The comparison of strain-compatible damping ratios of Col. A – Col. G with BE, LB and UB profiles.....	124
<b>Figure 6.10:</b> The variation of strain-compatible $G/G_{max}$ with depth for Col. A – Col. G profiles .....	127
<b>Figure 6.11:</b> The variation of strain-compatible damping ratio with depth for Col. A – Col. G profiles.....	130
<b>Figure 6.12:</b> The variation of $G_{max}$ values with depth for Col. A – Col. G profiles	131
<b>Figure 6.13:</b> The variation of small-strain and average strain-compatible shear moduli (G) with depth for (a) BE, (b) LB and (c) UB profiles.....	132

<b>Figure 6.14:</b> The variation of small-strain and average strain-compatible shear moduli (G) with depth for Col. A - Col. G profiles .....	134
<b>Figure 6.15:</b> Horizontal design target spectra.....	135
<b>Figure 6.16:</b> Foundation input motion obtained from best-estimate soil profile ....	136
<b>Figure 6.17:</b> Foundation input motion obtained from lower-bound soil profile.....	136
<b>Figure 6.18:</b> Foundation input motion obtained from upper-bound soil profile.....	136
<b>Figure 6.19:</b> Foundation input motion obtained from Col A soil profile .....	137
<b>Figure 6.20:</b> Foundation input motion obtained from Col B soil profile.....	137
<b>Figure 6.21:</b> Foundation input motion obtained from Col C soil profile.....	137
<b>Figure 6.22:</b> Foundation input motion obtained from Col D soil profile .....	138
<b>Figure 6.23:</b> Foundation input motion obtained from Col E soil profile.....	138
<b>Figure 6.24:</b> Foundation input motion obtained from Col F soil profile .....	138
<b>Figure 6.25:</b> Foundation input motion obtained from Col G soil profile .....	139
<b>Figure 6.26:</b> Comparison of ISRS at Region 1 for each soil profile.....	141
<b>Figure 6.27:</b> Comparison of ISRS at Region 2 for each soil profile.....	142
<b>Figure 6.28:</b> Comparison of ISRS at Region 3 for each soil profile.....	142
<b>Figure 6.29:</b> Comparison of ISRS at Region 4 for each soil profile.....	143
<b>Figure 6.30:</b> Comparison of ISRS at Region 5 for each soil profile.....	143
<b>Figure 6.31:</b> Comparison of ISRS at Region 6 for each soil profile.....	144



# **THE INFLUENCE OF SITE HETEROGENEITY ON THE SEISMIC RESPONSE OF NUCLEAR POWER PLANT STRUCTURES**

## **SUMMARY**

In order to ensure the safety of structures under earthquake loads and to evaluate the seismic response of the structures, the effect of local soil conditions on ground motions should be determined. The seismic response of structures considering the local site and soil-structure interaction effects, many variables are to be defined. It is necessary to know the simultaneous behavior of structure-foundation system and the soil, which is a part of this system, under earthquake loads.

The majority of civil engineering structures are designed assuming that the structure is fixed to the ground surface at the foundation level. For many years, this practice has been assumed conservative in terms of seismic design. However, local soil properties are directly influential at the design stage in determining the in-structure response spectra or in the calculation of earthquake loads, and also in the conduct of liquefaction analyses, or in the determination of earthquake-based loads for the design of ground structures such as retaining structures, engineering fills and slopes. It is a fact that the ground motion propagates through the soil media and the dynamic properties of soil medium have effects on the structures behavior. Therefore, the interaction between soil and structure should be taken into account.

The phenomenon of soil-structure interaction has been studied extensively, especially for nuclear power plants. The highest priority has to be given to nuclear reactor safety in nuclear power plant projects. The construction and operation of nuclear installations are strictly controlled and regulated by the regulatory authorities. Even if one in a million, always there is possibility of accident. An accident could result in dangerous levels of radiation that could affect the health and safety of the public living near these nuclear installations. The structure, which is the subject of analysis in this thesis, is a nuclear reactor building with containment structure that is identified as the most important structure in nuclear power plant designs. The reason why this kind of identification is given to that building is because that structure houses the most critical components. Thus, it is very important to understand the behavior of the subsurface media in order to achieve the safety goals of nuclear reactors.

Soil-structure interaction is a sophisticated issue that includes topics such as seismic field response, seismic wave motion, ground mechanics, geology, building mechanics and structural dynamics. In this subject, it is necessary to consider multi-variable elements such as soil behavior, structure behavior, and seismic wave propagation in the soil media. Moreover, if the ground environment below the structures shows heterogeneous features, it is very difficult to find a solution for modeling of that kind of systems.

In this thesis, the dynamic behavior of a nuclear power plant structure is investigated under an earthquake input motion with the influence of heterogeneous soil conditions. Within this context, site parameters and their variations in lateral and vertical directions are taken into account and transfer of the site heterogeneity effects to the super-structure is studied. The soil layers beneath the foundation are defined with related parameters taking into account the uncertainties of the soil profile. In this scope, strain dependent modulus degradation and damping curves are used to take into account the nonlinearity in the soil response analyses performed using DEEPSOIL and PLAXIS software for a variety of soil profiles. Accordingly, soil model with dynamic high-strain properties and foundation input motion that are incorporated into the soil-structure interaction analyses performed using ACS SASSI software based on the International Atomic Energy Agency safety guides and U.S. standards and guidelines.

The results are given as graphs that includes in-structure-response-spectra considering the effects of each soil profile in certain points of super-structure. Hence, the dynamic seismic response of the structure originating from the soil parameters and their influence on the outputs of the soil-structure interaction analyses are discussed over those graphs.

It is concluded that peak ground accelerations are not varying noticeably along the width of the foundation. But, the peak spectral accelerations are varying along with the north-south direction.

The change of the soil layers impedances in-depth influence the dynamic response of the structure remarkably. And also, it can be added that characteristic of soil profile which is identified as heterogeneous, considerably affects the foundation's dynamic response. Somehow, in the upper structure at the higher elevations, it is seen that this effect decreases.

Conclusively, it is observed that uncertainties taking into account the best estimate, upper bound and lower bound profiles does not accurately represent the subsurface soil that shows heterogeneous features. Hence, probabilistic soil-structure interaction approach is suggested to use in order to have more accurate results.

## TEMEL ZEMİNİNİN HETEROJENİTESİNİN NÜKLEER GÜÇ SANTRALİ YAPILARININ SİSMİK DAVRANIŞINA ETKİSİ

### ÖZET

Yapıların deprem yükü altındaki güvenliğini sağlamak ve sismik tepkisini değerlendirmek için yerel zemin koşullarının yer hareketi üzerindeki etkisi belirlenmelidir. Yapıların sismik tepkisi hesaplanırken yerel zemin koşulları ve yapı ile zeminin etkileşimini dikkate alan birçok değişken tanımlanmalıdır. Deprem yükleri altında yapı-temel sisteminin ve bu sistemin bir parçası olan zeminin eşzamanlı davranışını bilmek gerekir.

Yapıların büyük bir çoğunluğu, yapının temel seviyesinde zemin yüzeyine ankastre olduğu varsayılarak tasarlanmıştır. Uzun yıllar boyunca, bu uygulamanın sismik tasarım açısından oldukça muhafazakâr olduğu kabul edilmiştir. Ancak, yerel zemin özellikleri, tasarım aşamasında yapı içi tepki spektrumlarının belirlenmesinde veya deprem yüklerinin hesaplanmasında, bunun yanı sıra, sıvılaşma analizlerinin gerçekleştirilmesinde veya istinat yapılarında, mühendislik dolgularında ve şevlerde depremden kaynaklı olarak meydana gelen yüklerin belirlenmesinde doğrudan etkilidir. Yer hareketinin zemin ortamı içerisinde yayıldığı ve zemin ortamının dinamik özelliklerinin yapı davranışını etkilediği çok açık bir şekilde ortadadır. Bu nedenle, zemin ve yapı arasındaki etkileşimin bu tür hesaplamalarda dikkate alınması gerekmektedir.

Yapı zemin etkileşimi olgusu, şimdiye dek, özellikle nükleer santraller için kapsamlı bir şekilde çalışılmamıştır. Genel anlamda nükleer santraller doğal gaz kombine çevrim santrali veya fosil yakıt kullanan diğer herhangi bir termik santral gibi elektrik üreten termik santrallerdir. Atom çekirdeğinin parçalanması işlemi sırasında ortaya çıkan nükleer fisyon enerjisinden ısı üretici olarak faydalanılır. Sızdırmaz özellikteki kapalı ortamda gerçekleşen bu fisyon işlemi sırasında üretilen ısı suyu buhara dönüştürür. Kaynar sudan çıkan buhar türbinleri çevirir ve jeneratörler elektrik üretir.

Nükleer santral projelerinde her şeyden önce nükleer reaktör güvenliğine en yüksek öncelik verilmelidir. Nükleer tesislerin inşaatı ve işletilmesi düzenleyici otoriteler tarafından sıkı bir şekilde kontrol edilmekte ve ilgili mevzuata ilişkin düzenlemeler yapılmaktadır. Ancak bununla beraber, nükleer santrallerde, diğer herhangi bir tesiste de olabileceği gibi, milyonda bir bile olsa da her zaman kaza olasılığı vardır. Herhangi bir nükleer kaza, bu nükleer tesislerin yakın çevresinde yaşayan halkın sağlığını etkileyebilir. Bu kazalar, halkın ve çevrenin güvenliğini etkileyebilecek şekilde tehlikeli düzeyde radyasyona maruz kalmasına sebep olabilir. Bu tezde analiz konusu olan yapı, nükleer santral tasarımlarında en önemli yapı olarak tanımlanan ve bir korunak yapısına sahip bir nükleer reaktör binasıdır. Söz konusu tanımlamanın binaya atfedilmesinin nedeni, yapının en kritik bileşenleri barındırmasıdır. Bu nedenle, nükleer reaktörlerin nükleer güvenlik hedeflerine ulaşmak için yapı altındaki zemin ortamının davranışını saptayabilmek epey önem arz etmektedir.

Yapı-zemin etkileşimi, zeminin sismik etkiler altındaki tepkisi, sismik dalga hareketi, zemin mekaniği, jeoloji mühendisliği, yapı mekaniği ve yapı dinamiği gibi konuları içeren karmaşık bir husustur. Bu konuda, zemin davranışı, yapı davranışı ve zemin ortamındaki sismik dalga yayılımı gibi birçok değişken unsuru dikkate almak gerekir. Ayrıca, yapıların altında bulunan zemin heterojen özellikler gösteriyorsa, bu tür yapı-zemin sistemlerinin modellenmesi oldukça zordur.

Yapı-zemin etkileşimi konularındaki mühendislik uygulamaları ve bunun nükleer güvenliğe etkileri birçok düzenleyici mevzuat, standart ve kılavuzda ele alınmaktadır. Düzenleyici gerek dokümanları, karşılanması gereken hususlar anlamında bir çerçeve belirler. Bu bağlamda, konu özelinde, ülkelerarası mutabakat olarak Uluslararası Atom Enerjisi Ajansının güvenlik standartları ve kılavuzlarının yanı sıra uzun yıllardır Amerika Birleşik Devletinde kullanılagelen standart ve kılavuzlar oldukça yaygın bir şekilde kullanılmaktadır.

Bu çalışmada, tipik bir nükleer reaktör binasının oturduğu zeminin heterojen özellikler göstermesi durumunda bunun etkileri ve bu etkilerin üst yapıya ve ekipmanlara ne şekilde aktarıldığı hususu araştırılmıştır. Bu kapsamda, zemin tepki analizleri ve yapı-zemin etkileşimi analizleri yürütülmüş, bu analizlerin sonucunda çıkan kat tepki spektrumları yorumlanarak zemin heterojenitesinin üst yapının ve ekipmanların dinamik davranışına etkisi tartışılmıştır.

Tezin ilk bölümünde, nükleer santral kavramının daha iyi anlaşılması için nükleer santral yapısının kısa bir tarihçesi ve daha sonra nükleer santrallerde güvenlik kavramı ve güvenlik hedefleri irdelenmiştir.

İkinci bölümde, zemin tepki analizi ve bu tür analizlerde kullanılan en yaygın yöntemler ile dinamik yapı-zemin etkileşimi analizi ve bu analizlerde kullanılan çözüm yöntemleri hakkında akademik literatür bilgisi sunulmuştur. Ayrıca, yapı-zemin etkileşimi analizi konusunda nükleer endüstride kullanılan zorunlu mevzuatla birlikte daha detaylı bilgi içeren kılavuzlar hakkında bilgi verilmiştir.

Bu konuda yürütülmüş geçmiş çalışmaları ve analiz yöntemlerini özetleyen literatür taramasının ardından, üçüncü bölümde, zemin modelleme parametrelerinin belirlenmesi ve bunların değişimi ile ilgili bilgiler verilmiştir. Ek olarak, zemin tepki analizlerinde doğrusal olmama durumunu hesaba katan dinamik zemin kayma modülü ve sönüm oranı azalım eğrileri üçüncü bölümde sunulmuştur.

Daha sonra, zemin tepki analizi ile ilgili işlem adımlarında izlenen prosedür dördüncü bölümde anlatılmıştır. İlk olarak, sismik girdi hareketinin belirlenmesi konusunda ilgili standartlarda ve kılavuzlarda tanımlanan prosedürler izlenerek oluşturulan sismik girdi hareketi hakkında bilgi verilmiştir. Bunu takiben, zemin tepki analizi yapılmış ve farklı koşulları dikkate alan zemin tepki analizlerine ilişkin sonuçlar paylaşılmıştır.

Tezin beşinci bölümünde, derin eğimli tabakalaşmaya bağlı olarak heterojenliğin etkileri, DEEPSOIL yazılımı kullanılarak yapılan bir boyutlu eşdeğer doğrusal analizler ve PLAXIS 2D yazılımı ile gerçekleştirilen iki boyutlu zemin tepki analizlerinin karşılaştırılması yoluyla incelenmiştir.

Altıncı bölümde ilk olarak, seçilen tipik reaktör yapısının üç boyutlu modeli ve üst yapının dinamik özelliklerine dair bilgiler sunulmuştur. Sonrasında, yapı-zemin etkileşimi analizlerinde en çok kullanılan ve nükleer alanda endüstri standardı olarak kabul edilen SASSI metodolojisinden faydalanan ACS SASSI yazılımı kullanılarak yapılan yapı-zemin etkileşimi analizlerine dâhil edilen zemin modeli ve sismik girdi hareketine ilişkin detaylar verilmiştir.

Bu tez çalışmasındaki nükleer santral yapısının dinamik davranışı, heterojen zemin koşullarının etkisiyle birlikte bir deprem girdi hareketi altında incelenmiştir. Bu bağlamda, zemin parametreleri ve bunların yanal ve dikey yönlerdeki farklılıkları dikkate alınmakta ve zemin heterojenitesi etkilerinin üst yapıya aktarılması hususuna odaklanılmıştır. Temel altındaki zemin tabakaları, zemin profilinin ortaya çıkarılması aşamasındaki belirsizlikleri de dikkate alacak şekilde ilgili parametrelerle birlikte tanımlanmıştır. Buna göre, zemin tepki analizleri gerçekleştirilmiştir. Zemin tepki analizi sonucunda elde edilmiş olan dinamik zemin parametreleri ve sismik girdi hareketi, Uluslararası Atom Enerjisi Ajansı güvenlik kılavuzları ve Amerika Birleşik Devletleri standartlarına ve kılavuzlarına uygun bir biçimde yapı-zemin etkileşimi analizlerine dâhil edilmiştir.

Sonuçlar bölümünde, her bir zemin profilinin üst yapı içerisinde belirlenmiş bölgelerdeki etkileri yapı içi tepki spektrumlarını içeren grafikler aracılığıyla mercek altına alınmıştır. Bu bilgiler ışığında, zemin parametrelerinden kaynaklanan sonuçlar ve bunların SASSI çıktıları üzerindeki etkileri tartışılmıştır.

Burada, en yüksek yer ivmelerinin temel genişliği boyunca gözle görülür bir şekilde değişmediği, varılan sonuçlardan biridir. Ancak, en yüksek spektral ivmelerin kuzey-güney doğrultusu boyunca değişime uğradığı gözlemlenmiştir.

Zemin katmanlarının empedanslarının derinlikle birlikte değişiminin yapıda önemli ölçüde dinamik davranış değişikliğine yol açtığı görülmüştür. Ayrıca, heterojen özellik gösteren zemin profillerinin temel dinamik davranışını büyük ölçüde etkilediği sonucu da eklenebilir. Fakat, bu etkinin üst yapıda, yukarıdaki kotlara çıkıldıkça azaldığı görülmüştür.

Son olarak, belirsizlikleri dikkate alan ortalama, alt sınır ve üst sınır zemin profillerinin, heterojen nitelikteki zeminleri tam olarak temsil etmediği görülmüştür. Bu sebeple, daha isabetli sonuçlara ulaşabilmek için her daim zemin araştırmalarının kalitesinin artırılması doğal olarak gerekmele beraber, analiz yaklaşımı olarak da olasılıksal yapı-zemin etkileşimi analizinin kullanılması önerilmektedir.



## 1. INTRODUCTION

Nuclear power plants are electricity generating thermal plants just as natural gas combined cycle plant, coal-fired thermal power plant or any other thermal power plant. Nuclear fission energy from splitting the atomic nucleus utilized as heat generator. Water converts to steam because of the heat produced during this fission process that continues in a contained environment. Steam resulting from the boiling water turns turbines and generators produce electricity.

Around the world, nuclear power generating plants are divided into two main categories: pressurized water reactors (PWR) and boiling water reactors (BWR). Both systems boil water for steam generation in both cases the thermal energy of steam is converted into electric power. After this process, this steam is cooled in any case.

Schematic view of a typical pressurized water reactor system and boiling water reactor system are respectively shown in Figure 1.1 and Figure 1.2 (“Url-1,” n.d.).

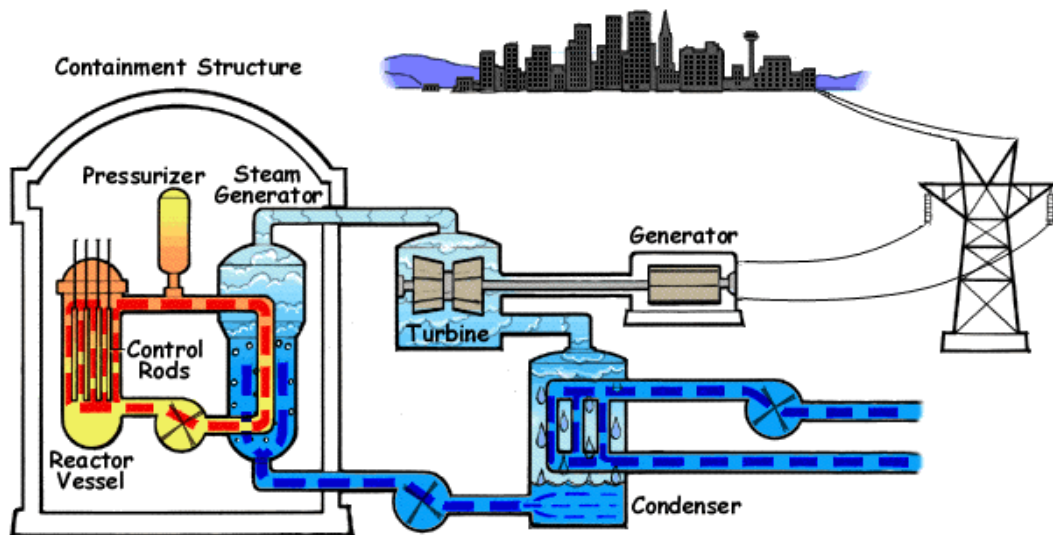


**Figure 1.1:** Schematic view of a typical pressurized water reactor

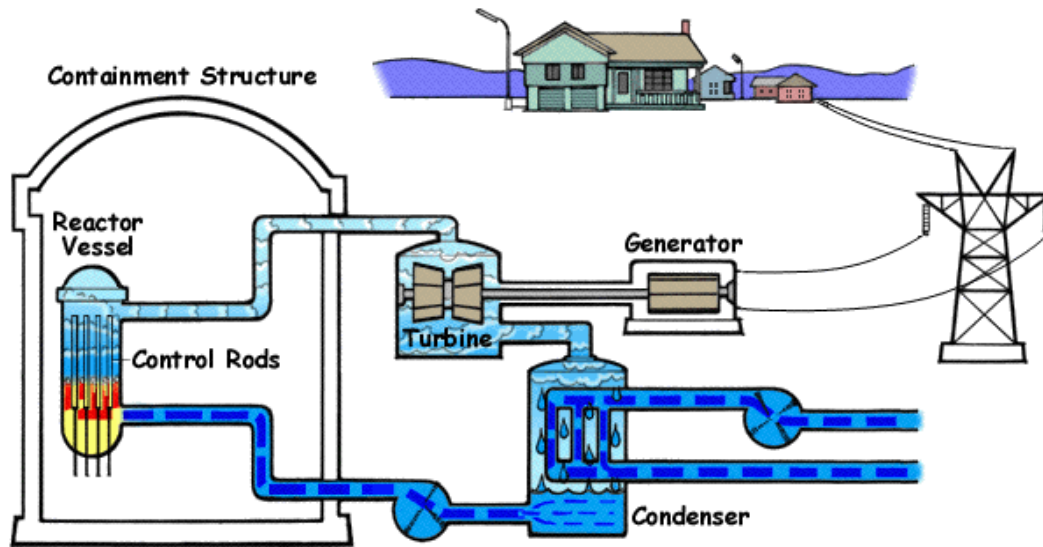


**Figure 1.2:** Schematic view of a typical boiling water reactor

It is not obviously seen in the abovementioned figures. However, the reactor coolant water is not the same water that boils to steam and powers the condenser. For instance, in a pressurized water reactor, the primary circuit, which contains radioactive coolant, is composed of a thermal-neutron reactor, reactor coolant loops, and a steam pressurizer. Each loop includes a steam generator and a reactor coolant pump, both connected with the reactor through cold and hot legs of the reactor coolant pipeline. The secondary circuit, which is nonradioactive, comprises the steam generators' steam generating part, main steam lines, one turbine, auxiliary equipment and associated systems, including those serving for heating and supplying feed water to the steam generators.

Electricity generation with nuclear has a considerable share to meet the world's energy need. There are 450 units in operation and 55 units under construction all around the world by the end of March, 2019 ("Url-2," n.d.). Distribution of the number of operational reactors by countries is presented in Figure 1.3. Most of the operational reactors are distributed in North America, Asia (Far East) and Western Europe. Additionally, the country with the highest number of reactors is United States of America with 97 reactors and France takes the second place with 58 reactors.



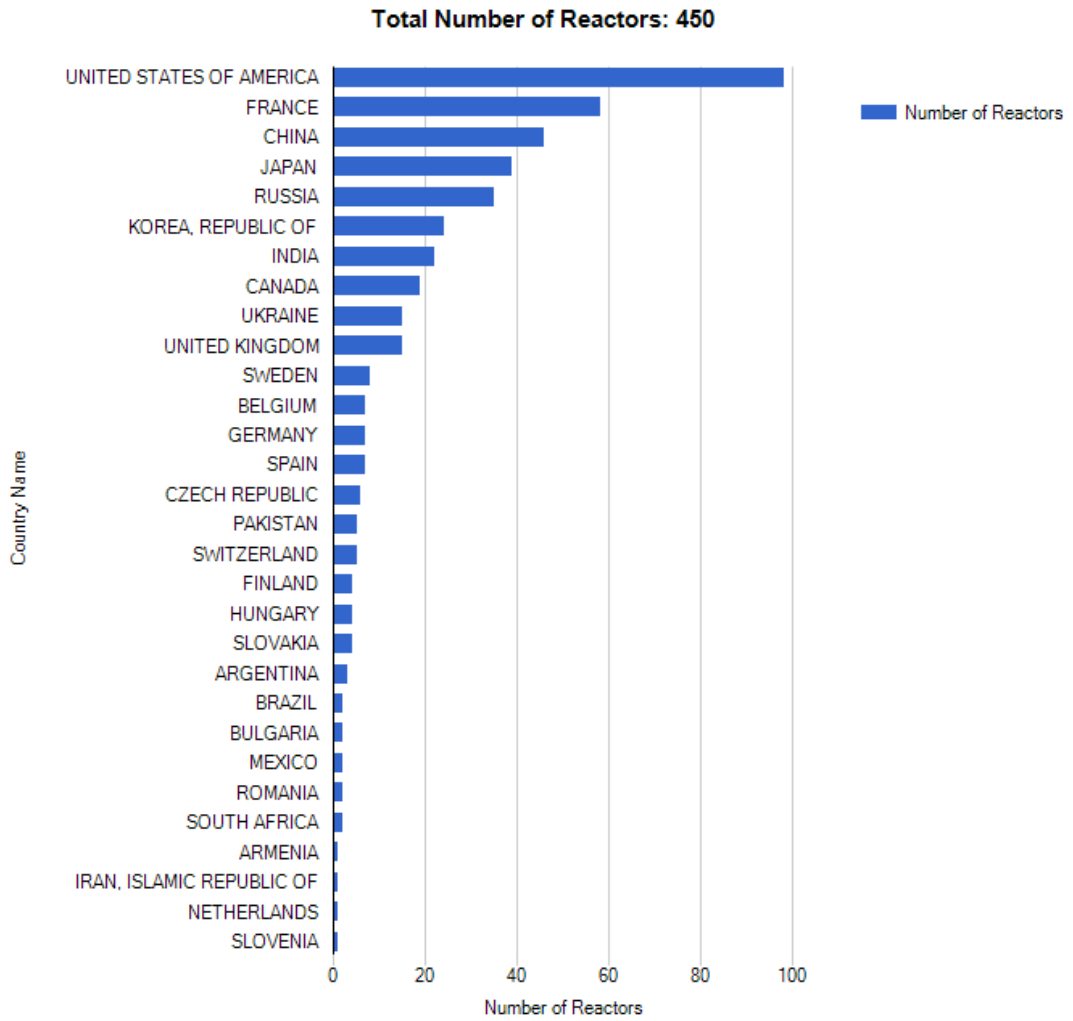


**Figure 1.3:** Number of operational reactors by countries in the world

Furthermore, the number of units under construction distributed by countries is shown in Figure 1.4. As of March 2019, in China 11, in India 7, in Russia 6 reactors are under construction. Besides, 1 unit is under construction in Turkey.

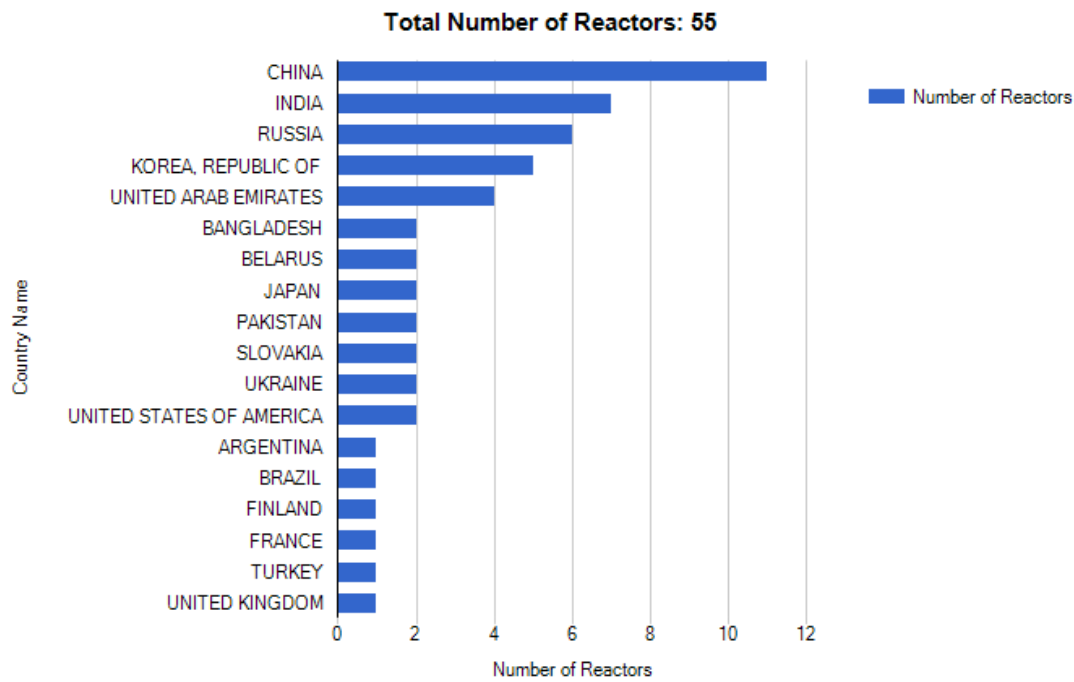


**Figure 1.4:** Number of under construction reactors by countries in the world

Throughout the development of nuclear reactors over a 60-year period, new generation plants using coolants such as gas, molten salt and liquid metals other than water, become more efficient in power generation. A light water type reactor design PWR, that uses pressurized water as the coolant to reduce the heat released by fission and transfer it to electrical generators, is predominantly constructed. By all means, full attention is thoroughly paid to reactor safety all over the world.

Major nuclear accidents, such as Three Mile Island, Chernobyl and Fukushima Daiichi, have caused severe damage in the past. Even though it shakes the confidence concerning nuclear power development for most countries, and especially have great influence on the development of nuclear power.

Aforementioned NPPs, namely Three Mile Island, Chernobyl and Fukushima Daiichi have the most common reactor technologies like pressurized water reactor and boiling water reactors. However, defects and problems in terms of safety confronted with the occurrence of these three major nuclear accidents.

The weaknesses of the NPPs have revealed after each nuclear accident and the critical importance of nuclear safety has become apparent. The opposition against this energy source continues in consequence of those accidents. Nevertheless, every nuclear accident leads up the improvement of nuclear safety (Gu, 2018).

## 1.1 A Brief History of Nuclear Power Plants Construction

The first nuclear power plant to be connected to an external grid goes operational on the 27<sup>th</sup> of June, 1954, in Obninsk, Russia. The nuclear reactor, which is shown in Figure 1.5, used to generate electricity, paved the way for Obninsk to be a Soviet scientific city and Obninsk still holds this soubriquet as the First Russian Science City (Nuclear Energy Agency, 2009).

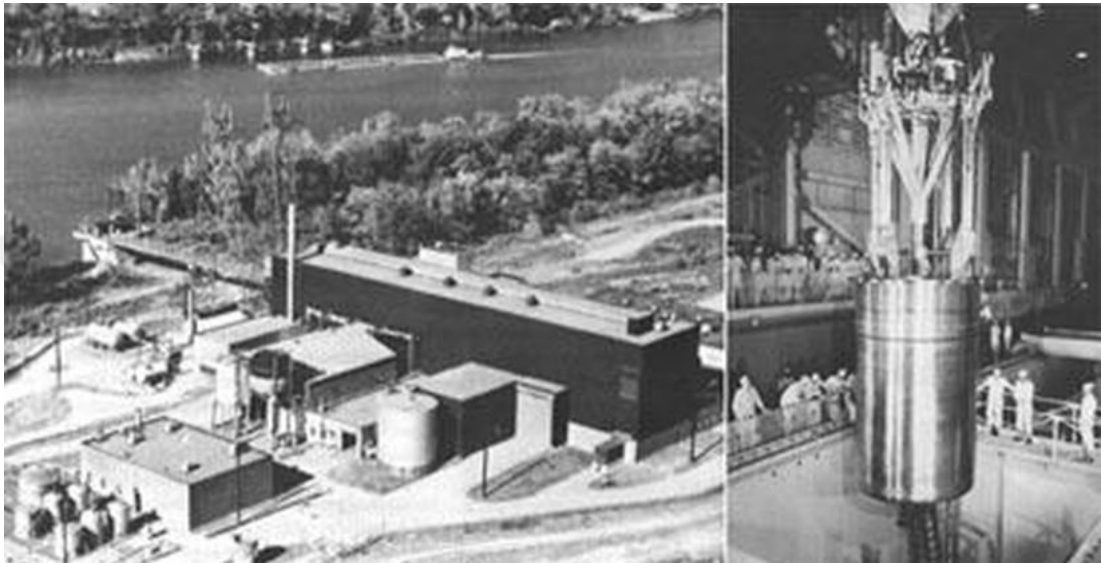


**Figure 1.5:** The first nuclear power plant, Obninsk NPP (“Url-3,” n.d.)

Obninsk city, currently houses more than 12 scientific research institutions and a technical university. Research is focused on nuclear-power engineering, nuclear physics, radiation technology, the technology of medical radiology and environmental protection (“Url-4,” n.d.).

Since 1954, after Obninsk NPP started operating, most of the industrialized western countries and countries like India and China, have welcomed nuclear power.

Two years after the first commercial NPP, Calder Hall was opened in the United Kingdom, with four 50 MWe reactors putting 200 MWe into the grid in 1956. The first commercial electricity-generating plant powered by nuclear energy in the U.S., is located in Shippingport, Pennsylvania. It reached its full design power in 1957. Light-water reactors like Shippingport use light water (i.e. ordinary water) to cool down the reactor core during the chain reaction. After Shippingport became critic, industry became more and more interested in developing light water reactors (Nuclear Energy Agency, 2009).

Later on, the first commercial pressurized water reactor (PWR) of 250 MWe was designed in U.S., Yankee Rowe, which started up in 1960 and operated to 1992. In the meantime, Argonne National Laboratory develops the boiling water reactor (BWR), and the first one, Dresden-1 of 250 MWe, designed by General Electric, is started up earlier in 1960. A prototype BWR, Vallecitos, ran from 1957 to 1963. By the end of the 1960s, PWR and BWR reactor units of more than 1000 MWe begins to be ordered.

Canada have developed reactors as well, but in a different way. These reactors were using natural uranium fuel and heavy water as a coolant and moderator. The first unit started up in 1962. Atomic Energy of Canada Limited still continues to improve this CANDU design.

France started out with a gas-graphite design and the first reactor started up in 1956. Commercial models operated from 1959. It then settled on three successive generations of standardised PWRs.

In 1964, two Soviet nuclear power plants start commissioning. A boiling water graphite channel reactor (100 MWe) begins operating in Beloyarsk (Urals). In Novovoronezh (Volga region) a new design, a small (210 MWe) pressurised water reactor known as a VVER (Vodo-Vodyanoi Energetichesky Reaktor or Water-cooled Power Reactor), is constructed.

In 1973, the first large 1000 MWe RBMK (Reaktor Bolshoy Moshchnosti Kanalnyy, High Power Channel-type Reactor) started up at Sosnovy Bor near Leningrad, and a VVER with a capacity of 440 MWe becomes critic in the Arctic northwest. This is superseded by a 1000 MWe version that becomes a standard design.

Other countries across the world, have decided on light-water designs for their nuclear power programmes, so that today 66% of the world capacity is PWR and 16% is BWR.

From the late 1970s to about 1990s, the historic growth in global nuclear generating capacity increases. Afterwards, nuclear power industry declines and stagnates. However, by the late 1990s, the first of the third-generation reactors, namely Kashiwazaki-Kariwa 6 (a 1350 MWe Advanced BWR), starts operating in Japan.

As a consequence of increasing electricity demand worldwide, especially in rapidly-developing countries, each country gives importance having assured access to affordable energy and thus re-starts their NPP construction programmes, in order to

meet demand at all times. Secondly, concerns about climate change for the need of carbon emissions limitation leads to an increase in the number of NPPs construction.

These factors coincided with the availability of a new generation of nuclear power reactors, and in 2004 the first of the late third-generation units is ordered for Finland – a 1600 MWe European Pressurized Water Reactor (EPR). Similarly, one other unit is constructed in France, and in the U.S. two new Westinghouse AP1000 units, each unit produces 1100 MWe, are built.

Afterall, plans and construction in Asia, particularly China and India, steal the spotlight from those in Europe and North America. The Republic of China alone marches forward to a huge nuclear power capacity. China plans to build more than one hundred further large units proposed and backed by credible political determination and popular support. Mostly, they are modernized Western design, or adaptations thereof. Besides, local designs are being constructed.

The history of nuclear power thus starts with science in Europe and then thrives in the UK and U.S. with the economic and technological development, decelerates for a few decades and later has a new growth spurt in East Asia. Almost over 17,000 reactor-years of operation have been accumulated within that period to satisfy the need of the world's electricity (Hardy, 1999).

An intergovernmental agreement was signed between Russian Federation and Republic of Turkey within the framework of the construction and operation of a nuclear power plant at the Akkuyu site in Turkey, in 2010. The first NPP in Turkey, which is a VVER design, is under construction since 2018.

## **1.2 Safety Considerations of NPPs**

The foundations of nuclear safety were laid after well-known speech by the U.S. president Dwight D. Eisenhower “Atoms for Peace”. It was a precursor of standardization and promotion of the peaceful use of atomic energy (Eisenhower, 2003).

Three fundamental terminology noted as “3S”; nuclear safety, nuclear security and nuclear safeguard serve as basis in nuclear regulation. International Atomic Energy Agency (IAEA) defines nuclear safety as “the achievement of proper operating conditions, prevention of accidents or mitigation of accident consequences, resulting

in protection of workers, the public and the environment from undue radiation hazards” (IAEA, 2007) (p.133). While, the IAEA defines nuclear security as “the prevention and detection of and response to, theft, sabotage, unauthorized access, illegal transfer or other malicious acts involving nuclear material, other radioactive substances or their associated facilities” (IAEA, 2007) (p.133). Nuclear safeguards specifies countermeasures to guarantee that governments obey the international regulations about nonuse of nuclear materials for nuclear explosives.

Bearing in mind the operation, decommissioning and waste disposal processes, at least 100 years dedication to maintain a sustainable national infrastructure may be needed for each nuclear power plant projects. The development of a nuclear power programme necessitates concentration to many interconnected and complex issues for a long period. Throughout these steps, the highest priority has to be given to nuclear reactor safety for each NPP projects in the world. Thus, it is very important to understand the safety considerations of nuclear reactors.

Nuclear safety requires commitments by all counterparts, such as the government, operator, regulatory body, nuclear technology and equipment suppliers and other parties, to ensure safety in all aspects of the nuclear power programme.

The fundamental safety objective is to protect people and the environment. Certainly, this objective has to be achieved without unreasonably limiting the operation of nuclear facilities and not posing to radiation risks. In order to maintain the highest standards of safety and to ascertain that facilities are operated safely, measures have to be taken:

- To limit the radiation exposure of people and the release of radioactive substances to the environment in a controlled manner,
- To minimize the possibility of events that might lead to a loss of control over a nuclear reactor core, nuclear chain reaction, radioactive source or any other source of radiation,
- To mitigate the consequences of events if they are to occur.

Those objectives should be applied to all nuclear facilities and activities and for the design and planning, siting, manufacturing, construction, commissioning and operation and decommissioning stages of a facility (IAEA, 2006).

Countries are responsible for the establishment of their nuclear safety regulations. However, radiation risks have no borders, and that makes nuclear safety a global issue. International collaboration is a must to enhance safety, to control hazards, to prevent accidents, to respond to emergencies and to mitigate any harmful consequences.

The IAEA safety standards reflect an international consensus on nuclear safety. However, these safety standards are high level of documents that constitutes a useful tool for all contracting parties under international conventions. Each member state have to fulfil it national and international obligations.

IAEA safety fundamentals establish safety objectives and principles. Safety requirements specify the requirements for the purpose of protecting people and environment from the harmful effects of radiation. Lastly, IAEA safety guides give recommendations to conform to the safety requirements with guidance in a more detailed way. The hierarchical structure of IAEA safety fundamental, requirements and guides is presented in Figure 1.6.

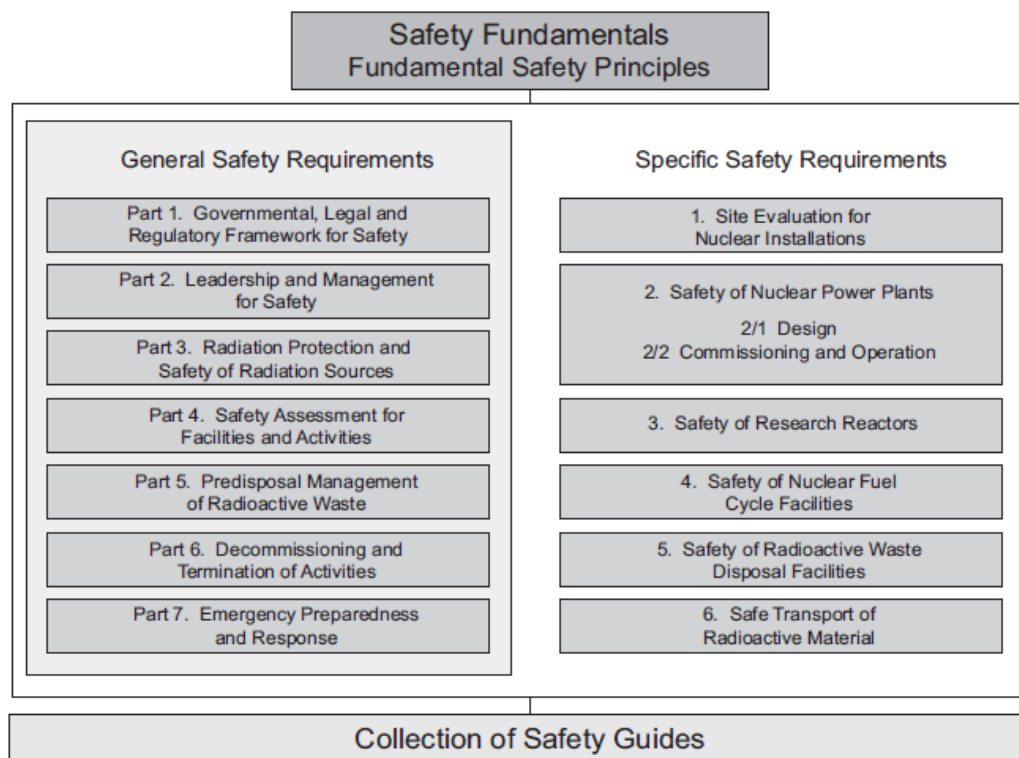


**Figure 1.6:** Structure of the IAEA Safety Standards Series

The main safety principles are described in IAEA Safety Fundamentals No. SF-1, Fundamental Safety Principles, 2006 (IAEA, 2006). IAEA establishes safety

requirements, recommendations and guidance to comply with by these safety principles.

According to IAEA, one of the major concepts, in terms of safety, entitled as defence-in-depth. The main idea behind this concept is multiple levels of protection. IAEA gives uttermost priority to it in its various aspects. Defence in depth can be described in association with:

- A well-established safety culture,
- Suitable site selection and engineering and designing features providing safety margins, diversity and redundancy, principally by the help of:
  - Design, technology and materials of high quality and reliability,
  - Control, limiting and protection systems and surveillance features,
  - Inherent and engineered safety features.
- Comprehensive operational procedures and practices likewise accident management procedures (IAEA, 2006).

Basically, nuclear safety aims to protect public and the environment from the detrimental effects of ionizing radiation. The strategy for defense in depth consists of two parts: first, to prevent accidents and second, if prevention fails, to limit the potential consequences of accidents and to prevent their evolution to more severe conditions. According to a report by International Nuclear Safety Advisory Group numbered as INSAG-10, defence in depth comprises of five levels (INSAG, 1996). Each level and their essential objectives by means of ensuring safety are shown in Table 1.1. This table consists of five levels of defense in depth. First four levels have the objective of prevention or control, and the fifth level aims the mitigation of radiological consequences of significant releases of radioactive materials.



**Table 1.1:** Levels of Defense in Depth

Levels	Objective	Essential means
Level 1	Prevention of abnormal operation and failures	Conservative design and high quality in construction and operation
Level 2	Control of abnormal operation and detection of failures	Control, limiting and protection systems and other surveillance features
Level 3	Control of accidents within the design basis	Engineered safety features and accident procedures
Level 4	Control of severe plant conditions, including prevention of accident progression and mitigation of the consequences of severe accidents	Complementary measures and accident management
Level 5	Mitigation of radiological consequences of significant releases of radioactive materials	Off-site emergency response

If one level were to fail, the subsequent level comes into play, and so on. Special attention is paid to hazards that could potentially impair several levels of defense, such as fire, flooding or earthquakes. Precautions are taken to prevent such hazards wherever possible and the plant and its safety systems are designed to cope with them.

Site heterogeneity effects to the seismic response of a typical reactor building is investigated in this study. In connection with the chosen nuclear facility structure type, a necessity for clarification how the structures, systems and components are classified in a nuclear power plant according to their importance to safety is arisen.

According to IAEA Safety Guide NS-G-1.6 (IAEA, 2003), the selected typical reactor building generally enters into Seismic Category 1 in almost every nuclear power plant design. Determination methods for each category have evolved in the light of experience gained in the design and operation of existing plants. Hence, this

categorization used in practice identifies that this type of structures deemed to have the highest importance to seismic safety. Seismic Category 1 structures, such as reactor building, should be designed to resist SL-2 earthquake level or in another terminology, Safe Shutdown Earthquake (SSE). In case of a SL-2 earthquake, all defence in depth levels should be available. Within the context of the defence in depth approach, as indicated in Table 1.1, earthquakes are included in Level 1 of defence in depth.

### **1.3 Objective and Scope**

Despite the fact that the construction and operation of nuclear installations are strictly controlled and regulated by the regulatory authorities all over the world, even if one in a million, always there is possibility of accident. An accident could result in dangerous levels of radiation that could affect the health and safety of the public living near these nuclear installations.

The structure, which is the subject of analysis in this thesis, is a nuclear reactor building with containment structure that is identified as the most important structure in nuclear power plant designs. The reason why this kind of identification is given to that building is because that structure houses the most critical components. During an earthquake, the properties of soil media affects the dynamic response of the super-structure. This dynamic effects transferred from the soil to the structure and vice versa, is named as soil-structure interaction (SSI).

In this study, a typical nuclear reactor building is considered to investigate site heterogeneity effects on the seismic response of the super-structure. Therefore, in the first chapter, a brief history of nuclear power plants construction and then safety considerations in NPPs conveyed in order to comprehend the nuclear safety concept better.

In Chapter 2 of this thesis, academic literature information is given regarding site response analysis and the most common methods used in this type of analysis, dynamic soil-structure interaction analysis and general solution methods of SSI analysis, and guidelines for SSI analysis along with requirements in nuclear standards and guides are presented as a subchapter.

Following the literature review summarizing the past studies and analysis methods in the second chapter, information regarding the determination of soil modelling

parameters and their variations is presented. Additionally, strain dependent modulus degradation and damping curves used to take into account the nonlinearity in the soil response analyses is submitted in Chapter 3.

Afterwards, process steps regarding site response analysis are followed in Chapter 4. Firstly, seismic input motion is generated following the procedures defined in the related standards and guidelines. Following this, site response analysis is performed, and the 1D equivalent linear site response analysis results are shared.

Within Chapter 5, the influences of heterogeneity due to the deeply inclined layering on the dynamic responses of the foundation are investigated through a comparison between 1D equivalent linear analyses using DEEPSOIL Hashash et al. (2016) and 2D site response analyses carried out with PLAXIS 2D software (Brinkgreve et al., 2006).

In Chapter 6, the super-structure model of chosen generic reactor building type and its dynamic properties are presented. Furthermore, soil model and input motion which are incorporated into the soil-structure interaction analyses performed using ACS SASSI software (GP Technologies Inc., 2014).

The results are given as graphs which includes in-structure-response-spectra considering the effects of each soil profile in certain points of super-structure. The results stemming from the soil parameters and their influence on the SASSI outputs are discussed.

It is discussed how the description of site effects could be refined by increasing the number of descriptive parameters as a future recommendation.



## **2. LITERATURE REVIEW**

### **2.1 Site Response**

Determining how the surface motions are affected by the soil layers above the bedrock, the propagation of the shear waves towards the upper part of the bedrock under a certain area, the development of fracture modeling from an earthquake source, and the development of the design response spectra can only be achieved by site response analyses.

In order to ensure the safety of structures under earthquake loads and to evaluate the seismic response of the structures, the effect of local soil conditions on ground motions should be determined. The seismic response of structures considering the local site and soil-structure interaction effects, many variables are to be defined. It is necessary to know the simultaneous behavior of structure-foundation system and the soil, which is a part of this system, under earthquake loads.

Under those earthquake loads, the free-field response of the soil above the bedrock is calculated. This calculation is named as “site response analysis”. Site response analyses are used to assess the effects of local soil conditions on the surface motion. The seismic waves propagate from bedrock to the surface with the influence of local soil conditions and it can be generally defined by the character of seismic sources, earthquake magnitudes, fracture mechanism and local soil conditions.

Local soil properties are directly influential at the design stage in determining the in-structure response spectra or in the calculation of earthquake loads, and also in the conduct of liquefaction analyses, or in the determination of earthquake-based loads for the design of ground structures such as retaining structures, engineering fills and slopes. In site response analysis, the propagation of shear waves, as shown in Figure 2.1, travelling from the bedrock to the ground surface is analyzed.

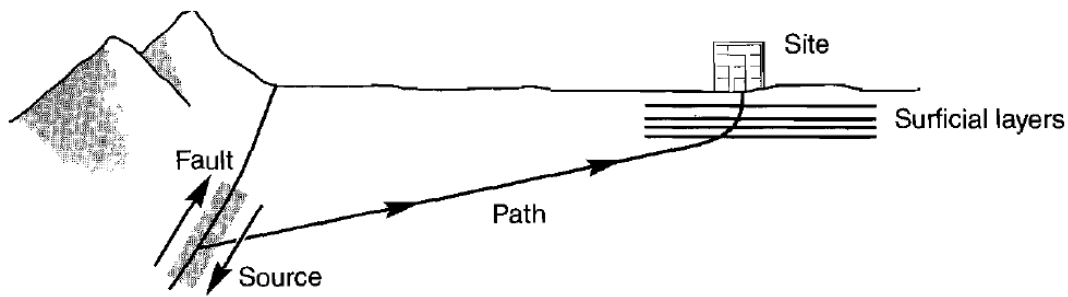


**Figure 2.1:** Wave propagation process to the ground surface (Kramer, 1996)

In order to perform site response analysis;

- Calculation or selection of the site-specific ground acceleration,
- Design ground motion determination,
- Determination of dynamic properties of soil layers,
- Selection of the dynamic behavior analysis method,

are required.

The ground acceleration and earthquake magnitude are obtained from the seismic hazard analysis. In the seismic hazard analysis, the distance from the active fault lines to the site and the empirical relations or taking into account the faulting mechanism.

As an input to the seismic soil-structure interaction analysis, the surface ground motion, in other words the free-field response spectra must be calculated. Free-field motion is the vibration of the soil media with the effect of earthquake in case without any structure on the ground.

In the seismic analysis of the structures built on the bedrock, it is observed that the ground motion seen in the basemat is similar to the ground motion before the building is constructed (Wolf, 1988). Based on the ground motion record on the ground surface in such soil media, it can be adopted as a reasonable approach to perform seismic response calculations of structures.

Design ground motion can be obtained from artificially generated acceleration records by using a series of earthquake acceleration records recorded in the past in regions with similar soil conditions, or by utilizing seismic hazard analysis. The dynamic properties of the soil layers are determined by the site investigations and in-situ experiments. The analysis of the soil layers behavior under the seismic effects

occurring in the bedrock and calculation methodology of the soil properties effects on the ground motion in the frequency domain can be one-dimensional, two-dimensional or three-dimensional (Kramer, 1996).

For many years, a couple of site response analysis methodologies have been developed. Those methodologies are grouped in regard to the dimensionality and the assumptions used in the analyses. Among these methods, the most commonly used method can be addressed as one-dimensional method in terms of dimensionality. The basic approaches within the scope of one-dimensional soil response analysis can be classified as linear, equivalent linear and nonlinear. Linear soil behavior has constant shear modulus and damping ratio for each soil layer. In the case of nonlinear soil behavior, the shear modulus and damping ratio vary according to the stress deformation relations.

Those methods have the advantages and disadvantages among each other. The selection of the methodology depends on the decision regarding the effectiveness of the local soil characteristics modeling.

However, in the one-dimensional site response analysis, a set of assumptions are considered as follows:

- All soil layers are parallel and horizontal,
- Seismic waves spreading from the main rock in the vertical direction cause the ground to react,
- Ground and main rock surfaces are infinite in third dimension.

Equivalent linear site response analyses are carried out with programs such as SHAKE2000 (Schnabel et al., 2009) and DEEPSOIL (Hashash et al., 2016) using frequency-domain equivalent linear approach. In addition to this, finite element programs such as OpenSees (Mazzoni et al., 2009), ABAQUS (Dassault Systemes, 2005) and LS-DYNA (LSTC, 2009) are mostly used in time-domain nonlinear analysis. DEEPSOIL, which is used in this thesis for the one-dimensional equivalent linear analyses, can also be used to perform nonlinear time-domain site response analysis.

### 2.1.1 Equivalent linear site response analysis

It is widely known that the soil medium shows nonlinear behavior under the seismic loads. The equivalent linear approach is practically applied taking into account the nonlinearity by approximating the nonlinear properties of soil for its computational efficiency and reasonable approximations. This simplified approach uses strain-compatible, linear material properties of the soil.

Firstly, the equivalent linear approach for site response analysis is suggested by Idriss and Seed (1967) that estimates nonlinear soil response through a linear analysis. Later, Schnabel et al. (1972) implemented this method in the frequency-domain and created SHAKE software, which is widely used in engineering applications. The equivalent linear method in frequency-domain is still current practice in nuclear industry.

In the equivalent linear method, either in the frequency or the time-domain, the soil layer properties are iteratively adjusted with a series of linear analyses. A linear analysis is first performed using the initial values of shear modulus and damping ratio, and the high-strains in the soil layers are computed. An effective shear strain is then calculated for each layer by multiplying the high shear strain by an effective shear strain ratio. This strain value, along with the assumed or experimentally determined modulus reduction and damping curves, is used to update the shear modulus and damping ratio of each layer.

The dynamic properties of the soil media under dynamic loads such as earthquakes are largely dependent on the shear-strain ratio characteristics under the cycling loading. These characteristics can be listed as follows:

- Shear modulus value  $G_{\max}$ , obtained at very small shear strains (generally less than 0.001%)
- Relationship between the maximum shear modulus  $G_{\max}$  and  $\gamma$  (this relationship is usually denoted as  $G/G_{\max} - \gamma$  curves),
- Damping ratio variation with shear strain ( $\zeta - \gamma$ ),

The relationship between shear stress  $\tau$  and  $\gamma$  is shown in Figure 2.2. In this figure, when the shear strain is low, the shear modulus increases while the shear modulus



decreases with the increase of shear strain. The hysteresis curves of different cycling shear strain can be combined accordingly.

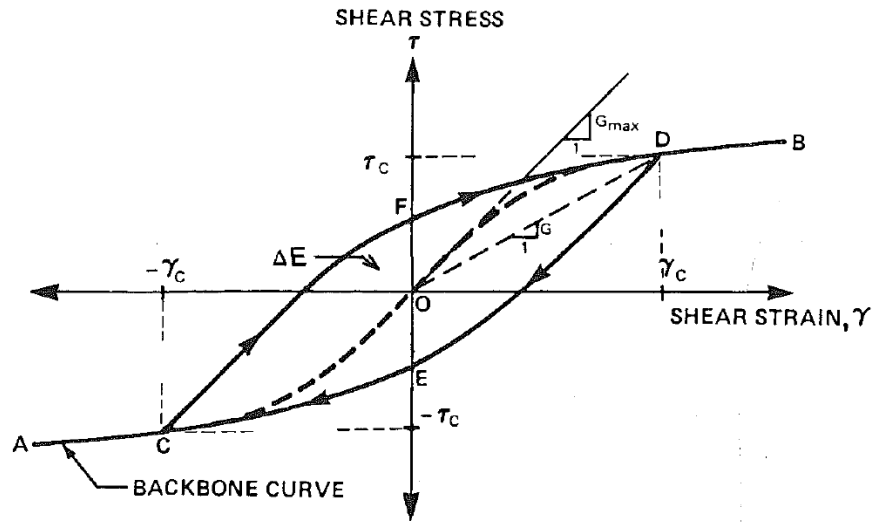


**Figure 2.2:** First-cycle stress-strain curve (Vucetic & Dobry, 1991)

$G_{max}$  value is degraded with the increase of shear strain and the shear modulus ratio  $G/G_{max}$  will be less than 1.0. Hence, the overall stiffness is dependent on  $G/G_{max}$  together with the other parameters such as the shear strain ratio and the damping ratio. The strain-dependent shear modulus degradation and damping ratio curves are shown in Figure 2.3. These relationships are described through certain laboratory studies.

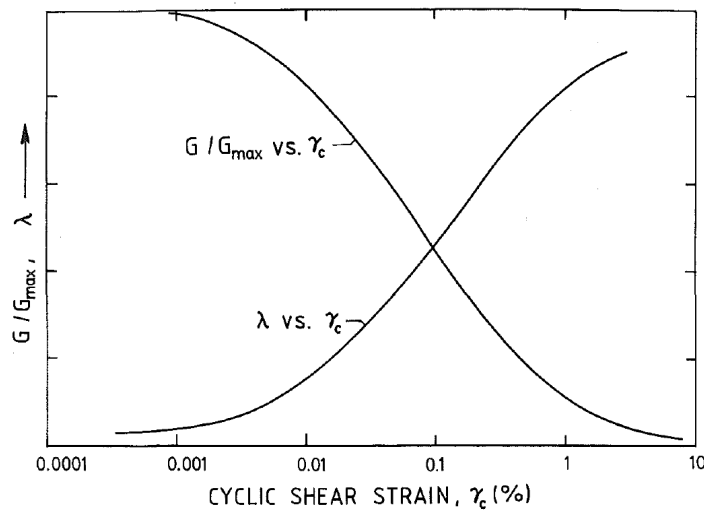


**Figure 2.3:** Strain-dependent shear modulus degradation and damping ratio curves (Vucetic & Dobry, 1991)

Calculation steps using equivalent linear approximation method to represent nonlinear soil behavior can be described as follows:

1. Initial values of  $G$  ( $G_{\max}$ ) and damping ratio ( $\zeta_0$ ) are taken for each soil layer. Generally, they correspond to the same shear strain ratio. Small-strain values are generally used in initial values,
2.  $G_{\max}$  and  $\zeta_0$  values are used to calculate the soil response and the shear strain of each layer,
3. The effective shear strain ratios at each layer ( $\gamma^{(i)}$ ) is obtained from the maximum shear strain within the time-dependent change of the calculated shear strain,
4. Sequent equivalent linear values  $G^{(i+1)}$  and  $\zeta^{(i+1)}$  are selected from the effective shear strain ratio for the next iteration,
5. The process from the second step to the fourth step until the difference between the shear modulus and the damping ratio calculated in the two iterations is below the value previously determined for all layers (Schnabel et al., 1972).

It was observed that the ground reactions determined based on these assumptions were consistent with the measured responses during many earthquakes.

Equivalent linear approach is adopted by the computer programs such as SHAKE (Schnabel et al., 2009) and SASSI (Lysmer et al., 1999). In this thesis, DEEPSOIL and SASSI programs are used for the seismic response incorporating one-dimensional equivalent linear analyses.

### **2.1.2 Nonlinear site response analysis**

The realistic behavior of the soil under cyclic loading can be modeled by nonlinear and backbone curves namely nonlinear hysteretic model. The main idea for modeling the dynamic behavior of the soil with different shear stress-strain curves is that this behavior varies depending on the amplitude of cyclic loading. When the amplitude of the motion such as earthquake vibration is low, linear behavior is observed on the surface, while nonlinear behavior due to plastic deformation is observed due to shifts between the soil grains in cyclic and large amplitude motions. Due to the intrinsic properties of the earthquakes, such as frequency content, duration and amplitude of the dynamic motion, and the engineering properties of the soil, the soil behavior is

expected to be complex. Some complex material models, such as Kodner-Zelasko model (Lee and Finn, 1978), and modified version of this model (Matasovic, 1993) were developed using experimental data on the basis of Masing rules (Masing 1926). Nonlinear hyperbolic soil model to define loading and unloading behavior with extended Masing rule is shown in Figure 2.4.

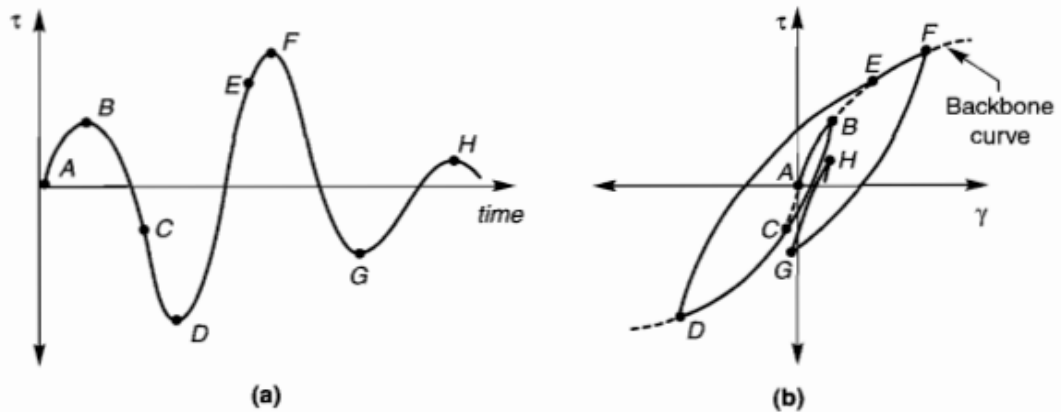


**Figure 2.4:** Extended Masing rules: (a) variation of shear stress with time; (b) resulting stress-strain behaviour (backbone curve indicated by dashed line) (Kramer, 1996)

Based on these models, computer programs such as OpenSees (Mazzoni et al., 2009), ABAQUS (Dassault Systèmes, 2005), LS-DYNA (LSTC, 2009) and DEEPSOIL (Hashash et al., 2016) were developed.

In this method, site response analyses are carried out with mainly lumped mass approach and finite element approach. In the lumped mass approach, the soil layers are modeled as individual lumped masses linked with springs. Equations of motion is calculated and integrated for each soil layer. On the other hand, the soil layers are modelled with solid elements. The lumped mass and finite element approaches are sketched in Figure 2.5.

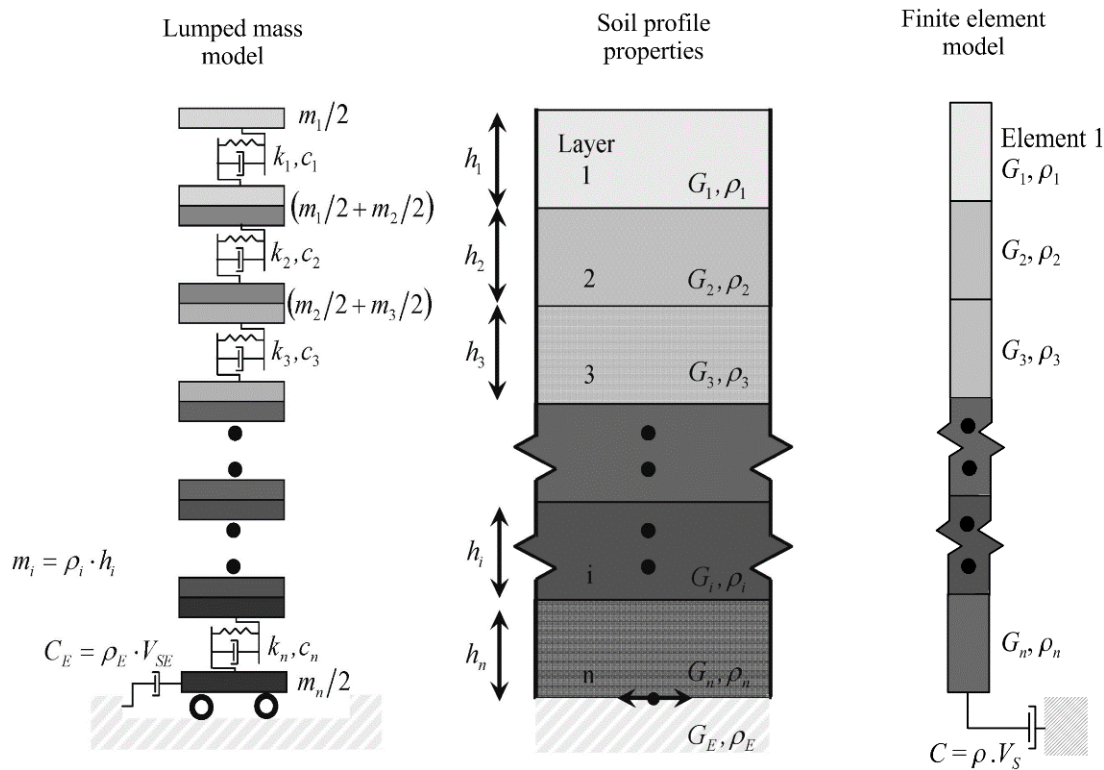


**Figure 2.5:** The lumped mass and finite element approaches in nonlinear site response analysis (Bolisetti, et al., 2014)

The soil profiles are modeled in a more realistic way with a nonlinear approach. However, this approach is not practically used in the structural engineering of nuclear field.

## 2.2 Dynamic Soil-Structure Interaction

The earthquake resistant design of the majority of civil engineering structures are performed with assuming that the structure is fixed to the ground surface at the foundation level. For many years, this practice has been assumed to be conservative in terms of seismic design (Bhaumik & Raychowdhury, 2013). However, the ground motion propagates through the soil media and it is an undeniable fact that the dynamic properties of soil medium, particularly soft soils have effects on the structures' behavior. Therefore, the interaction between soil and structure should be taken into account. This interaction is named as soil-structure interaction (SSI).

Soil-structure interaction is a sophisticated issue that includes topics such as seismic field response, seismic wave motion, ground mechanics, geology, building mechanics and structural dynamics. In this subject, it is necessary to consider multi-variable

elements such as soil behavior, structure behavior, and seismic wave propagation in the soil media.

The interaction is caused by the diffusion of the ground motion waves from the foundation surface and by the structural damping of the vibrations and energy. Due to these effects, the deformation (displacements, velocities and accelerations) in the soil surrounding the structure are different from the deformation on the free surface. Thus, the dynamic behavior of a structure supported by a soft soil can be different from an identical structure on a very hard soil or rock considering the amplitude and frequency content. The soil-structure system shows higher structural response at a relatively low frequency compared to a similar structure resting on the rigid floor. However, the structural response is also affected by the radiation damping and material damping that occur in the soil media.

The deformations of a structure during earthquake shaking are affected by interactions between three linked systems: the structure, the foundation, and the geologic media underlying and surrounding the foundation. A seismic Soil-Structure Interaction (SSI) analysis evaluates the collective response of these systems to a specified free-field ground motion. A seismic soil-structure interaction analysis evaluates the collective response of the structure, the foundation, and the geologic media underlying and surrounding the foundation, to a specified free-field ground motion. The term free-field refers to motions that are not affected by structural vibrations or the scattering of waves at, and around, the foundation. SSI effects are absent for the theoretical condition of a rigid foundation supported on rigid soil. Accordingly, SSI accounts for the difference between the actual response of the structure and the response of the theoretical, rigid base condition.

SSI effects are categorized as inertial interaction effects, kinematic interaction effects, and soil-foundation flexibility effects. The terms kinematic and inertial interaction are introduced in 1975 by Robert Whitman at MIT.

The SSI effects can be listed as below:

- Inertial effect: The deformations at the foundation level due to inertial effect would amplify the free field motion.
- Kinematic effect: The rigid boundary had a kinematic effect on the response and creates incoherency on the shear waves reaching to the foundation. If the

soil profile has deeply inclined layers, this incoherency effect is more considerably pronounced. This kinematic interaction would deamplify the free-field motion.

- Soil-foundation flexibility effect: The weight of the foundation increased the stresses in the soil, which in turn increased the shear wave velocities and the moduli of the soil layers. Increased shear wave velocities and/or shear moduli would amplify accelerations with higher frequency components to the surface and cause lower internal damping (Kausel, 2010).

The properties of soil are not directly considered in conventional structures and modeling and analysis of the structures are carried out using only certain soil parameters. Therefore, the soil-structure interaction is ignored. Currently almost every high-level standard and regulation establish requirements considering this phenomenon which may be critical for facilities like nuclear power plants.

Firstly, in 1867, a theory was proposed by Winkler based on the assumption that reactions of subsoil are directly proportional to settlement of a foundation structure (Winkler, 1867). However, this study and numerous studies have focused only on the foundation behavior until 1950s. In 1954 by R.G. Merrit and Prof. George Housner observed that horizontal records obtained at the foundation are similar to motion records on structure nearby, concluding that the lateral compliance of the foundation has a very little effect on these motions (Merrit & Housner, 1954). In 1957, Housner investigated the interaction of a building and the soil during an earthquake. In this study, the significant effects were observed on the rocking motion of a building resting on a soft soil (Housner, 1957).

Most of the studies were numerical until the recent studies carried out during 2000s (Kausel, 2010). Ductility effects accounting for nonlinearity of structures under dynamic conditions with SSI effects due to rocking were investigated (Mylonakis and Gazetas, 2000). Many experimental studies conducted internationally in addition to the numerical considerations. A number of experiments were performed by scientists including Maugeri et al. (2000), Knappett et al. (2004), Turan et al. (2009), and Qin and Chouw (2010) using shaking table.

In 1991, Gazetas used Winkler springs with elastic stiffness for modeling a machine foundation. His study involves a number of impedance functions in frequency domain

for surface mount of embedded foundations and different shape of foundations (Gazetas, 1991).

The studies by Veletsos and Wei (1971) and Luco and Westman (1971, 1972) focused on the dynamic behavior of structures. Circular plates above elastic half-spaces with a wide range of frequencies were investigated. After these pioneering works, the advancement in the field of study of SSI accelerated, especially in the nuclear industry (Kausel, 2010).

Thereupon, in the nuclear sector, the effects on the containment structures' integrity considering nonlinearity was investigated by Evans and Keogh in 1987. It was shown that variations in soil media characteristics affect the containment structures' response (Evans & Keogh, 1987). Analyses performed by Venancio-Filho et al. in 1997 addressing the substructure and frequency domain methods to investigate the effect of dynamic soil-structure interaction on NPP containment structures and identified different foundation impedance functions (Venancio-Filho et al., 1997). Later, in 2010, nonlinear dynamic response analyses carried out by Zentner and this study was concluded with the interpretation of equipment fragility curves (Zentner, 2010). One year later, Saxena et al. specifically studied on the effects of slip and separation at the interface due to seismic behavior of a NPP structure. In conclusion of this study, those effects were found influential. More recently, Saxena and Paul reached a conclusion that the foundation embedment depth is significant considering those effects (Saxena et al., 2011), (Saxena & Paul, 2012).

### **2.2.1 Solution methods**

Soil-structure interaction solution methods that are used to evaluate the kinematic effects and inertial effects can be examined in two different approaches (Wolf, 1985).

- Direct method,
- Substructuring (subsystem) method.

In the direct method, the superstructure and the soil are modeled by being idealized as a single system. In contrast to direct method, soil media and superstructure are modeled as separate subsystems in the substructuring method. This approach, which is more suitable for practical applications, also significantly reduces the analysis time

and allows the structural engineer and the geotechnical engineer to interact with each other on separate system models.

### 2.2.2 Direct method

In the simplest terms, direct method can be described as a combined single step soil-structure system solution in SSI analysis. The direct method does not refer to superposition. He can solve the problem of structure-ground interaction in the frequency domain and solve the time domain. The direct method can be applied as an analysis in the linear or nonlinear time domain.

The simplest method of direct method is the simplified ground spring method. Except for the simplified soil spring method, structures and soil media are normally modeled by either finite element or finite difference method. In order to represent the semi-infinite soil environment with a separate model, the imaginary boundaries should be determined and appropriate boundary conditions should be applied. Finite element model with lateral boundaries that used in SSI direct approach is shown in Figure 2.6.

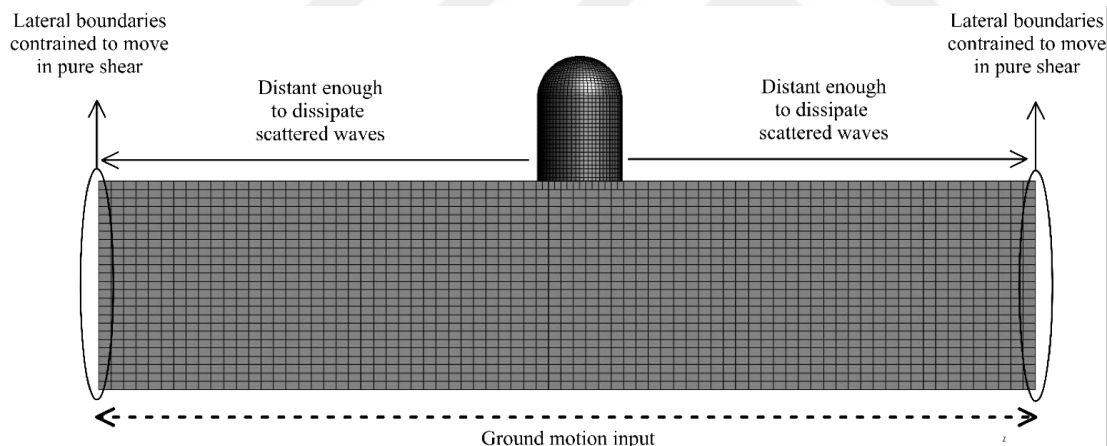


**Figure 2.6:** Soil-structure modelling in direct method (Bolisetti, 2015)

Once consistent motion is determined at the boundaries of discrete media, soil-structure interaction analyses are performed in one or two steps.

In general, the structure-ground interaction analysis by direct method involves the following steps:

1. Modeling the structure,
2. Foundation modeling: geometry, rigidity and interface,
3. Modeling of the soil,



- a. Determination of soil material properties (linear, non-linear),
  - b. Soil discretization,
  - c. Determining the lower boundary and horizontal boundaries of the soil-structure model,
4. Specifying the input motion to be applied at the borders,
  5. Conducting soil-structure interaction analysis,
  6. Performing a second step analysis for a more detailed structural response, if necessary (ASCE, 2017).

Direct approach is mostly performed in time domain nonlinear analyses. Computer programs such as LS-DYNA (LSTC, 2009), ABAQUS (Dassault Systèmes, 2005) and OpenSees (Mazzoni et al 2009) widely used for finite element modelling in time domain.

### **2.2.3 Substructuring method**

In the substructuring approach, the soil and structure are considered in two different substructures and those substructures are analyzed separately.

All the substructures are combined by superposition, assuming that soil and structure behavior is linear, in practice it is an equivalent-linear approach. The calculation steps in substructuring method are as follows:

- Determination of foundation input motion. This motion should not be confused with the free-field motion. The difference between foundation input motion and free-field motion is specified with a transfer function in frequency domain. This transfer function involves the solution of only the kinematic interaction problem.
- The frequency dependent impedance functions describe the stiffness and damping characteristics of the soil-foundation interaction system. Material and geometrical properties of foundation and soil with equivalent linear properties are taken into account in this step.
- Response of the upper structure by the frequency dependent excitation soil springs using rocking and translational components of foundation input motion is calculated (NIST, 2012).

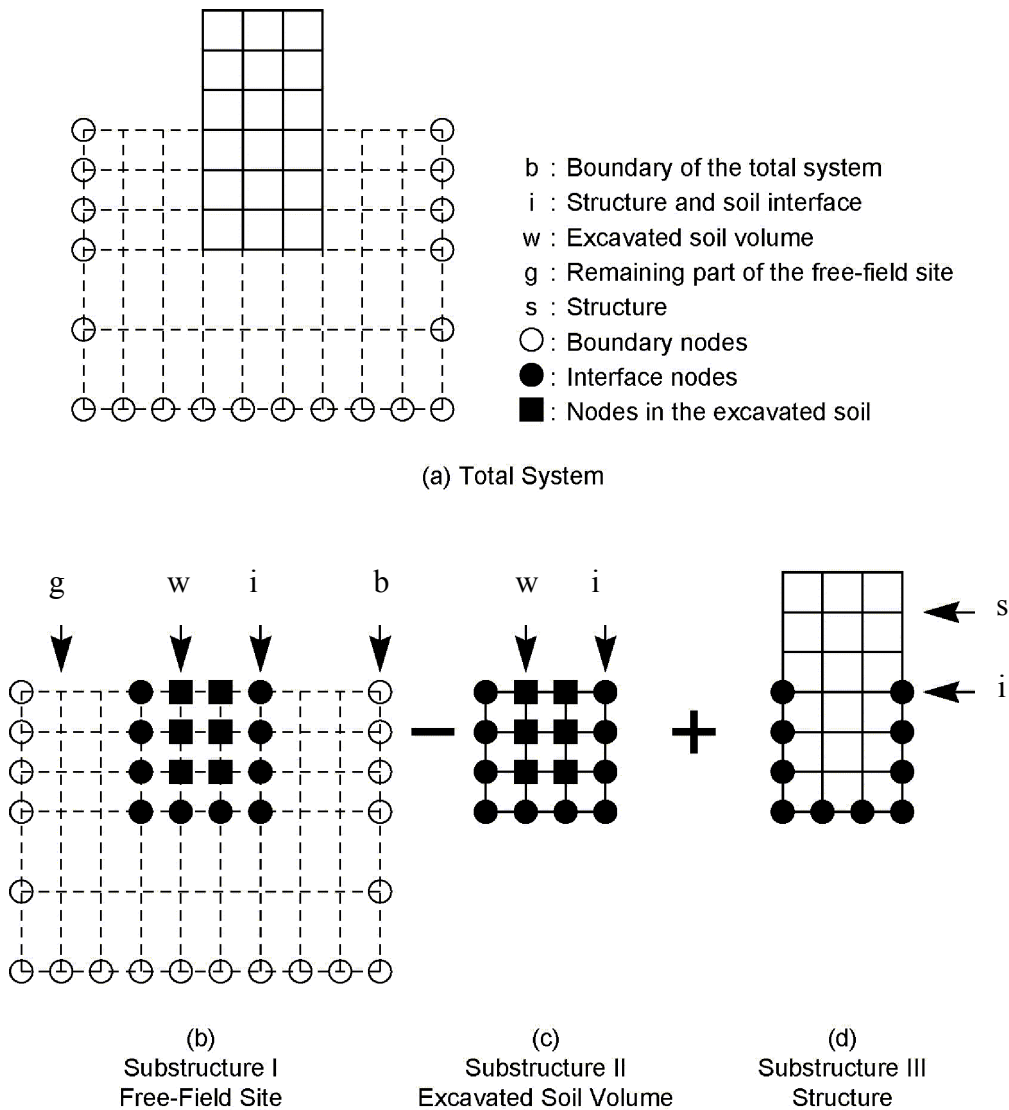


**Figure 2.7:** Substructuring in soil-structure interaction analysis (adapted from (Lysmer F. Ostandan, and C.C. Chin., 1999))

Most commonly preferred computer programs using the substructuring method are SASSI (A System of Analysis of Soil-Structure Interaction) (Lysmer F. Ostandan, and C.C. Chin., 1999) and CLASSI (Continuum Linear Analysis of Soil-Structure Interaction) (Wong and Luco, J.E., 1970).

Conceptually, substructuring methods can be classified into four types depending on how the structure and the soil interact in their degrees of freedom. These are the followings:

1. Rigid boundary method: rigid is used here for the boundary between the floor and the foundation or partial buried structure,
2. Flexible boundary methods,

3. Flexible volume method,
4. Sub-structure subtraction method (ASCE, 2017).

For the solution of these four substructuring methods, the sub-problems of the seismic soil-structure interaction analysis which have to be solved before are shown in Figure 2.8.

Method \ Analysis	Rigid Boundary	Flexible Boundary	Flexible Volume	Subtraction
Site Response Analysis (a)				
Scattering Analysis (b)			None	None
Impedance Analysis (c)				
Structural Response Analysis (d)	Standard	Standard +	Standard +	Standard +

**Figure 2.8:** Types of substructuring methods (Ostadan, 2006)

Key elements of the SASSI approach can be described as follows:

- The site is modeled in semi-infinite elastic or viscoelastic horizontal layers on a rigid base or semi-infinite elastic or viscoelastic halfspace.
- Structures are idealized with standard two or three-dimensional finite elements. Each node may have six degrees of freedom.
- The excavated soil is idealized with standard plane unit deformation or three-dimensional solid elements.
- The nodes in the boundaries between the finite element models of structures and the excavated soil are common.
- Both the flexible volume method and the subtraction method or the extended (modified) subtraction method can be used for impedance analysis. The interaction between the excavated soil and the semi-infinite space occurs at all

nodes in the flexible volume method. The extended subtraction method accepts the interaction at the boundary nodes and at selected nodes in the excavation area.

- All interconnected nodes are located at the floor layer interfaces with degrees of freedom.
- Material damping is taken into account with complex moduli, which allows effective damping ratios to be frequency independent and vary from element to element
- The seismic environment may include an arbitrary three-dimensional overlap of inclined body and surface waves.
- Earthquake simulation is defined by the acceleration record in the time domain namely, control motion.
- The control motion is applied to the control point defined on the free surface or at a point in the soil column.
- Fast Fourier transform technique is used for time histories.

### **2.3 SSI Analysis of NPPs Within Standards and Requirements**

The engineering application of soil-structure interaction and its effect in terms of nuclear safety is discussed in a number of regulatory requirements, standards and guides. The regulatory requirements establish a framework of high-level issues to be met. As an international consensus IAEA, in addition to that, U.S. standards and guides are introduced in this chapter.

#### **2.3.1 IAEA safety guides**

The soil-structure interaction analysis in the guidelines of the International Atomic Energy Agency is mainly addressed in the NS-G-3.6 (IAEA, 2004) and NS-G-1.6 (IAEA, 2003) documents. Additionally, the requirements regarding design basis ground motion including site response analysis, response spectra and time histories, and other relevant articles considering seismic hazard assessment are placed in SSG-9 (IAEA, 2010) specific safety guide.

IAEA Safety Guide NS-G-3.6 (IAEA, 2004) is one of the basic guidelines used in nuclear industry. This nuclear safety guide gives recommendations on input parameters, analysis methods and solutions steps for the soil-structure interaction analysis. This document describes coupling and combination criteria which are

required in order to determine the dynamic response of the structure together with the foundation. The soil-structure system mainly includes the following factors:

1. The structure's dynamic properties in the course of the structural modelling,
2. The foundation impedance,
3. The dynamic response of the coupled soil–structure system.

According to NS-G-3.6 (IAEA, 2004), solution steps for the dynamic soil–structure interaction analysis under earthquake loads involve;

- Site response analysis,
- Foundation scattering analysis,
- Foundation impedance analysis,
- Structural modelling,
- Analysis of the coupled system interaction response.

In addition to these, NS-G-3.6 recommends on the information that should be available in the design considering input parameters, such as  $V_s - V_p$  profiles, number and thickness of soil layers, dynamic characteristics for each layer at small strain, the depth of embedment, geometrical information of foundation and mass, stiffness and damping parameters of the structures. IAEA recommends that nonlinear soil behavior should be considered using equivalent linear material properties for each soil layer.

With respect to analysis methods, IAEA recommends the designer to take into account the uncertainties, the contributions of different types of damping, the effects of soil layering, embedment and strain dependent soil properties.

IAEA Nuclear Safety Guide NS-G-3.6 categorizes the site into three types according to the best estimate small strain shear wave velocity just beneath the foundation level:

- Type 1:  $V_s > 1100$  m/s,
- Type 2:  $1100$  m/s  $> V_s > 300$  m/s,
- Type 3:  $300$  m/s  $> V_s$

IAEA recommends soil–structure interaction analysis to be carried out for Type 2 or Type 3 sites. However, IAEA states that, for Type 1 sites, a fixed base assumption may be used in the aseismic modelling of NPP structures (IAEA, 2004).

Another IAEA document gives guidance about the seismic design and qualifications of nuclear structures, namely NS-G-1.6 (IAEA, 2003). This document also provides information regarding design basis earthquakes that are grouped as SL-1 (seismic level 1) and SL-2 (seismic level 2). According to IAEA, generally, SL-2 corresponds to a level with an exceedance probability of  $10^{-4}$  per reactor per year and SL-1 corresponds to a level with a probability of being exceeded of  $10^{-2}$  (mean value). Within the scope of this document, recommendations are given considering the appropriate modelling of soil-structure system defining the subsurface conditions, material properties, taking into account for radiative effects of seismic waves and justification of input ground motion (IAEA, 2003).

IAEA-SSG-9 (IAEA, 2010) gives recommendation on seismic levels, design basis response spectra and time histories. According to this document, time histories should satisfactorily reflect all ground motion parameters represented in the response spectra with the addition of other parameters such as duration, phase and coherence.

### **2.3.2 U.S. standards and guides**

The first generation NPPs in the U.S. were commissioned during the 1960s. Seismic design requirements were not specific to nuclear industry and undetailed. In 1970s, the seismic design requirements applicable to safety related nuclear structures, systems and components were established in a more detailed way. The experience and lessons learned in this area of expertise were gradually reflected in new standards for NPPs.

U.S. NRC establishes requirements in Appendix S to 10 CFR 50 (U.S. NRC, 2014b) regarding earthquake safety of nuclear power plants. It states that a seismic safety evaluation of safety related structures, systems and components must take into account soil-structure interaction effects under a Safe Shutdown Earthquake (SSE). Safe Shutdown Earthquake level corresponds to SL-2 level earthquake in IAEA terminology.

According to this regulation following safety goals under SSE; reactor coolant integrity, the capability to shutdown the reactor and maintain it in a safe shutdown condition, and prevention or mitigation of the consequences of accidents have to be maintained (U.S. NRC, 2014b).

U.S. NRC Regulatory Guide 1.60 (U.S. NRC, 2014a) specifies generic horizontal and vertical response spectra to be used as the design basis response spectra.

In 2007, U.S. NRC Regulatory Guide 1.208 (U.S. NRC, 2007a) was published. This guide provides a method embracing a performance-based approach, also including probabilistic seismic hazard analysis methods, for the determination of site-specific earthquake ground motion. The performance-based approach adopted in Regulatory Guide 1.208 is based on ASCE 43-05 standard (ASCE, 2005).

U.S. NRC has prepared a set of document, namely NUREG-0800 Standard Review Plan (SRP), to establish criteria for the review of nuclear power plants' construction and operating license applications. These documents are intended to use in evaluating whether an applicant or designer meets the regulations of U.S. NRC. However, the designers also make use of them in order to meet those criteria.

SRP 3.7.1 (U.S. NRC, 2007b) determines criteria regarding the seismic input motion or also known as control motion. The spectrum from the artificial ground motion time history must envelop the free-field design response spectra for all damping values used in the seismic response analysis. According to this document, the frequency intervals at which spectral values are determined are to be sufficiently small when spectral accelerations are calculated from the artificial time history. Table 2.1, which is adapted from SRP 3.7.1, provides a set of frequencies to be employed at the response spectra calculation. An artificial time history was incorporated into the calculations in this thesis. Therefore, those frequency intervals were taken into account for the response spectra calculation.

**Table 2.1:** Suggested frequency intervals for response spectra calculation (U.S. NRC, 2007b)

Frequency Range (hertz)	Increment (hertz)
0.2 - 3.0	0.10
3.0 - 3.6	0.15
3.6 - 5.0	0.20
5.0 - 8.0	0.25
8.0 - 15.0	0.50
15.0 - 18.0	1.0
18.0 - 22.0	2.0
22.0 - highest frequency of interest	3.0

U.S. NRC staff reviews soil-structure analyses more deeply according to Standard Review Plan numbered as 3.7.2 (U.S. NRC, 2007c). SRP 3.7.2 gives specific guidelines for SSI analysis. These guidelines can be summarized as follows:

- The nonlinear soil behavior can be approximated by linear methods. These methods may be with the use of equivalent linear soil material properties determined from iterative linear analysis.
- Strain-dependent soil properties should be consistent with the geotechnical data obtained. Strain-dependent modulus degradation and damping ratio may be determined from laboratory tests, or this information can be obtained from the literature.
- Variability of soil properties should be taken into account, at least, as best estimate (BE), lower bound (LB) and upper bound (UB).
- If direct solution method is used;
  - Each SSI analysis is performed in one step.
  - Finite element or finite difference methods are used to spatially discretize the soil-structure system.
  - Bottom and horizontal boundaries are well-defined.
- If substructuring solution method is used;
  - Free-field motion, assuming the foundation is massless, is determined.
  - The frequency-dependent foundation impedance functions are determined.
  - SSI analysis is performed.

It is obvious that, nuclear facilities demand much stricter requirements on structural analysis methods compared to conventional structures. Thus, American Society of Civil Engineers (ASCE) published a standard for the seismic analysis of safety-related nuclear structures, namely ASCE 4. Published version of 1998 (i.e. ASCE 4-98) is still valid for the nuclear structures (ASCE, 2000).

Section 3.3 of ASCE 4-98 (ASCE, 2000) defines requirements on soil-structure interaction modeling and analysis. This standard allows fixed-base assumption if the



structure rests on rock that corresponds to a shear wave velocity ( $V_s$ ) greater than 1100 m/s. In other cases, SSI effects should be considered.

ASCE 4-98 introduces a variety of provisions on uncertainties of properties, solution methods such as direct method and impedance method (substructuring method), embedment effects, seismic input motion and generation of in-structure response spectra, frequency (suggested frequency intervals are also presented in Table 2.1). All of the SSI analyses requirements within the scope of SRP 3.7.1 and SRP 3.7.2 are established in ASCE 4-98 standard.

In 2016, an updated version of ASCE 4, ASCE 4-16 (ASCE, 2017) was published. In addition to older version ASCE 4-98, this newer version presents methods for probabilistic soil-structure interaction analysis. Section 5.5 of this standard establishes the requirements for the performance of probabilistic SSI with two simulation approaches, namely Monte Carlo simulation and Latin Hypercube simulation. According to ASCE 4-16 (ASCE, 2017) standard, a minimum 200 simulations are required when Monte Carlo methods are used and a minimum of 30 simulation considered when Latin Hypercube simulation is done (ASCE, 2017).



### 3. MODELLING OF SOIL MEDIUM

Doubtlessly, ASCE 4 standard is widely used in terms of seismic analysis, particularly soil-structure interaction analysis and site response analysis in nuclear industry. Within this scope, ASCE 4-98 (ASCE, 2000) establishes the requirements considering uncertainties and variability of soil properties that should be taken into account. According to this standard, the mean values of soil investigation data, hereafter as best estimate (BE), lower bound (LB) and upper bound (UB) soil data considering the uncertainties of soil investigation data should be incorporated into the soil-structure interaction analysis.

The foundation soil layers are defined with related parameters and one-dimensional small-strain shear wave velocity soil profiles (BE (best estimate), UB (upper bound) and LB (lower bound)) that should be used in soil-structure interaction analyses as per ASCE 4-98 (ASCE, 2000). Since the studied hypothetical site show heterogeneous features, additional 7 one-dimensional soil profiles to investigate the site heterogeneity are also incorporated into calculations. The strain compatible soil profiles (degraded shear modulus and damping profiles) to be used in soil-structure interaction analysis are computed in one-dimensional equivalent linear site response analysis.

For the reason that the studied site has deeply inclined soil layering, the site is modelled with the help of seven different 1D soil profiles. In order to investigate the variation of soil layering, average shear wave velocity depth profiles are obtained for seven cross sections: Cross-section A-A (BH01 and BH02), cross-section B-B (BH03 and BH04), cross-section C-C (BH05 and BH06), cross-section D-D (BH07 and BH08), cross-section E-E (BH09 and BH10), cross-section F-F (BH11 and BH12) and cross-section G-G (BH13 and BH14). The locations of cross-sections with the 80-m-width-foundation footprint are shown in the site layout map in Figure 3.1.

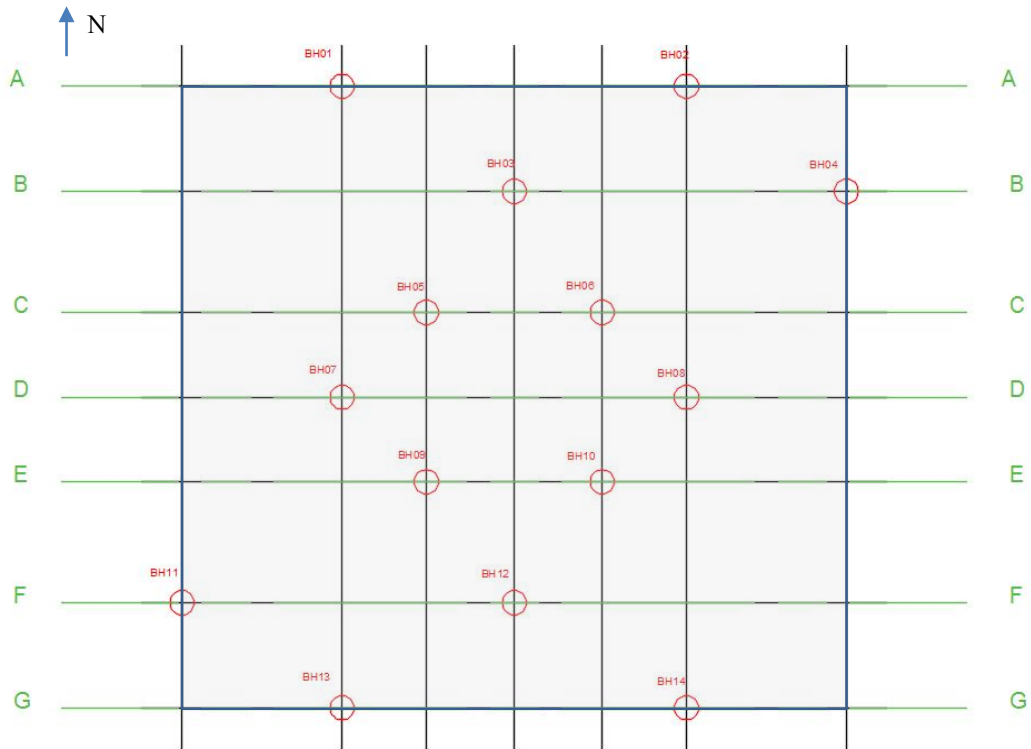


**Figure 3.1:** Borehole layout

According to the borehole data, the site has layering as shown schematically in Figure 3.3. Regarding average shear wave velocity variations with depth, the  $V_s$  profiles on the most south and the most north sections of the site significantly differ from the  $V_s$  profiles on the middle sections. This deviation is contributed to the deep slope layering of the rock over each other in north-south direction. This layering scheme repeats itself on the east-west direction as shown in Figure 3.2.

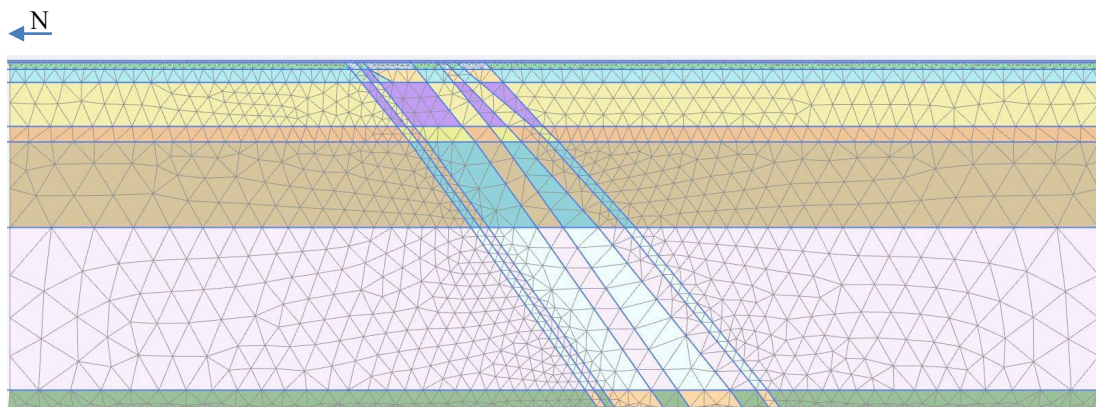


**Figure 3.2:** Schematic representation of the studied site with inclined layers

The borehole data shows that the site has 2 types of rock at the site (rock 1 (R1) and rock 2 (R2)), rock1 (R1) being less rigid, with three degrees of weathering along with the depth. Weathering degrees of rock, such as high, medium and low weathered rock, respectively indicated as RA, RB and RC in Figure 3.3.

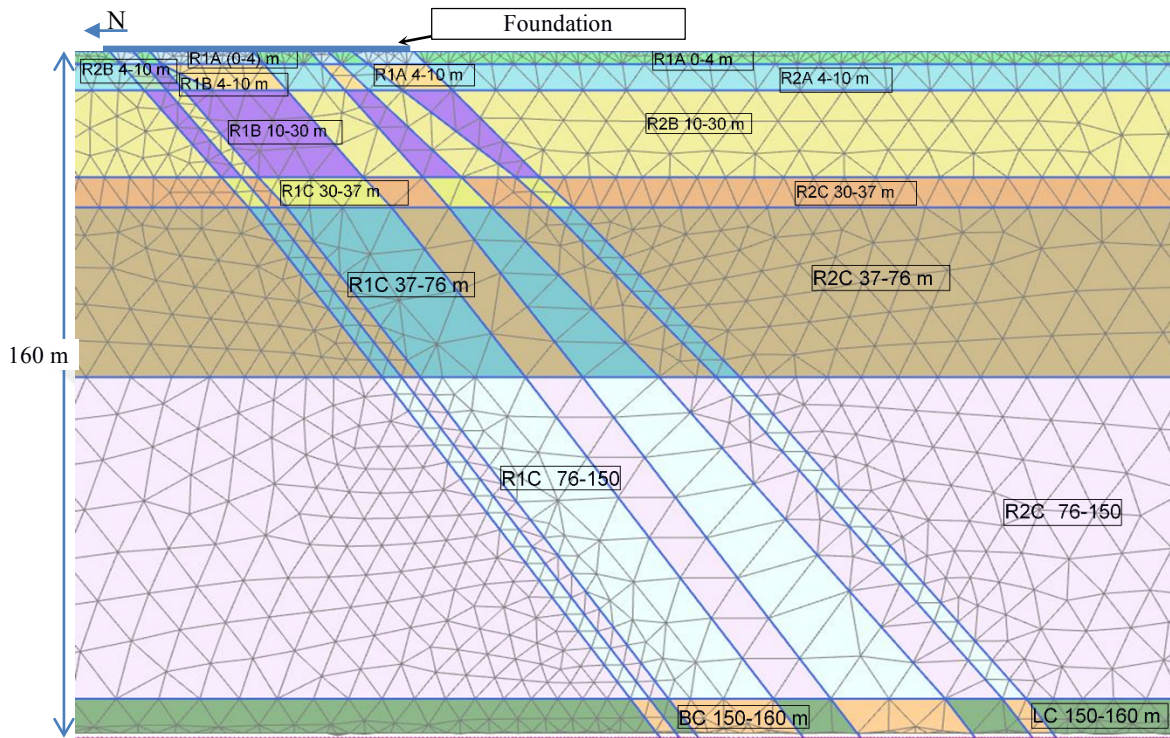


**Figure 3.3:** Schematic representation of the soil under the foundation

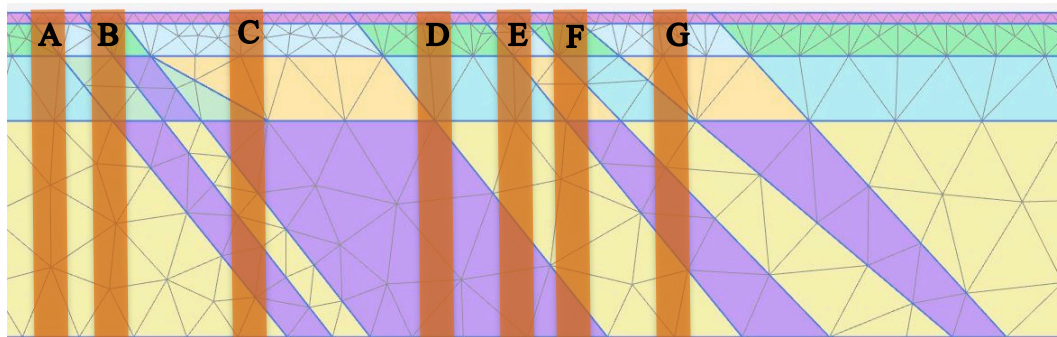
The soil medium is represented by a rigid half-space and the interaction surface is flexible, however the soil-structure system is fully bonded at the interface. The interaction surface is modelled as surface mount, which also match with the geometry of the finite element model of the structure. Thereby, the coupling of the soil-structure system is achieved using the strain compatibility at the interaction nodes.

Properties of undersurface foundation material is shown in Table 3.1. Each of the two types of rock (R1 and R2) are subclassified as A, B and C in relation with their material properties. In the first column of the table including rock types, the values indicated in parentheses define the depth range of those sections. In this table,  $\rho$  refers to density,  $c$  defines the cohesion,  $\phi$  is the internal friction angle,  $E_{50}$  refers to secant stiffness in drained triaxial test and  $E_{ur}$  is unloading/reloading stiffness from drained triaxial test.

**Table 3.1:** Properties of undersurface foundation material

Rock Type	$\rho$ (g/cm <sup>3</sup> )	c (kPa)	$\phi$	$E_{50}$ (MPa)	$E_{ur}$ (MPa)
R1-A (0-4 m)	2.47	287	24	60	180
R1-A (4-10 m)	2.47	287	24	60	180
R1-B (4-10 m)	2.68	703	26	170	510
R1-B (10-30 m)	2.68	703	26	170	510
R1-C (30-37 m)	2.81	1011	28	370	1110
R1-C (37-76 m)	2.81	1011	28	370	1110
R1-C (76-150 m)	2.81	1011	28	370	1110
R1-C (150-160 m)	2.81	1011	28	370	1110
R2-A (0-4 m)	2.68	589	24	93	279
R2-A (4-10 m)	2.68	589	24	93	279
R2-B (4-10 m)	2.74	1031	26	165	495
R2-B (10-30 m)	2.74	1031	26	165	495
R2-C (30-37 m)	2.83	1337	28	730	2190
R2-C (37-76 m)	2.83	1337	28	730	2190
R2-C (76-150 m)	2.83	1337	28	730	2190
R2-C (150-160 m)	2.83	1337	28	730	2190

One-dimensional (1D) equivalent linear site response analyses are performed in 7 one-dimensional soil columns representing the 2D heterogeneity of the foundation soil and BE, UB and LB using 1994 Northridge Earthquake horizontal time history scaled according to PSHA (Probabilistic Seismic Hazard Analysis) done for the site. Those 7 one-dimensional soil columns are indicated in Figure 3.4. During this study, DEEPSOIL software is used to determine the response spectra on the foundation level and the top of rock (Hashash et al., 2016).

**Figure 3.4:** Locations of the 7 1D soil columns

As input for soil-structure interaction analysis of the building, the strain-compatible shear modulus-depth and damping ratio-depth profiles of the foundation soil are computed from each ten one-dimensional equivalent linear site response analyses.

### **3.1 Soil Parameters and Their Variations**

The hypothetically chosen site, in general, is composed of soft rock and stiff rock with low damping characteristics.

According to ASCE 4-98 (ASCE, 2017), small-strain shear modulus ( $G_{max}$ ) best estimate (BE), upper bound (UB) and lower bound (LB) soil profiles with depth are determined statistically starting from the bottom level of the foundation. BE profile is determined as the mean of all the maximum shear moduli determined at the relevant depths. For determination of UB and LB profiles, the coefficient of variation  $C_v$  is computed for all depths. The coefficient of variation  $C_v$  is greater than 0.5 for the first 10 m of the foundation soil evidencing higher heterogeneity in the corresponding soil layers. Additionally, 7 one-dimensional soil profiles are used in the site response analyses to investigate the site heterogeneity.

The shear wave velocities are obtained and plotted starting from the foundation mat bottom elevation, which corresponds the bottom level of the unit foundation.

The shear wave velocity and the compressional wave velocity data for 7 soil profiles and BE, LB and UB profiles plotted with depth as shown in Figure 3.5 and Figure 3.6.

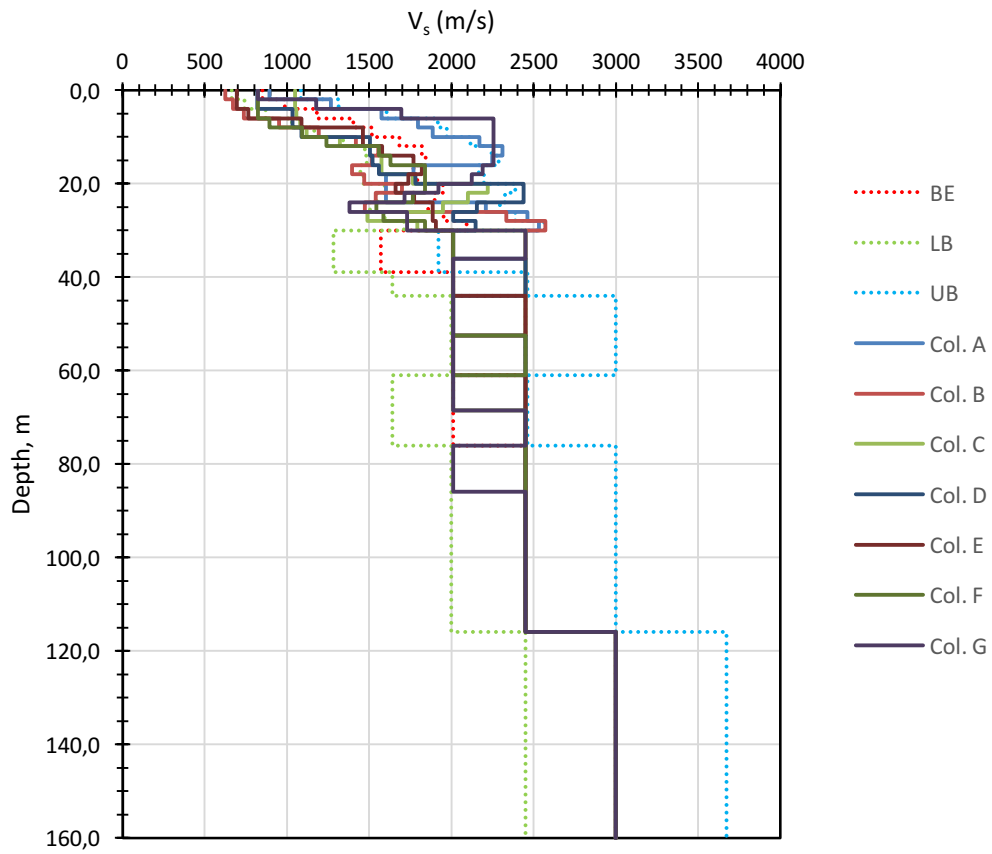


**Figure 3.5:**  $V_s$  values of the soil profiles



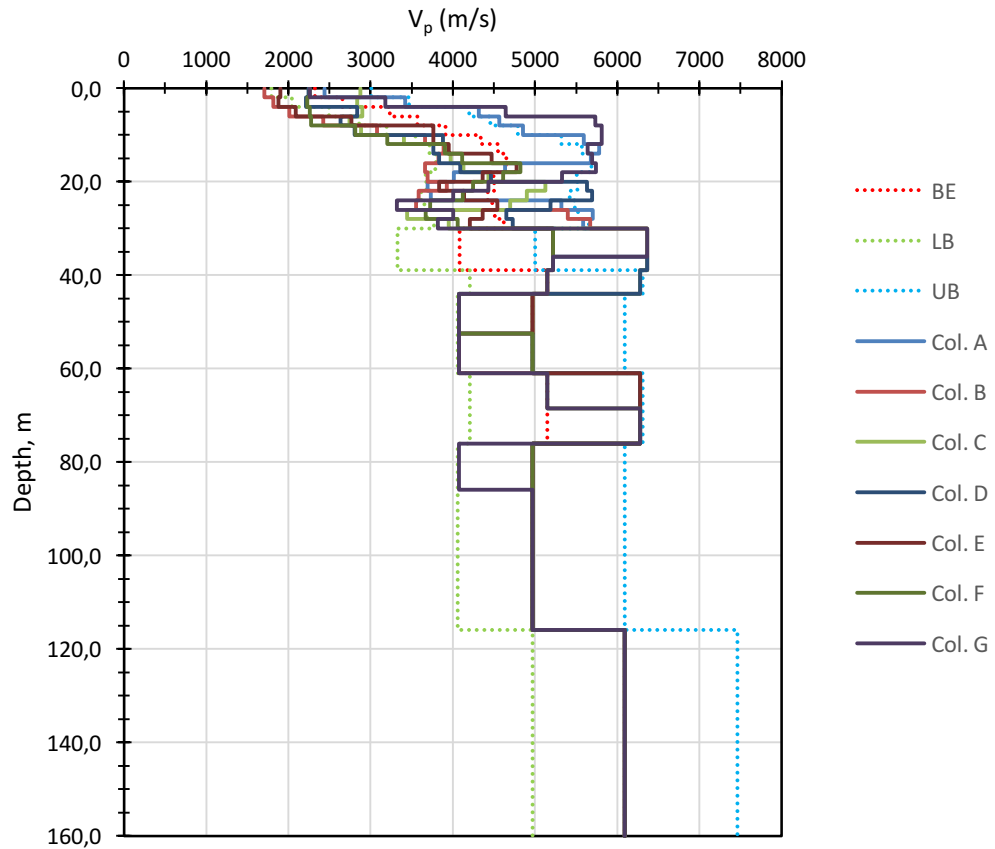


**Figure 3.6:**  $V_p$  values of the soil profiles

The small-strain shear moduli of the each soil layer are determined from the shear wave velocities and the mean mass density value of soil layers as described in equation (3.1).

$$G = \rho \cdot V_s^2 \quad (3.1)$$

In this equation,  $G$  refers to the small-strain shear modulus,  $V_s$  is shear wave velocity and  $\rho$  denotes the mass density of a soil layer.

The mean ( $\mu$ ) and the standard deviation ( $\sigma$ ) of the shear moduli data are obtained in terms of depth. Coefficients of variation with depth are determined as described in equation (3.2) and plotted as in Figure 3.7.

$$C_v = \mu/\sigma \quad (3.2)$$

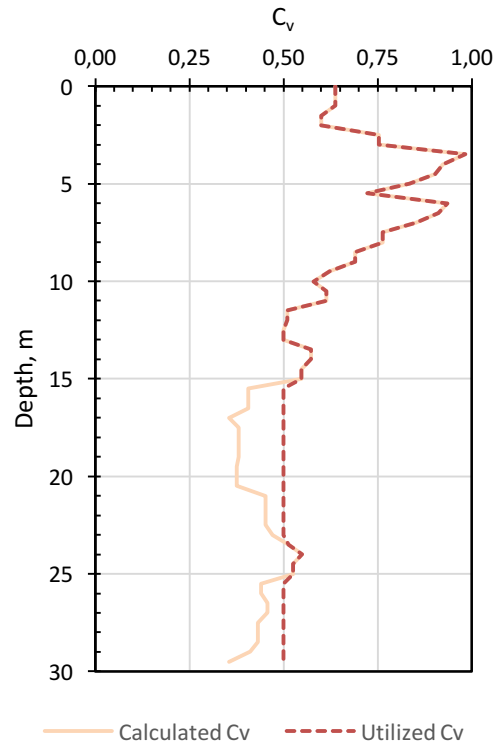


**Figure 3.7:**  $C_v$  values change in depth

According to ASCE 4-98 standard,  $C_v$  values should be at least 0.5. In lieu of this requirement, all the values below 0.5 are taken into account as 0.5 for the calculation of upper bound (UB) and lower bound (LB) soil profiles' parameters from best estimate (BE) values.

The importance of the analysis depth in site response analysis when input motion is applied at the bedrock is not discussed. For soil-structure interaction analysis, the soil profiles are determined for down to 160 m, which corresponds to the depth of influence, which is the width of the foundation multiplied by two.

### 3.2 Strain Dependent Modulus Degradation and Damping Curves

In order to predict the changes of the soil properties under dynamic loads corresponding to the loads caused by earthquakes, it is necessary to have a set of curves of dependences of the dynamic shear modulus and damping ratio (internal damping of each soil layer) on the shear strains, which for each type of soil describe the apparent decrease of dynamic shear modulus and increase of damping ratio depending on the shear strain.

The soil sections that are related to the nuclear facility's foundation soil are provided without any field and laboratory data. Since then, backbone curves as referred in EPRI 1993 publication are utilized in the site response analysis (EPRI, 1993).

The strain-dependent modulus degradation and damping curves are presented in Figure 3.8 and Figure 3.9.

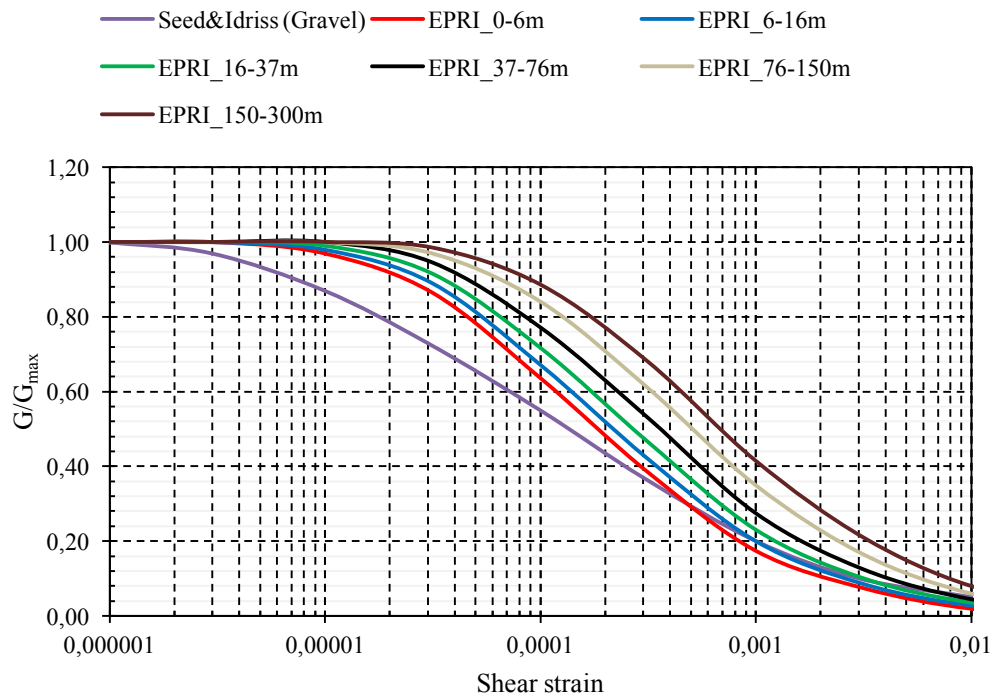


**Figure 3.8:** Shear modulus degradation with shear strain

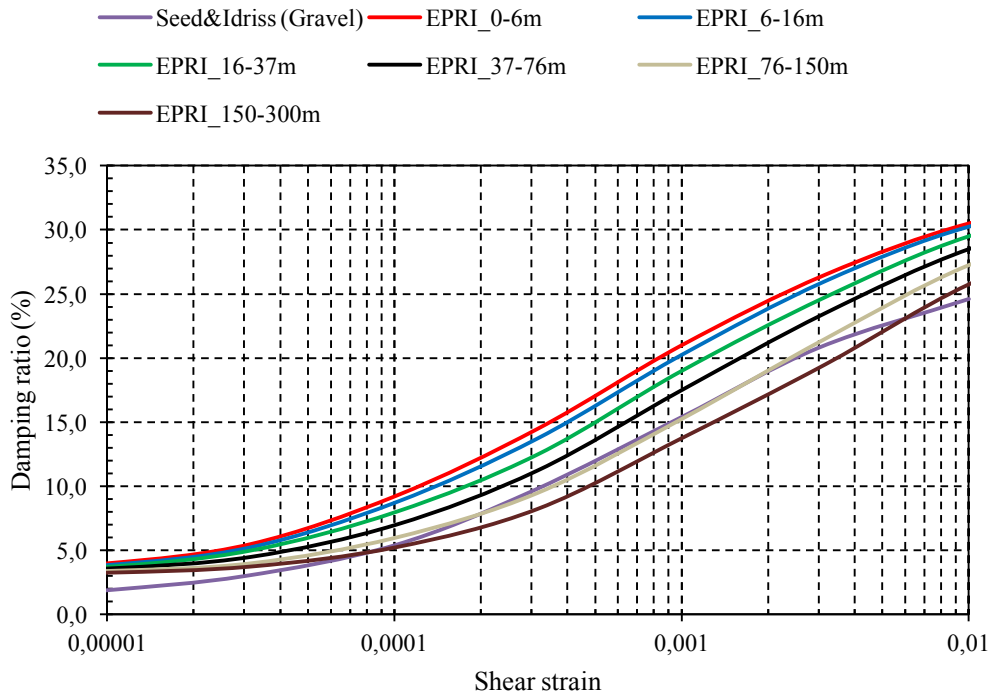


**Figure 3.9:** Damping variation with shear strain

As seen on Figure 3.8,  $G_{\max}$  values of each reference curve are degraded with the increase of shear strain and the shear modulus ratios  $G/G_{\max}$  become less than 1.0. It is also seen on Figure 3.9 that damping ratios of each reference curve increase proportionally with the shear strain. Besides, it can be inferred that the dynamic behavior of the existing soil media becomes more linear as the depth increases.

#### **4. SITE RESPONSE ANALYSIS PROCEDURE AND SEISMIC INPUT MOTION**

For the purpose of this study, in total ten 1D equivalent linear site response analyses are performed using 1994 Northridge Earthquake horizontal time history. In addition to seven soil profiles, BE, UB and LB profiles with the coefficient of variation ( $C_v$ ) values are taken into account for the site response analyses. Each site is 160 m deep and is underlain by a rigid boundary.

Unit weights ranging from  $26.0 \text{ kN/m}^3$  to  $27.8 \text{ kN/m}^3$  are assigned for soft and stiff rock, respectively. Considering the all hypothetical sites,  $V_s$  values are in the range of 620 m/s and 3000 m/s.

Firstly, deconvolution analyses are carried out to obtain the acceleration time histories at the base rock at 160 m depth since 10 earthquake records for the studied soil profile are surface record. However, for the reason that the responses resulting from these records are very similar, only Northridge Earthquake record is used for the evaluation of site heterogeneity. Afterwards, site response analyses are performed assuming that all soil strata are horizontal and the earthquake waves are propagated vertically. Besides, it is assumed that the foundation is massless, and vertically propagating shear waves produce only horizontal translations and compressional waves produce only vertical motions in the free-field conditions.

During this study, DEEPSOIL v6.1 software is used to determine the response spectra on the foundation level and on the top of rock (Hashash et al., 2016). As input for soil-structure interaction analysis of the building, the strain-compatible shear modulus depth and damping ratio depth profiles of the foundation soil are computed from each ten one-dimensional equivalent linear site response analyses.

#### 4.1 Seismic Hazards and Input Time Histories

IAEA Specific Safety Guide SSG-9 (IAEA, 2010) is widely used in order to establish the design basis ground motions for the nuclear installations. In lieu of this, input time histories should sufficiently reflect the design response spectra and other spectral representation with the addition of other parameters such as duration and time step. Additionally, this document provides the following guidance towards their development in terms of selection and scaling time histories, and also provides techniques to match ground motions and design response spectra taking into account the phase characteristics.

The ground motion time history is developed for the random horizontal components of the target design response spectra using the ASCE 7-10 requirements (ASCE, 2013), which are in conformity with the nuclear regulations referred above.

The importance of the ground motion selection and spectrum compatible ground motion generation methodologies has been comprehensively studied by the PEER Ground Motion Selection and Modification Working Group (Vegge et al., 2001). The basic criterion is that the spectrum of the time series provides a good match to the user's target spectrum over the spectral period range of interest. This approach produces scaled recordings that provide the best match to the spectral shape of the target spectrum over the user-specified period range of interest, but whose spectra will oscillate about the target.

Based on probabilistic seismic hazard analyses of the hypothetical site, the earthquake record is surface record for this soil profile with average shear wave velocity ( $V_{s30}=1100$  m/s). Deconvolution analyses of the 10 earthquake records are performed in DEEPSOIL software to obtain the acceleration time histories at the base rock at approximately 160 m, which is a recommended depth of influence for a foundation width of around 80 m.  $G/G_{max}$  and damping curves shown in Figure 3.8 and Figure 3.9 are used in deconvolution analyses. Deconvolution procedure is basically schematized in Figure 4.1.

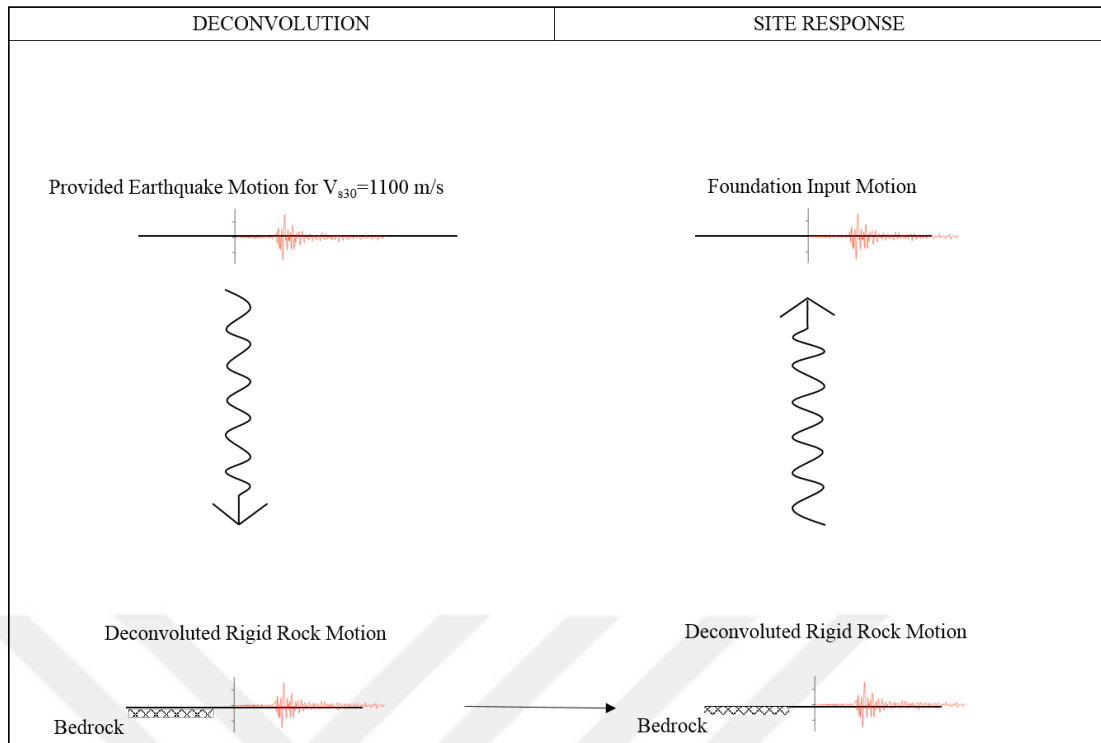


**Figure 4.1:** Deconvolution procedure

Deconvolution analyses are performed for 10 acceleration records (for 5 input motions with two lateral components). These records are namely “koca\_090”, “koca\_180”, “lomap\_000”, “lomap\_090”, “lomaplo\_000”, “lomaplo\_090”, “northr06\_000”, “northr06\_270”, “sfern\_111” and “sfern\_201”. According to the deconvolution analysis in BE profile, peak ground accelerations (PGA) are reduced down to 0.13 - 0.20 g on top of rock from about 0.39 g at the surface. The predominant period of all the input records are around 0.15 sec, whereas the first and second predominant periods are around 0.15 sec and 0.4 - 0.5 sec for the top of rock records. The response spectra of all the input and the deconvoluted acceleration records obtained for BE small-strain  $V_s$  profile are presented in Figure 4.2.

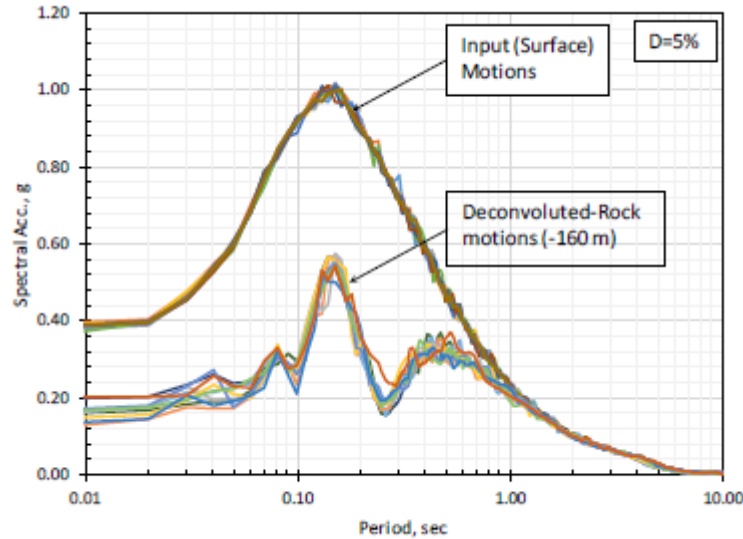


**Figure 4.2:** The response spectra obtained in deconvolution analyses for BE small-strain Vs profile

The highest PSA values at the first predominant period and the second predominant period are 0.52 - 0.57g and 0.32 - 0.36 g, respectively. PGA and PSA values of surface and rock motions obtained from deconvolution analyses of BE soil profile for ten earthquakes are indicated in Table 4.1.

**Table 4.1:** PGA and PSA values of surface and rock motions obtained from deconvolution analyses of BE soil profile for five earthquakes

Earthquake	Surface Motion		Rock Motion (deconvoluted)	
	PGA (g)	PSA(g)	PGA (g)	PSA(g)
koca_090	0.39	1.01	0.20	0.57
koca_180	0.37	1.00	0.16	0.54
lomap_000	0.39	1.00	0.16	0.57
lomap_090	0.39	1.01	0.13	0.57
lomaplo_000	0.38	1.02	0.16	0.57
lomaplo_090	0.39	1.01	0.15	0.57
northr06_000	0.39	1.00	0.17	0.55
northr06_270	0.39	1.01	0.17	0.54
sfern_111	0.38	1.01	0.13	0.52
sfern_201	0.39	1.00	0.20	0.54

Deconvolution analyses are then performed in LB small-strain Vs profile using all the input motions. The PGA values are reduced down to 0.14 - 0.22 g from about 0.39 g.



The response spectra of all the input and the deconvoluted acceleration records obtained for LB small-strain Vs profile are presented in Figure 4.3.

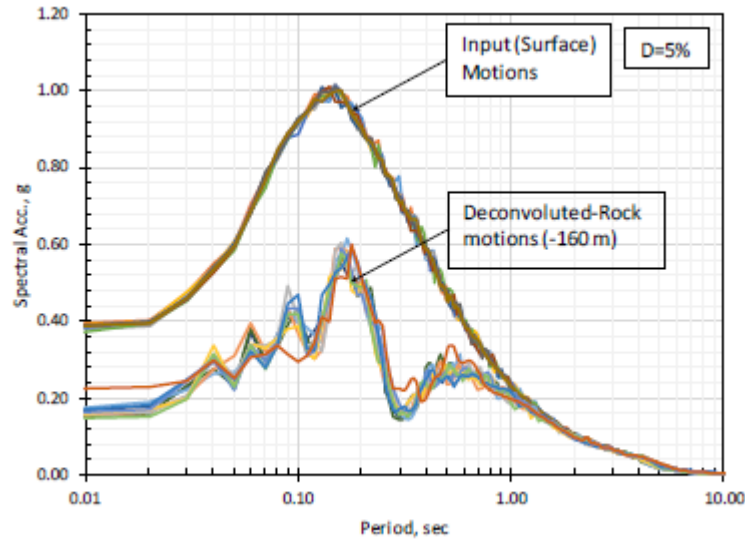


**Figure 4.3:** The response spectra obtained in deconvolution analyses for LB small-strain Vs profile

Although several spectral peak values are observed in top of rock motions, the highest PSA values (0.58 - 0.60 g) are observed at around 0.16 - 0.18 sec. The second peak after the highest PSA that is also observed in BE profile analysis is also observed at around 0.5 - 0.6 sec period with much lower spectral values (0.3 - 0.33g). PGA and PSA values of surface and rock motions obtained from deconvolution analyses of LB soil profile for five earthquakes are indicated in Table 4.2.

**Table 4.2:** PGA and PSA values of surface and rock motions obtained from deconvolution analyses of LB soil profile for five earthquakes

Earthquake	Surface Motion		Rock Motion (deconvoluted)	
	PGA (g)	PSA(g)	PGA (g)	PSA(g)
koca_090	0.39	1.01	0.16	0.55
koca_180	0.37	1.00	0.15	0.56
lomap_000	0.39	1.00	0.17	0.61
lomap_090	0.39	1.01	0.16	0.59
lomaplo_000	0.38	1.02	0.16	0.60
lomaplo_090	0.39	1.01	0.16	0.58
northr06_000	0.39	1.00	0.16	0.59
northr06_270	0.39	1.01	0.14	0.57
sfern_111	0.38	1.01	0.17	0.59
sfern_201	0.39	1.00	0.22	0.60

Lastly, deconvolution analyses are performed in UB profile. The PGA values are reduced down to 0.13 - 0.22 g on top of the rock from about 0.39 g at the surface. The response spectra of all the input and the deconvoluted acceleration records obtained for UB small-strain Vs profile are presented in Figure 4.4.

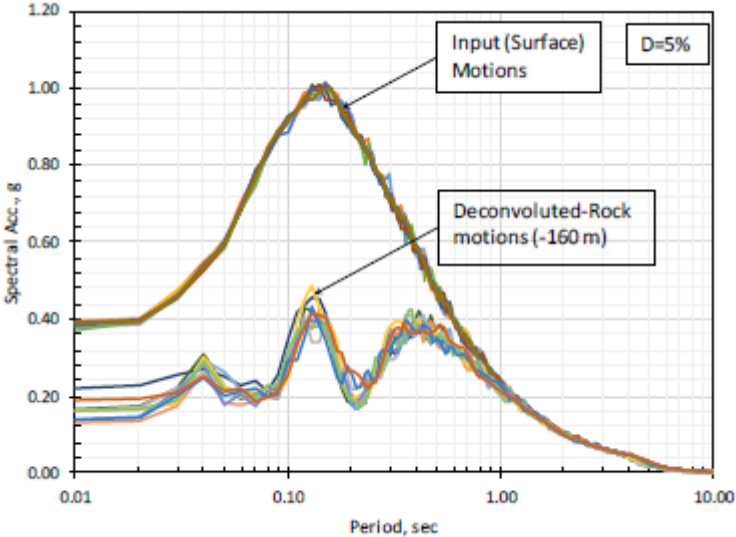


**Figure 4.4:** The response spectra obtained in deconvolution analyses for UB small-strain Vs profile

The PSA values (peak spectral acceleration) are observed at 0.13 sec and 0.4 sec with 0.39 - 0.45 g and 0.4 g, respectively. PGA and PSA values of surface and rock motions obtained from deconvolution analyses of UB soil profile for five earthquakes are indicated in Table 4.3.

**Table 4.3:** PGA and PSA values of surface and rock motions obtained from deconvolution analyses of LB soil profile for five earthquakes

Earthquake	Surface Motion		Rock Motion (deconvoluted)	
	PGA (g)	PSA(g)	PGA (g)	PSA(g)
koca_090	0.39	1.01	0.22	0.45
koca_180	0.37	1.00	0.16	0.43
lomap_000	0.39	1.00	0.16	0.41
lomap_090	0.39	1.01	0.13	0.42
lomaplo_000	0.38	1.02	0.16	0.41
lomaplo_090	0.39	1.01	0.16	0.49
northr06_000	0.39	1.00	0.14	0.39
northr06_270	0.39	1.01	0.16	0.42
sfern_111	0.38	1.01	0.14	0.43
sfern_201	0.39	1.00	0.19	0.41

According to the related design codes, at least five earthquake records should be considered in the structural dynamic design. However, the results of deconvolution analyses for BE, LB and UB soil profiles show that responses taking into account the five different earthquake records are very similar. Therefore, in order to reduce the computational complexity, only Northridge Earthquake record (north06\_000) is chosen for the evaluation of site heterogeneity.

The chosen earthquake record, based on seismicity of the site for the target response spectra depicted in Figure 4.5, is obtained from PEER database and by using ACS SASSI.

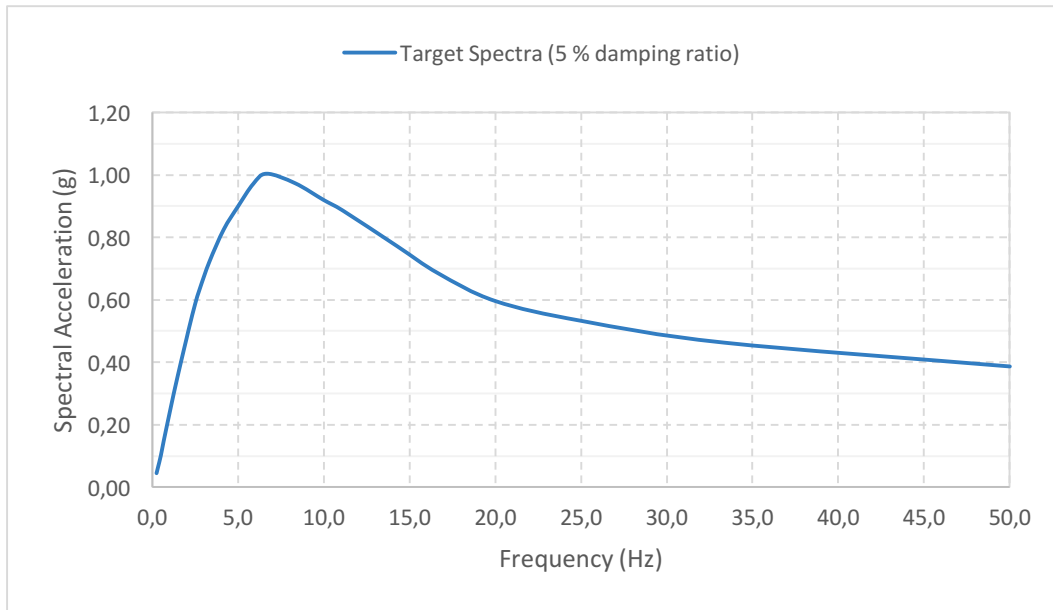


**Figure 4.5:** Target spectra

Spectra as above are developed in line with procedures stated in the guideline document NUREG/CR-6728, Section 4.9. (McGuire Silva et al., 2001) and U.S. NRC Regulatory Guide 1.60 (U.S. NRC, 2014a). In order to generate ground motion time histories data based on the acceptance in ASCE 43-05 (ASCE, 2005), spectral matching method are applied using ACS-SASSI software and PEER database. Input ground motion time history on the bottom rigid boundary is shown in Figure 4.6.

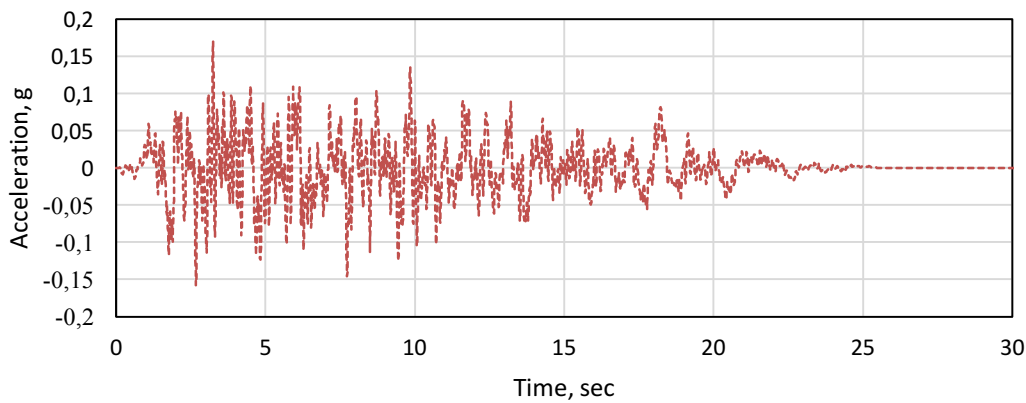


**Figure 4.6:** Deconvoluted input ground motion time history

Information regarding the seismic event of the input ground motion used in the spectral matching application is presented in Table 4.4.

**Table 4.4:** The chosen input ground motion

Earthquake Name	Year	Station Name	Magnitude ( $M_w$ )	Mechanism
Northridge	1994	Los Angeles Griffith Park Observatory	6.69	Reverse

Magnitude of 1994 Northridge Earthquake is 6.69. However, PSHA (Probabilistic Seismic Hazard Analysis) studies of the hypothetical site has resulted with the magnitude  $M_w=7.2$ . Original horizontal time history of Northridge Earthquake is scaled to this magnitude.

#### **4.2 Site Response Analyses for Different Soil Profiles**

Within the context of this study, DEEPSOIL v6.1 software is used for determining the free-field surface motions spectra (Hashash et al., 2016). The software, developed by Professor Youssef M. A. Hashash at the University of Illinois, facilitates carrying out 1D equivalent linear and nonlinear site response analysis in frequency domain and time domain. Because one-dimensional analysis in the engineering applications is much preferred, the software is well accepted in academic and engineering research interests. It is also preferable owing to the user interface is simplified with respect to the user's convenience.

Furthermore, the software provides the opportunity to analyze the frequency domain and time domain in the user interface. In both cases, backbone curves which are determined with the experimental studies carried out by Darendeli 2001, Seed & Idriss 1991, Meng 2007, Roblee & Chiu 2004, Andrus 2003, Amir – Faryar et al. 2016 and Vucetic & Dobry 1991 for the cohesive and cohesionless soils, and also user-defined reference curves could be incorporated whilst defining the material properties as shown in Figure 4.7.

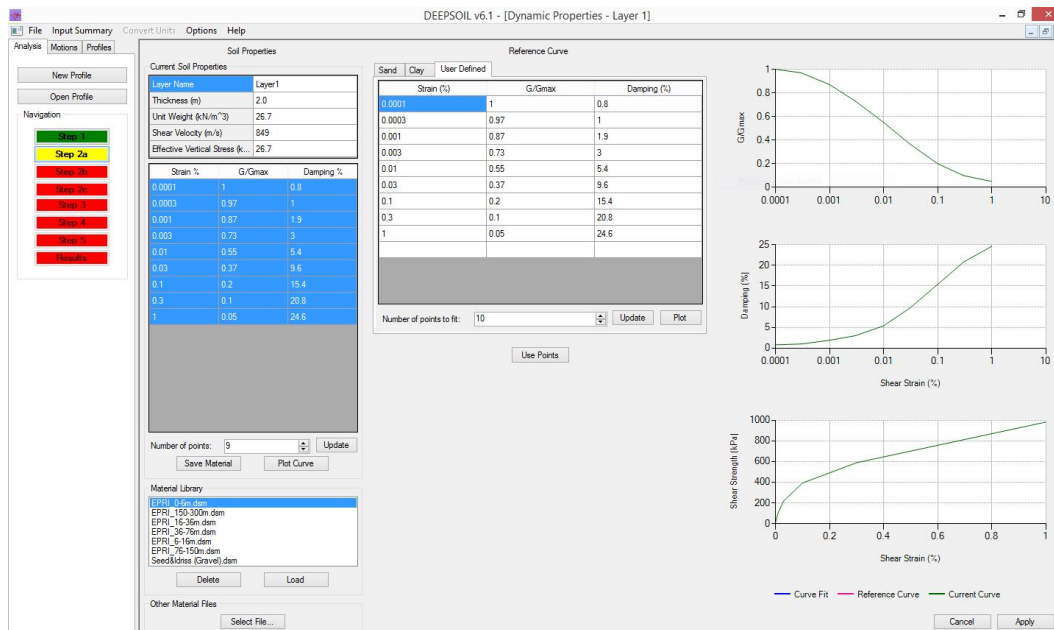


**Figure 4.7:** Material properties interface of DEEPSOIL software

Typically, a maximum frequency of 15 Hz is used for the site response analysis of conventional structures. However, a higher frequency is recommended for nuclear installation structures. For the reason of this necessity, for all soil layers' maximum frequency should generally be a minimum of 30 Hz. Hence, the soil layer thicknesses are chosen in the range of between 2 m and 10 m. In conjunction with this, thirty-two soil layers are introduced for 160 m depth in the site response analyses.

The soil layers under the nuclear installation's foundation mat are defined with related parameters such as dynamic shear modulus ( $G$ ) and one-dimensional small-strain shear wave velocities ( $V_s$ ). Idealized soil profiles for the ten different soil columns (BE, LB and UB and 7 one-dimensional columns representing the 2D heterogeneity) that are considered in site response analysis performed using DEEPSOIL software, are presented in Figure 4.8 – 4.17.

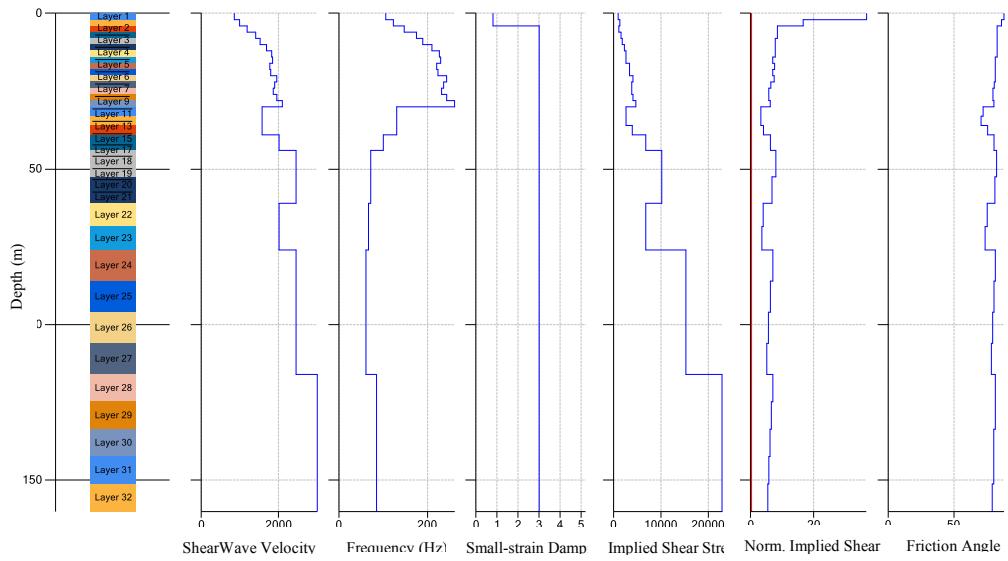


**Figure 4.8: Best-estimate (BE) soil profile and its soil properties**

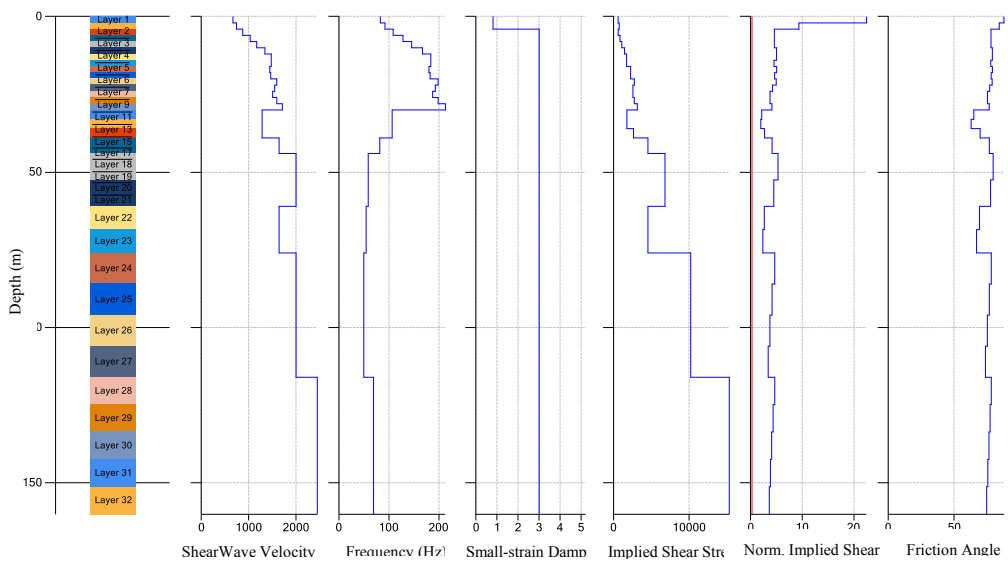


**Figure 4.9: Lower-bound (LB) soil profile and its soil properties**

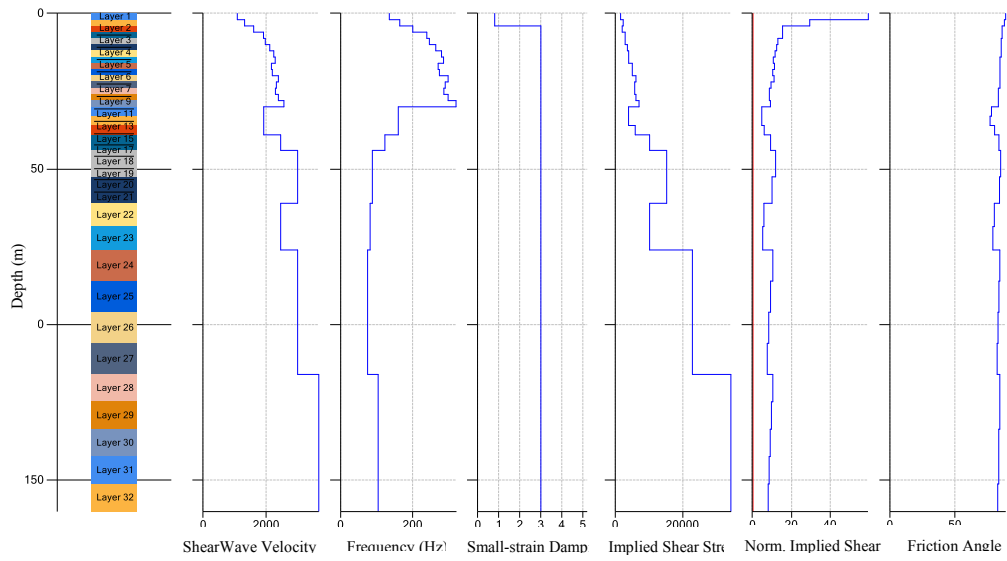


**Figure 4.10: Upper-bound (UB) soil profile and its soil properties**

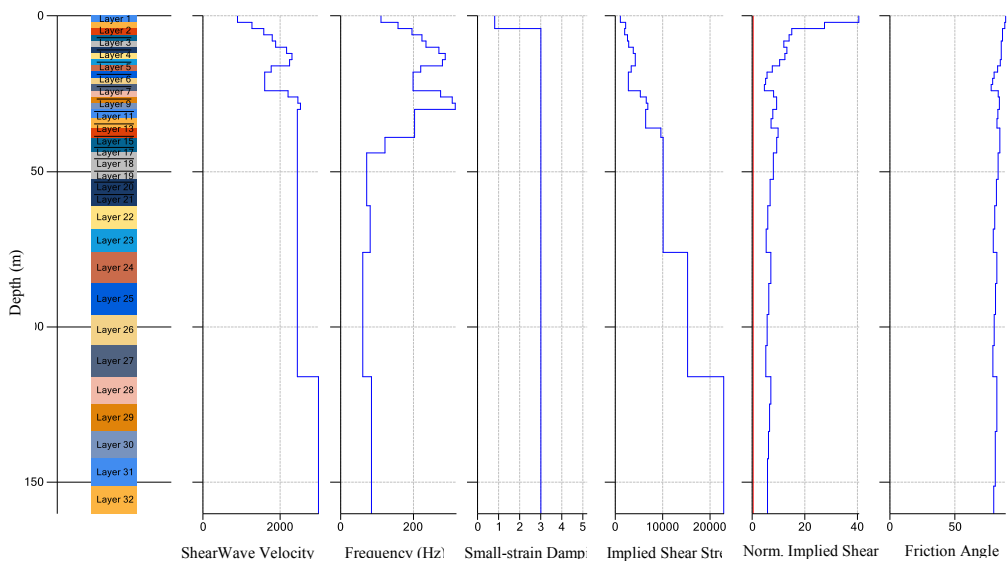


**Figure 4.11: Column A soil profile and its soil properties**



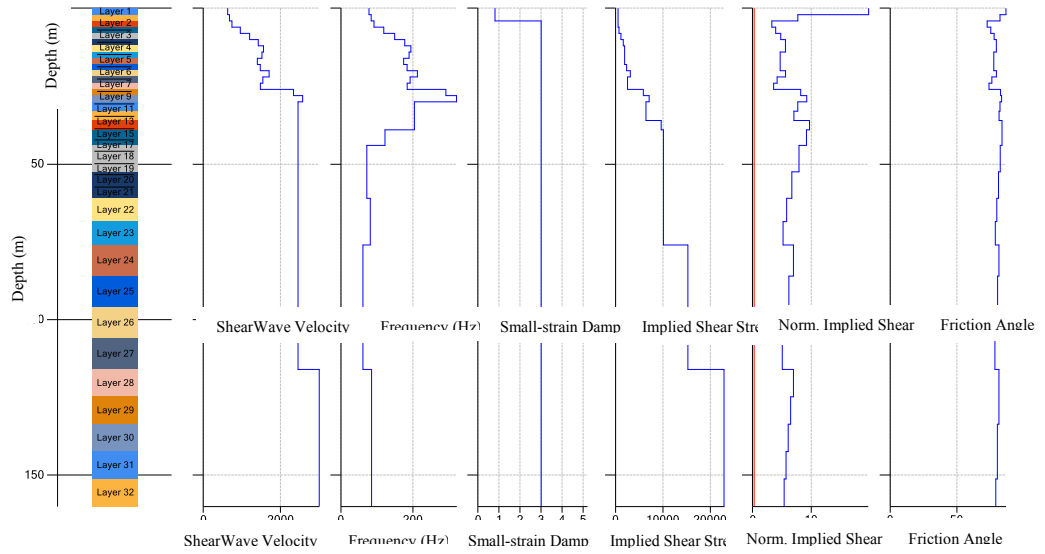


**Figure 4.12: Column B soil profile and its soil properties**

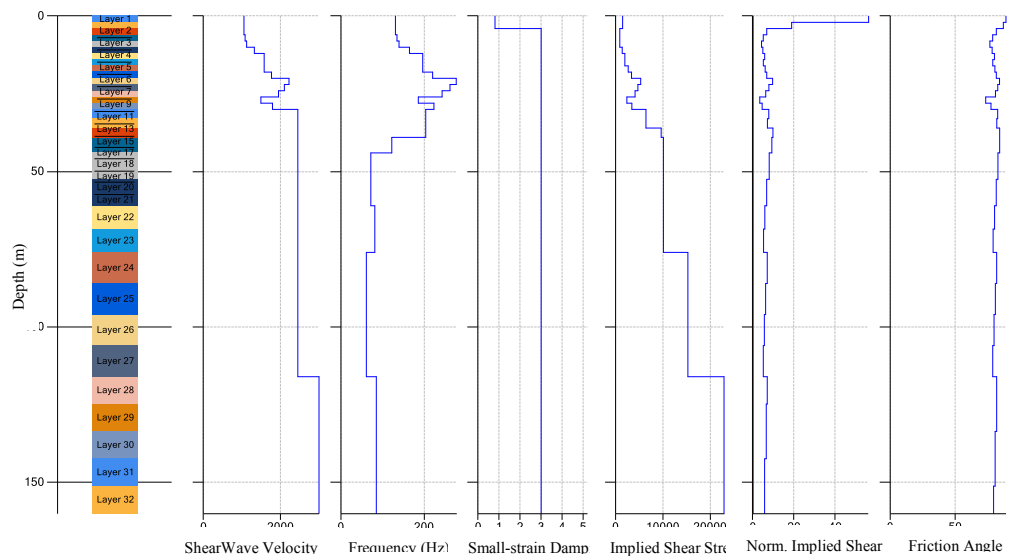


**Figure 4.13: Column C soil profile and its soil properties**

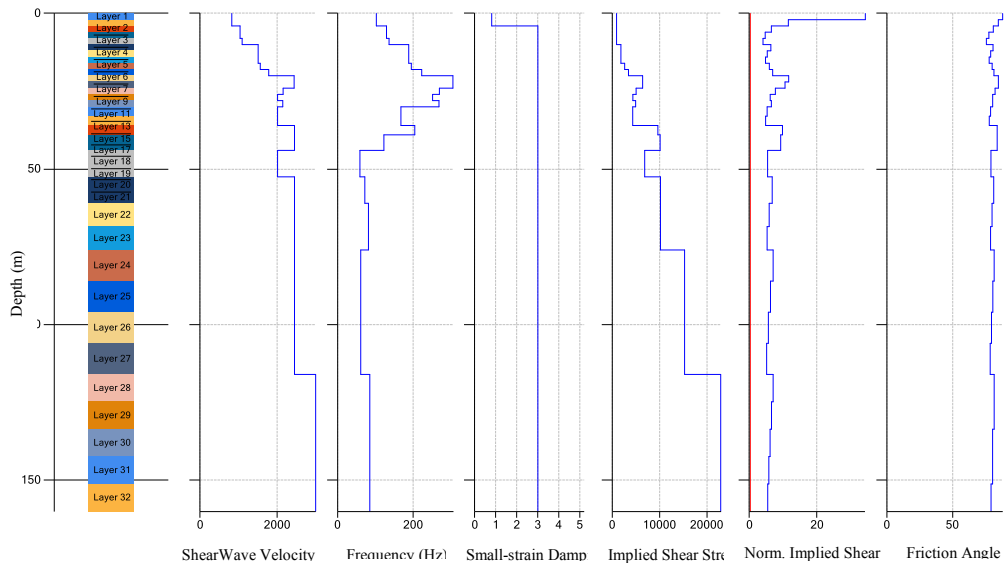


**Figure 4.14: Column D soil profile and its soil properties**

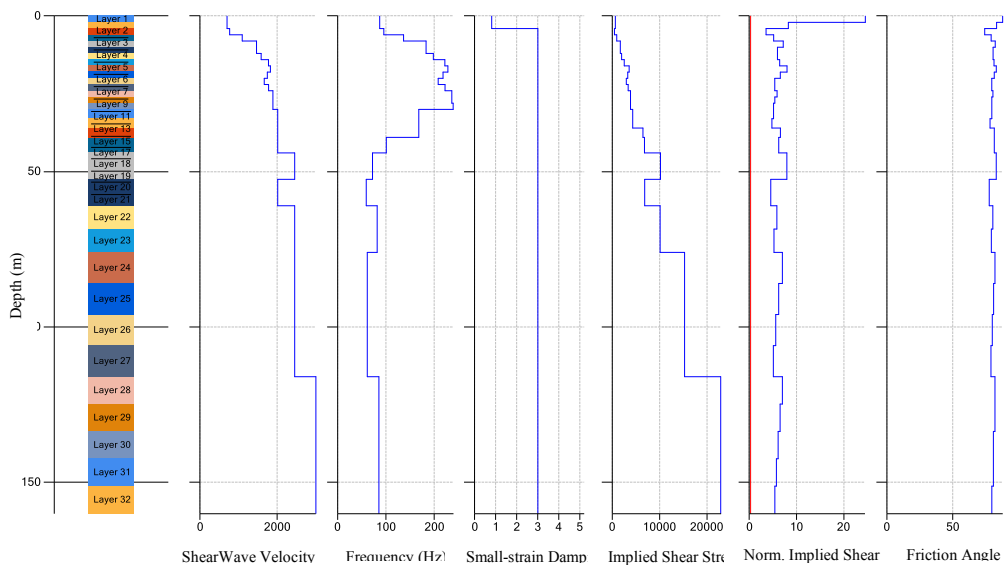


**Figure 4.15: Column E soil profile and its soil properties**

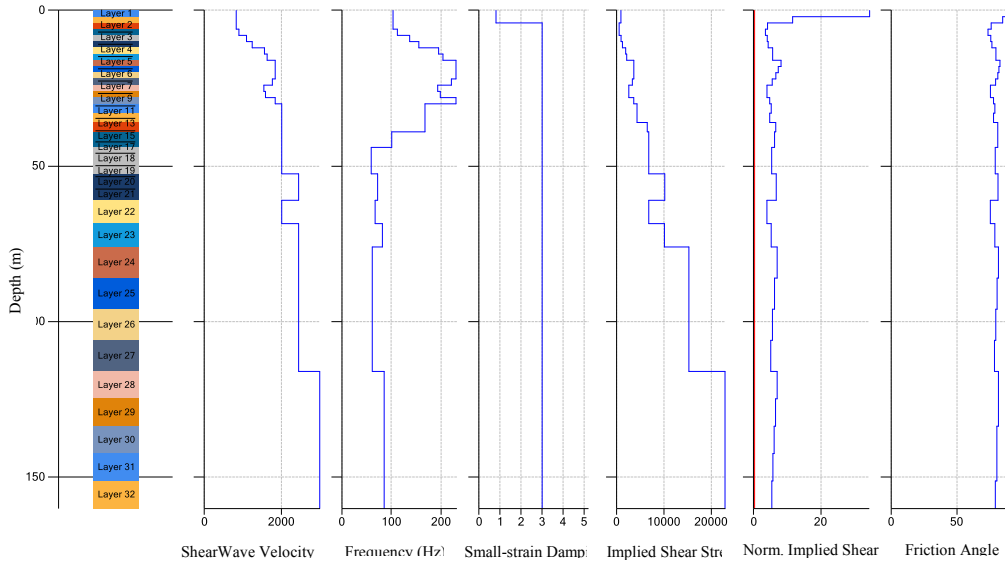


**Figure 4.16:** Column F soil profile and its soil properties

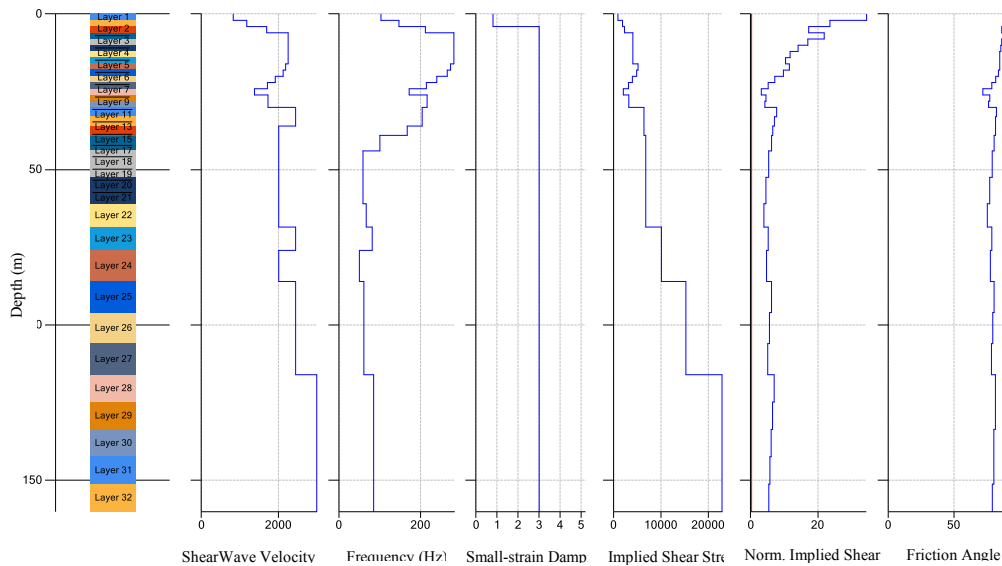


**Figure 4.17:** Column G soil profile and its soil properties

The fundamental periods for BE, LB and UB small-strain  $V_s$  profiles are determined as, respectively, 0.29 s, 0.36 s and 0.24 s, and also 0.27 s, 0.30 s, 0.28 s, 0.29 s, 0.30 s, 0.30 s and 0.28 s for the 7 different one-dimensional soil columns. The earthquake input motion is applied at the bottom of the soil profiles using rigid bedrock option for the bedrock. The fundamental periods for the 7 one-dimensional soil columns are quite close and bounded by the fundamental periods of the BE, UB and LB profiles.

Effective shear strain ratio is entered as 0.62 for the analyses, since the earthquake magnitude for the site is determined as  $M_w=7.2$ . 15 iterations and frequency

independent complex shear modulus formulation are used in the analyses as described in equation (3.3).

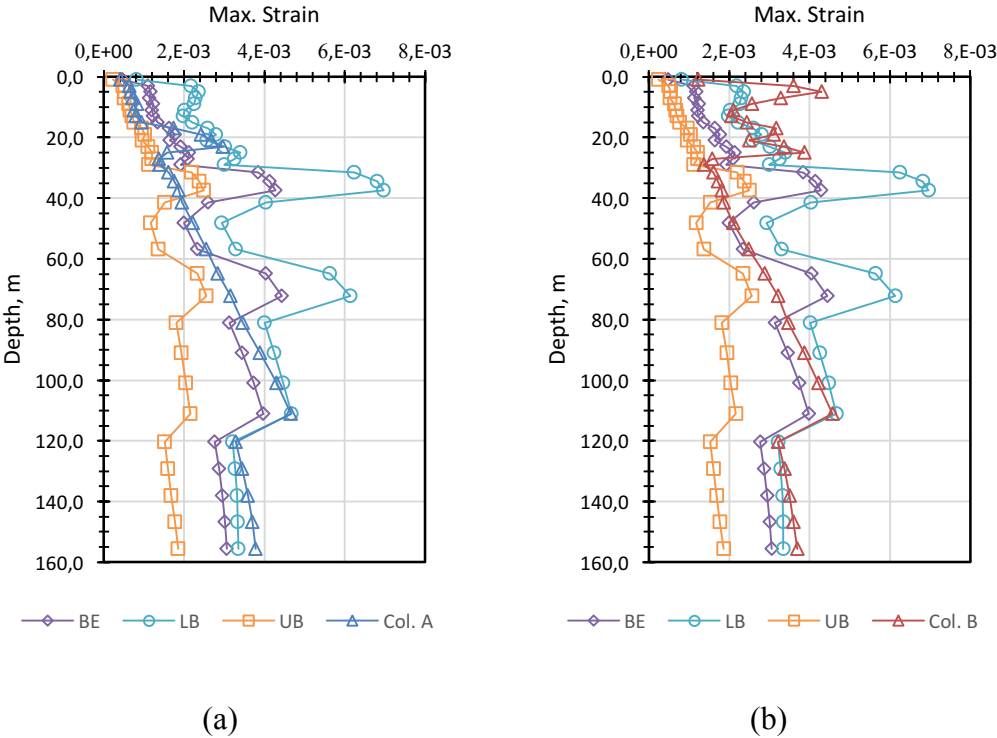
$$G^* = G(1 + 2i\xi) \tag{3.3}$$

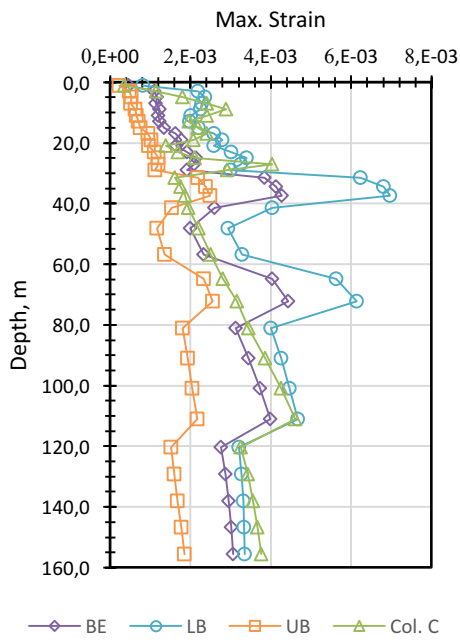
### 4.3 One-Dimensional Equivalent Linear Analysis Results

One-dimensional (1D) equivalent linear site response analyses incorporating 7 one-dimensional soil columns and one for each BE, UB and LB profiles accounting for the coefficient of variation ( $C_v$ ) are performed using 1994 Northridge Earthquake horizontal time history.

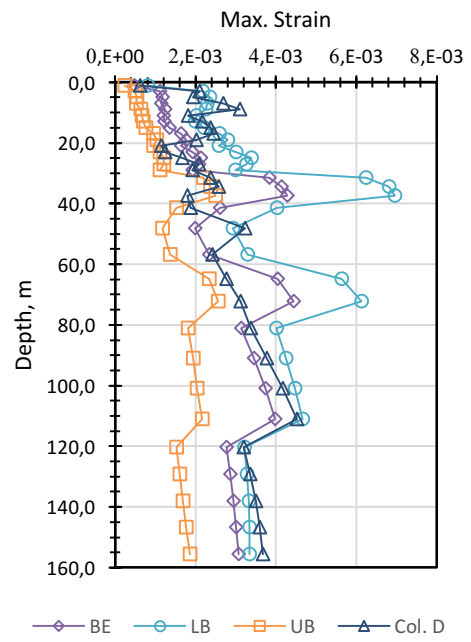
Aforementioned ten separate site response analyses are carried out for all 10 different soil profiles idealized in 32 layers with  $V_s$  values ranging from 620 m/s to 3000 m/s.

As a result of these site response analyses, maximum strain values for each soil layer and the response spectra at the free-field surface are obtained using DEEPSOIL software. Maximum strain values with the corresponding depth are shown in Figure 4.18.

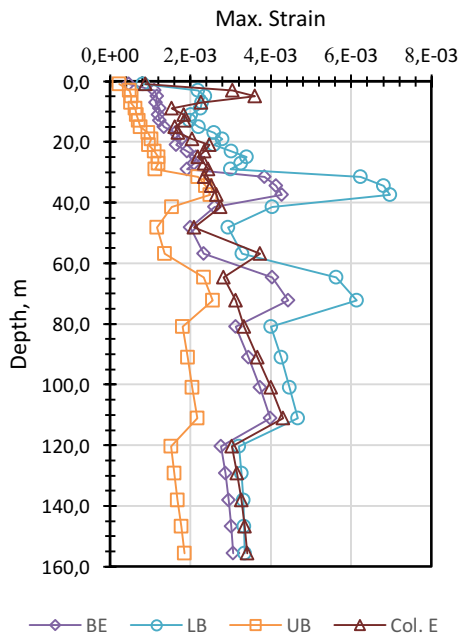




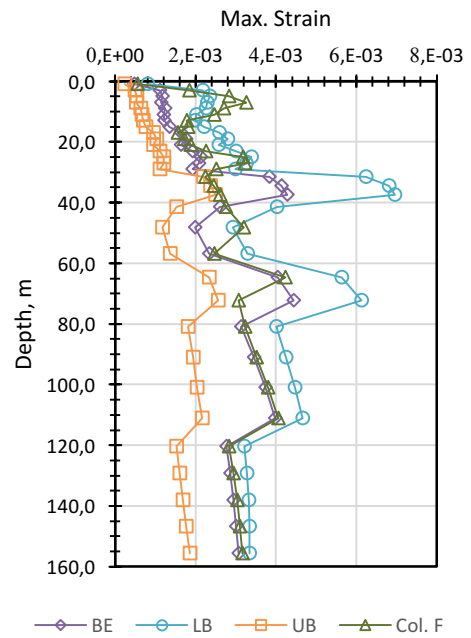
(c)



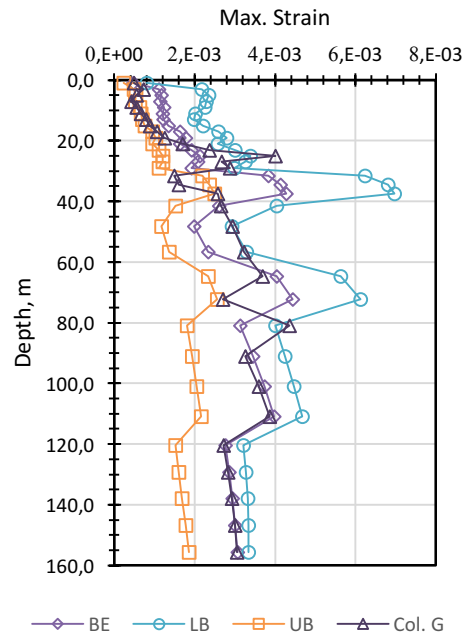
(d)



(e)



(f)



(g)

**Figure 4.18:** The comparison of maximum strain values of Col. A – Col. G with BE, LB and UB profiles

The comparison of the response spectra considering spectral acceleration values at the surface and the top of rock corresponding to each period is presented in Figure 4.19 and Figure 4.20.

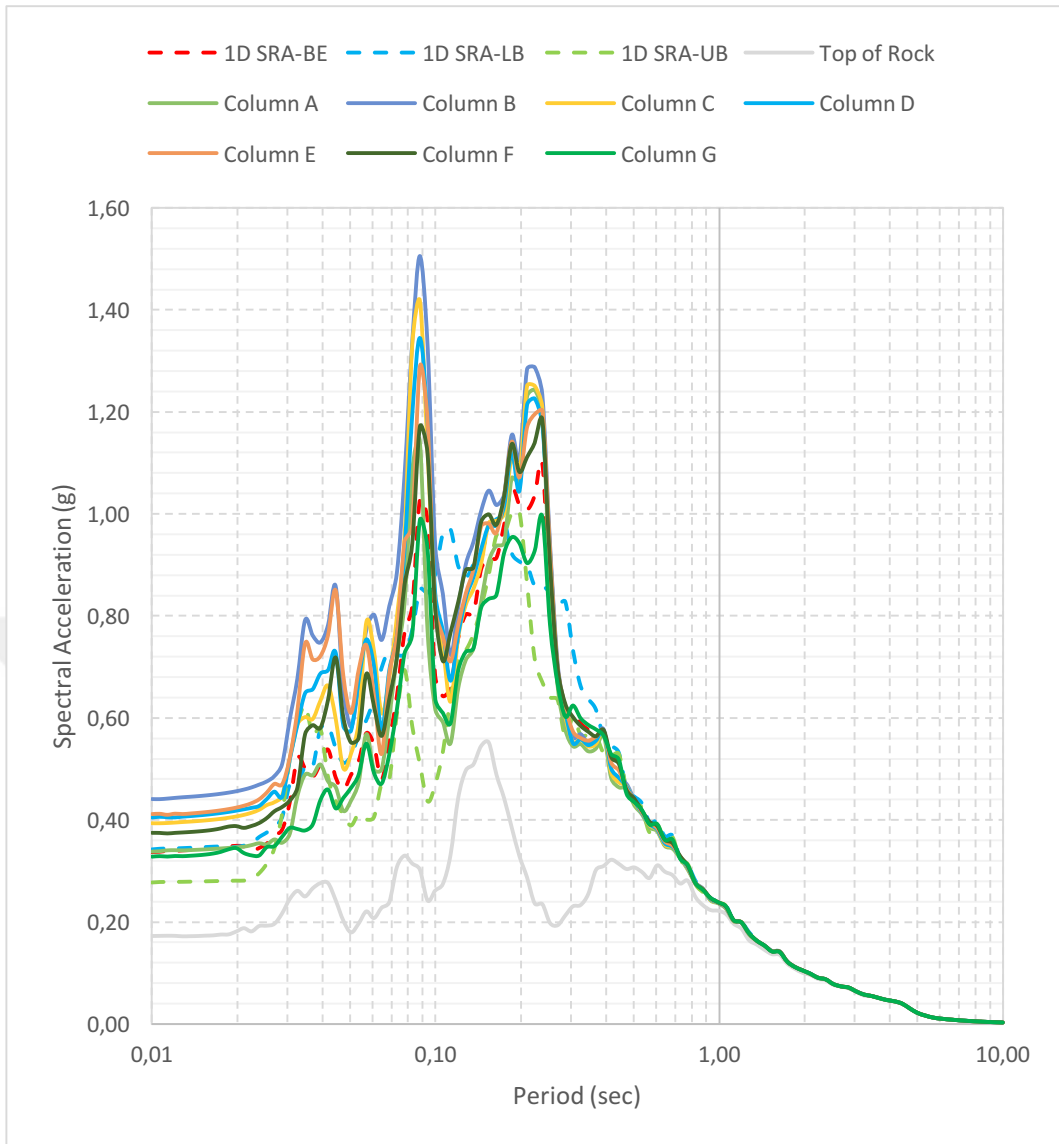
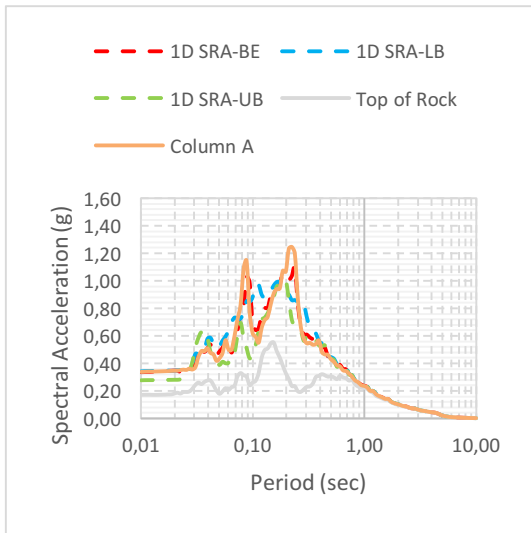
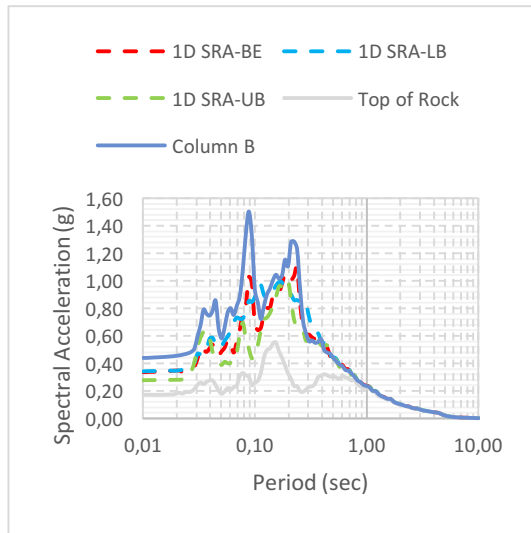


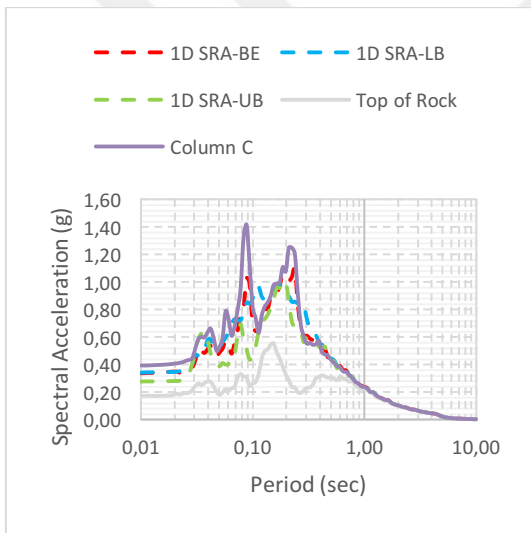
**Figure 4.19:** The response spectra at the surface and the top of rock



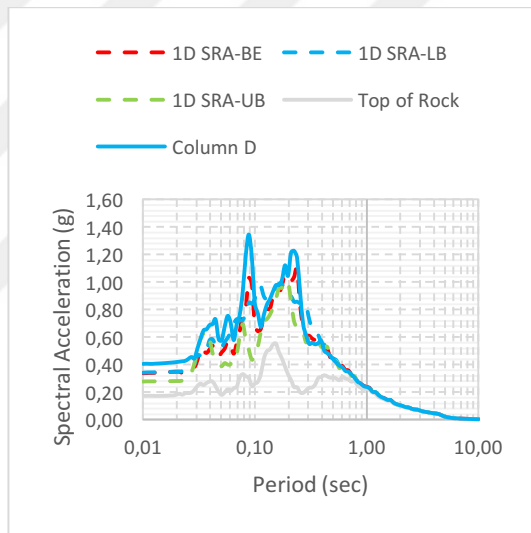
(a)



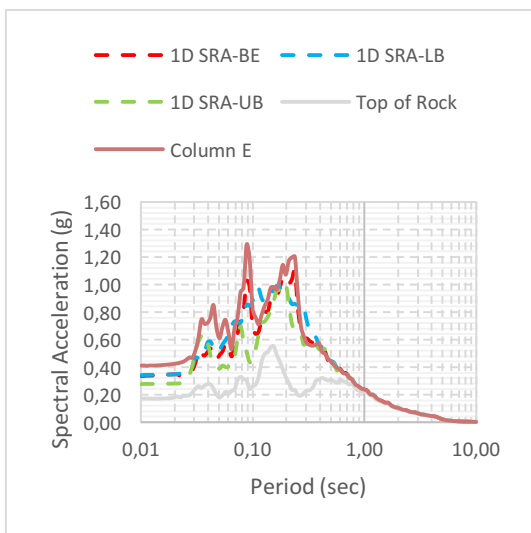
(b)



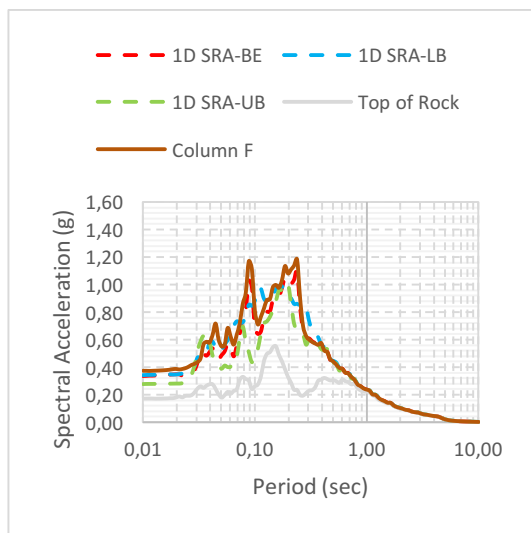
(c)



(d)

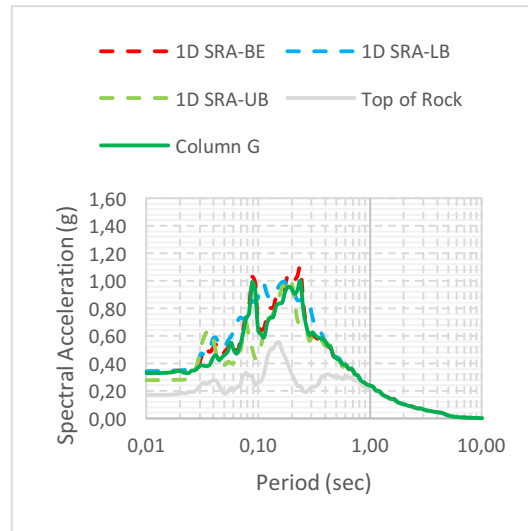


(e)



(f)





(g)

**Figure 4.20:** Comparison of the response of each column with BE-LB-UB results

According to the site response analyses results in all ten profiles, peak ground accelerations are amplified from about 0.17 g on the top of rock, up to 0.44 g at the surface. The first and second predominant periods of all the input records are around 0.08 – 0.11 s and 0.17 - 0.24 s for the surface records. The second predominant periods of the surface records are close to the fundamental period of the BE soil profile (0.29 s). The highest peak spectral acceleration values for the surface records, at the first predominant period and the second predominant period, are 0.70 - 1.50 g and 0.99 - 1.29 g, respectively. Those values are presented as a tabulated format in Table 4.5.

**Table 4.5:** Predominant periods, PSA and PGA values of input rock and surface motions obtained in site response analyses of each soil profile

Soil Profile	Fundamental Period (s)	Predominant Period (s)		PSA (g)		PGA (g)	Amplification (Surface PGA / Rock PGA)	Amplification (Surface PSA / Rock PSA)	
		T1	T2	@T1	@T2			@T1	@T2
Input rock	-	0.08	0.15	0.31	0.55	0.17	-	-	-
BE	0.29	0.09	0.24	1.03	1.10	0.34	2.0	3.3	2.0
LB	0.36	0.11	0.17	0.97	0.99	0.34	2.0	3.1	1.8
UB	0.24	0.08	0.20	0.70	1.00	0.28	1.6	2.3	1.8
Col. A	0.27	0.09	0.22	1.14	1.24	0.34	2.0	3.7	2.3
Col. B	0.30	0.09	0.22	1.50	1.29	0.44	2.6	4.8	2.3
Col. C	0.28	0.09	0.22	1.42	1.25	0.39	2.3	4.6	2.3
Col. D	0.29	0.09	0.22	1.34	1.23	0.40	2.4	4.3	2.2
Col. E	0.30	0.09	0.24	1.29	1.20	0.41	2.4	4.2	2.2
Col. F	0.30	0.09	0.24	1.17	1.18	0.37	2.2	3.8	2.1
Col. G	0.28	0.09	0.24	0.99	0.99	0.33	1.9	3.2	1.8

Due to low modulus degradation in the soil, the surface responses are amplified due to stiff formations with low damping characteristics. Therefore, the soil has characteristics that are more rigid and the soil fundamental periods are close to the predominant period of the characteristic earthquake record, the amplifications are quite high.

PGA values are not significantly changing in Columns A, F and G. However, the highest PGA value is observed in Column B, and those values are considerably high

in Columns C, D and E, comparing to BE (best-estimate), LB (lower-bound) and UB (upper-bound) profiles. The spectral acceleration values in Column A is very similar to BE values, but only at the periods of  $T_1$  and  $T_2$ , the PSA values of Column A are observed as slightly higher than the values of BE profile at the same periods. However, those values are lower than LB and UB except for some periods.

When it is focused on the Column B, it can be said that spectral acceleration values are overwhelmingly higher than BE in the order of 1~1.5 (ranging up to 50%), up to the period of  $T_2$ . Besides, those values are also higher than LB and UB in almost all periods.

Considering Columns C, D and E, likewise, spectral acceleration values are significantly higher than BE, but in the order of 1~1.4 (ranging up to 40%). And also, they exceed the values of LB and UB profiles except for a couple of periods.

When it comes to Column F, this deviation is about 10%. The PGA of Column G is nearly the same as that of the BE profile. Moreover, spectral acceleration values of Column G are less than BE, LB and UB in almost all periods.

In the light of all this information, it can be interpreted that the investigated site has characteristics apparently varying vertically and horizontally. It is inferred that the variation of soil profiles obtained considering standard deviation values, such as BE (best-estimate), LB (lower-bound) and UB (upper-bound), do not satisfactorily reflect the behavior of heterogeneous configuration of soil layers. Those values are considered insufficient to represent the heterogeneous subsurface soil media in the free-field conditions.



## **5. INFLUENCE OF INCLINED LAYERS ON SITE RESPONSE ANALYSIS**

In this part of the study, besides estimation of the dynamic parameters of soil layers for SSI analysis, the influences of heterogeneity due to the deeply inclined layering on the dynamic responses of the foundation are investigated.

The effect of deeply inclined layering at the site on the foundation input motion is investigated in this chapter through equivalent linear site response analyses in free-field.

Within this context, the results acquired with a two-dimensional site response analysis using PLAXIS 2D software (Brinkgreve et al., 2006) are obtained via personal communication (Bayat & Alver, 2018).

The foundation soil layers are defined with related parameters and one-dimensional small-strain shear wave velocity of four different soil profiles to investigate the site heterogeneity through a comparison between 1D equivalent linear and 2D site response analyses.

### **5.1 1D Equivalent Linear Analysis of Soil Profiles**

Idealized one-dimensional layer thicknesses of 32 soil layers with the account for dynamic shear modulus ( $G$ ) and one-dimensional small-strain shear wave velocities ( $V_s$ ) are introduced to DEEPSOIL software for the four different soil profiles that are considered in site response analyses.

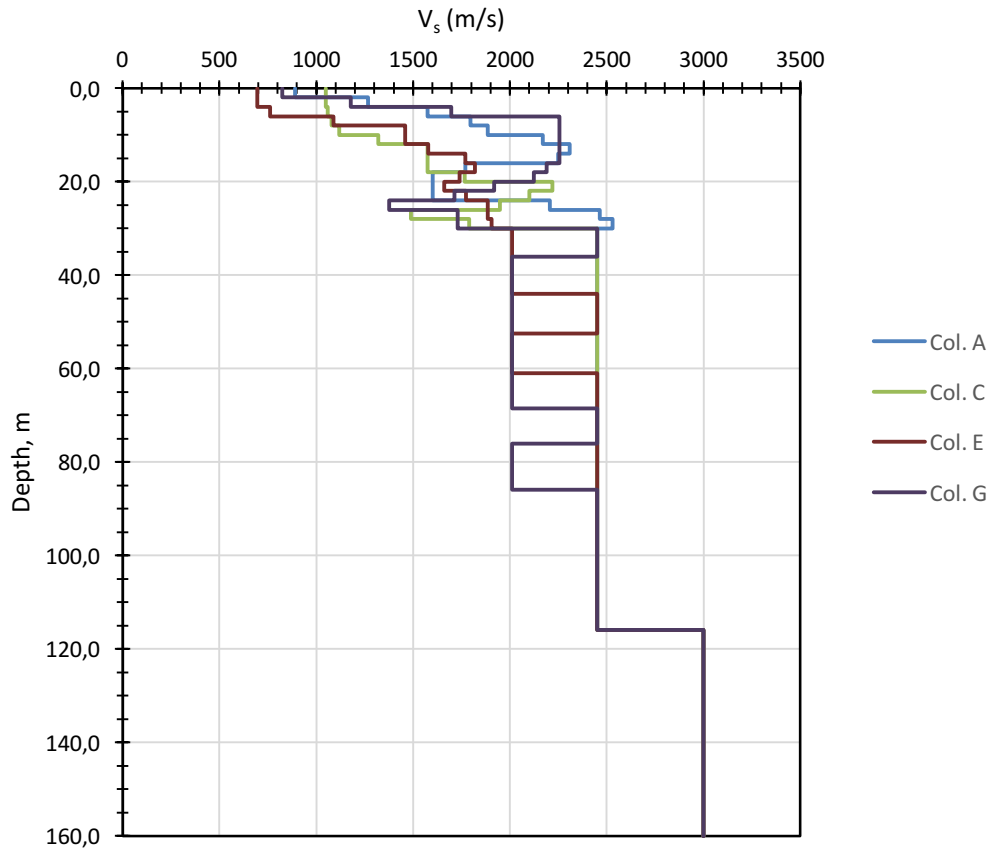


**Figure 5.1:**  $V_s$  profiles chosen for the comparison purposes with 2D results

## 5.2 Comparison With Plaxis 2D Analysis

The results obtained for four different soil profiles with one-dimensional equivalent linear analyses and the results of 2D site response analysis using PLAXIS software are compared. True nonlinear analysis in PLAXIS and equivalent linear analysis where nonlinear characteristics are implemented iteratively in DEEPSOIL. The compliant base boundary at the bottom of the soil profile and free field boundary at the sides of the model are used in PLAXIS.

Model dimensions in x and y directions are 500 m by 160 m. Figure 5.2 demonstrates a section of the mesh along the foundation width footprints.

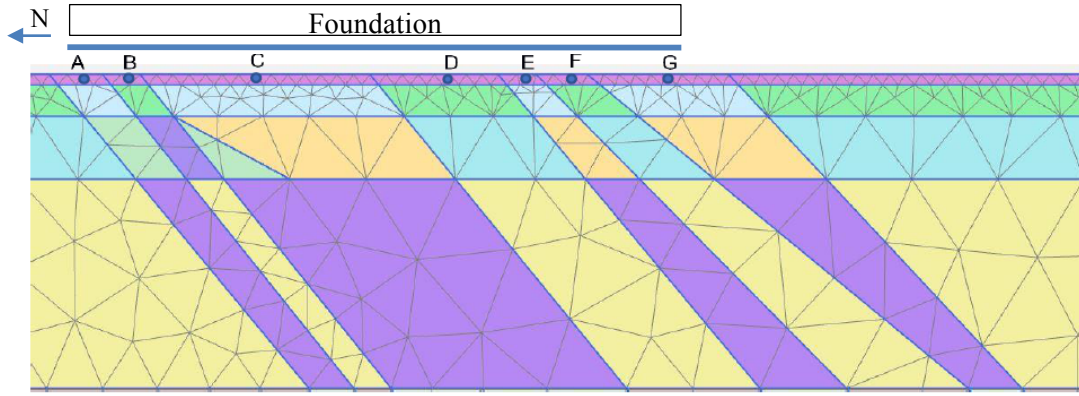


**Figure 5.2:** Schematic foundation soil representation including surface points to compare (Bayat & Alver, 2018)

The model mesh consists of 3885 triangular elements and 32738 number of nodes for inclined profile. According to the given suggestion in the software, a very fine mesh model option is used to generate the mesh, ending with the average element size of 5.756 m. According to Kuhlmeier & Lysmer (1973) suggestion, average element size should be less than one-eighth of the wavelength associated with the maximum frequency component of the input wave.

The minimum shear wave velocity input ( $V_s$ ) in the soil model is 620 m/s and the maximum frequency component of the input motion  $f_{max}$  is 10 Hz. In line with the Equation (5.1), the elements size are  $\lambda/8 = 7.75$  (Bayat & Alver, 2018).

$$Average\ element\ size \leq \frac{\lambda}{8} = \frac{V_{s,min}}{8f_{max}} \quad (5.1)$$

The Hardening soil model with small-strain stiffness (HSsmall) in Plaxis 2D is used. The model stiffness parameters are  $E_{50}$ ,  $E_{oed}$ ,  $E_{ur}$ ,  $G_0$  and  $\gamma_{0.7}$ , where the first three of them are static parameters.  $E_{50}$  was secant stiffness in drained triaxial test,  $E_{oed}$  is tangent stiffness for oedometer loading and  $E_{ur}$  is unloading/reloading stiffness from drained triaxial test.  $G_0$  is the shear modulus at very small strains and  $\gamma_{0.7}$  is the threshold shear strain.  $G_0$  values in the profile are calculated using the shear wave velocity and the density of the corresponding soil layers. Another dynamic input for HSsmall model is  $G_0^{ref}$  and could be found from the following relation between  $G_0^{ref}$  and  $G_0$  as shown in Equation (5.2).

$$G_0 = G_0^{ref} \left( \frac{c \cos \phi - \sigma'_3 \sin \phi}{c \cos \phi + p^{ref} \sin \phi} \right)^m \quad (5.2)$$

where  $m$  is taken 0.5 for most soils,  $c$  is the cohesion,  $\phi$  is the internal angle of friction,  $\sigma'_3$  is the effective confining stress and  $p^{ref}$  is the reference stress (100 kPa).

Static soil parameters ( $E_{50}$ ,  $E_{oed}$ ,  $E_{ur}$ ) are estimated using pressuremeter test results. However, for dynamic analysis, there is a limit value for  $E_0/E_{ur}$  or  $G_0/G_{ur}$  ratio in HSsmall model and the permitted maximum ratio is 20. In dynamic analysis,  $G_0$  values obtained from shear wave velocity measurements are kept constant and for the  $G_0/G_{ur}$  ratios greater than 20,  $G_{ur}$  values are recalculated by considering the permitted limit value. Also,  $G_0^{ref}$  is estimated by using  $G_0/G_{ur}=20$  relation.  $G_{ur}$  is related to  $E_{ur}$  as in the Equation (5.3).

$$G_{ur} = \frac{E_{ur}}{2(1 + \nu)} \quad (5.3)$$

In HSsmall model, stiffness degradation or stress-strain relationship is written as in Equation (5.4).

$$\tau = G_s \gamma = \frac{G_0 \gamma}{1 + 0.385 \frac{\gamma}{\gamma_{0.7}}} \quad (5.4)$$

The threshold strain ( $\gamma_{0.7}$ ) is the strain at which secant modulus  $G_s = 0.70G_0$ . The threshold strain ( $\gamma_{0.7}$ ) is selected from the modulus degradation and damping curves used in 1D site response analysis and presented in Section 3.2. The model stiffness degradation has been cut off at  $\gamma_{cut-off}$  value since the model itself represents the modulus degradation. Therefore, small-strain stiffness reduction curve has a cut-off shear strain beyond which the tangent shear modulus ( $G_t$ ) is equal to unloading-reloading shear modulus ( $G_{ur}$ ). Calculation of the cut-off shear strain value is given in Equation (5.5).

$$\gamma_{cut-off} = \frac{1}{0.385} \left( \sqrt{\frac{G_0}{G_{ur}}} - 1 \right) \gamma_{0.7} \quad (5.5)$$



Rayleigh damping is used in the model for each material in order to prevent the mesh from very high and low frequencies. Minimum damping 0.5% for target frequencies of 1 Hz and 10 Hz are applied.

Site response analysis is performed in inclined layers modelled in Plaxis 2D software to investigate the effect of non-horizontal deeply inclined soil/rock layers on the ground accelerations and displacements. Free field and compliant base boundary options are used in the model for vertical and lateral (base) boundaries, respectively (Bayat & Alver, 2018). The Hardening soil model is used and the model parameters assigned in the program are presented in Table 5.1.

**Table 5.1:** Soil parameters used in dynamic analyses of the inclined Plaxis 2D model

Rock Type	$\rho$ (g/cm <sup>3</sup> )	$c$ (kPa)	$\phi$	$V_s$ (m/s)	$G_0$ (MPa)	$G_0^{\text{ref}}$ (MPa)	$E_{50}^{\text{ref}}$ (MPa)	$E_{\text{ur}}^{\text{ref}}$ (MPa)	$\gamma_{0.7}$
R1-A (0-4 m)	2.47	287	24	620	949	998	63	189	7.5E-05
R1-A (4-10 m)	2.47	287	24	620	949	949	60	180	7.5E-05
R1-B (4-10 m)	2.68	703	26	1190	3795	3791	178	535	7.5E-05
R1-B (10-30 m)	2.68	703	26	1190	3795	3575	168	504	8.8E-05
R1-C (30-37 m)	2.81	1011	28	2010	11353	10386	488	1464	1.4E-04
R1-C (37-76 m)	2.81	1011	28	2010	11353	9725	457	1371	1.8E-04
R1-C (76-150 m)	2.81	1011	28	2010	11353	8519	400	1201	2.1E-04
R1-C (150-160 m)	2.81	1011	28	2010	11353	7867	370	1109	2.9E-04
R2-A (0-4 m)	2.68	589	24	790	1673	1715	95	286	7.5E-05
R2-A (4-10 m)	2.68	589	24	1050	2955	2945	141	424	7.5E-05
R2-B (4-10 m)	2.74	1031	26	1560	6668	6660	311	932	8.8E-05
R2-B (10-30 m)	2.74	1031	26	1560	6668	6383	298	894	8.8E-05
R2-C (30-37 m)	2.83	1337	28	2450	16987	15837	707	2122	1.4E-04
R2-C (37-76 m)	2.83	1337	28	2450	16987	15014	671	2012	1.8E-04
R2-C (76-150 m)	2.83	1337	28	2450	16987	13436	600	1800	2.1E-04
R2-C (150-160 m)	2.83	1337	28	2450	16987	12540	560	1680	2.9E-04

Comparisons of 1D DEEPSOIL and Plaxis 2D results for the same free-field surface points are presented in Figure 5.3 – 5.7.

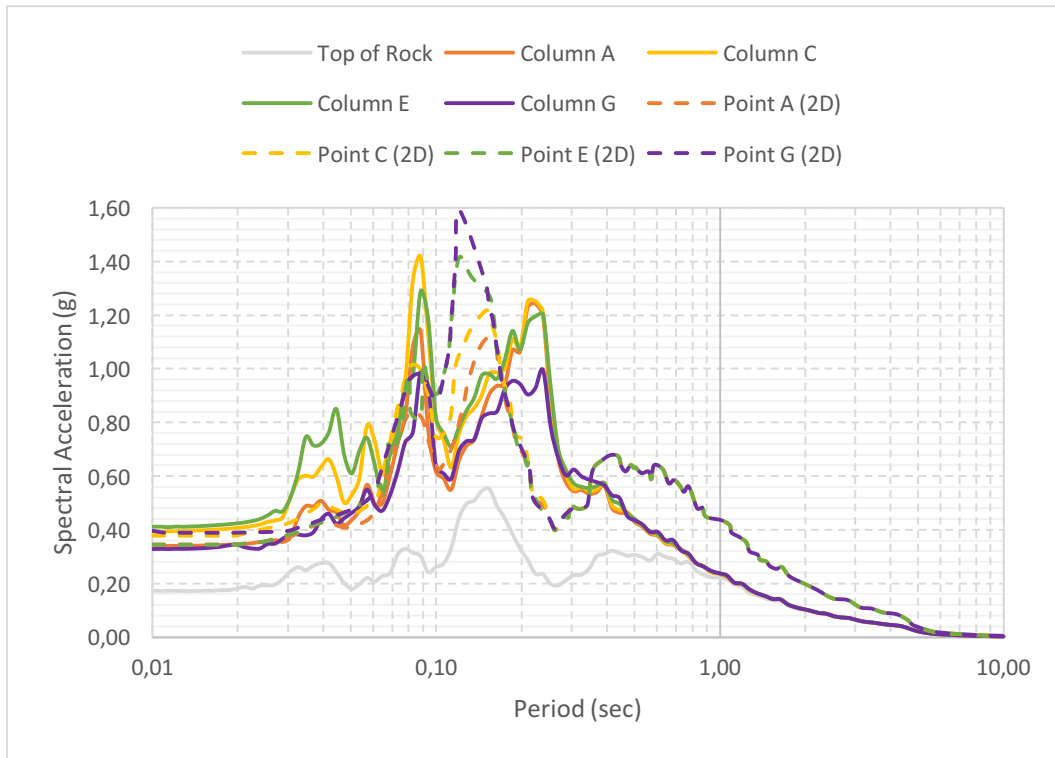


**Figure 5.3:** Comparisons of 1D and 2D site response analyses for the corresponding soil columns in 1D and surface points counterparts in 2D analyses

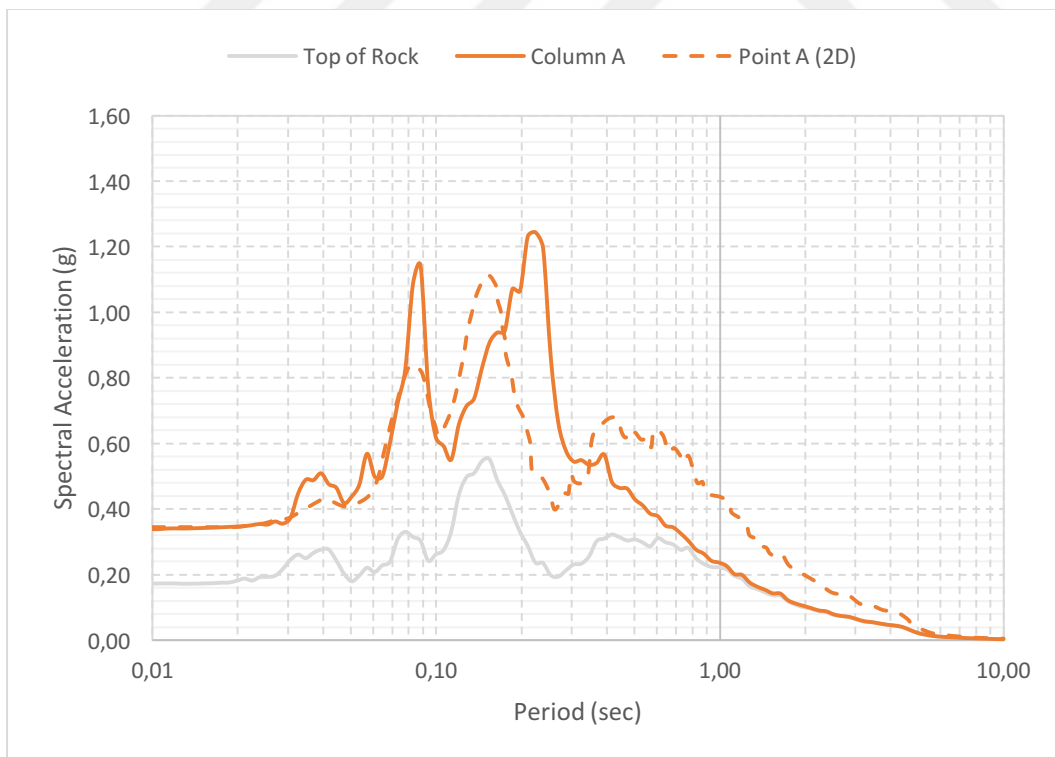


**Figure 5.4:** Comparison of the response of Column A with Plaxis 2D results at the same location

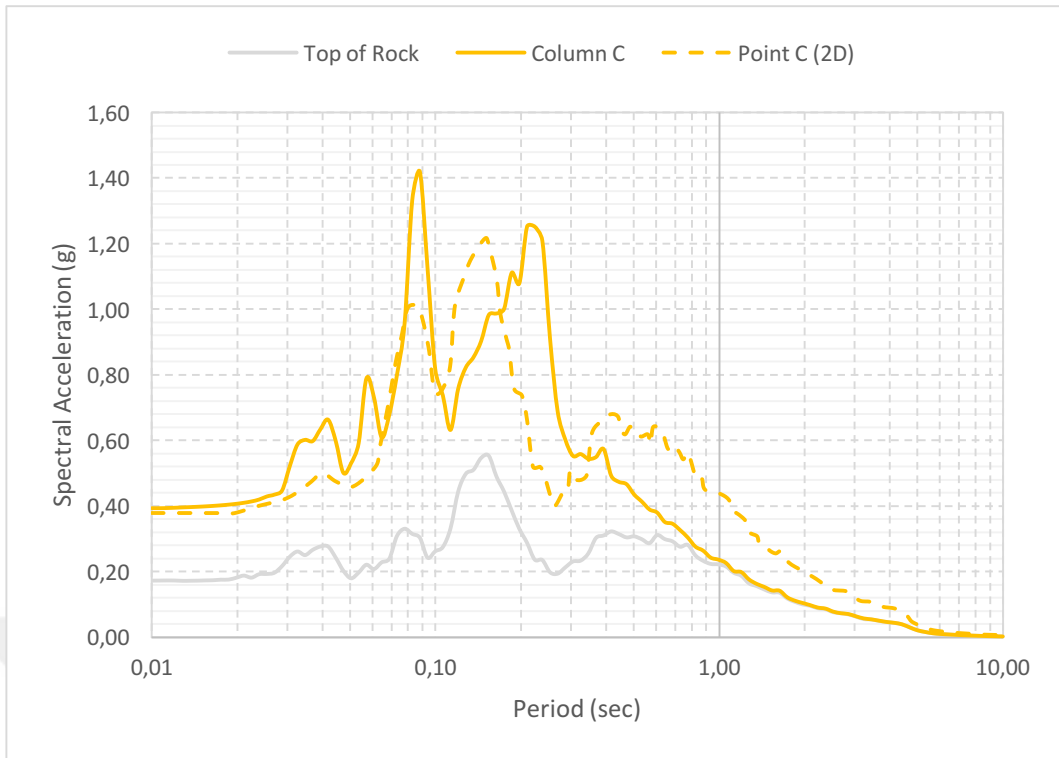


**Figure 5.5:** Comparison of the response of Column C with Plaxis 2D results at the same location

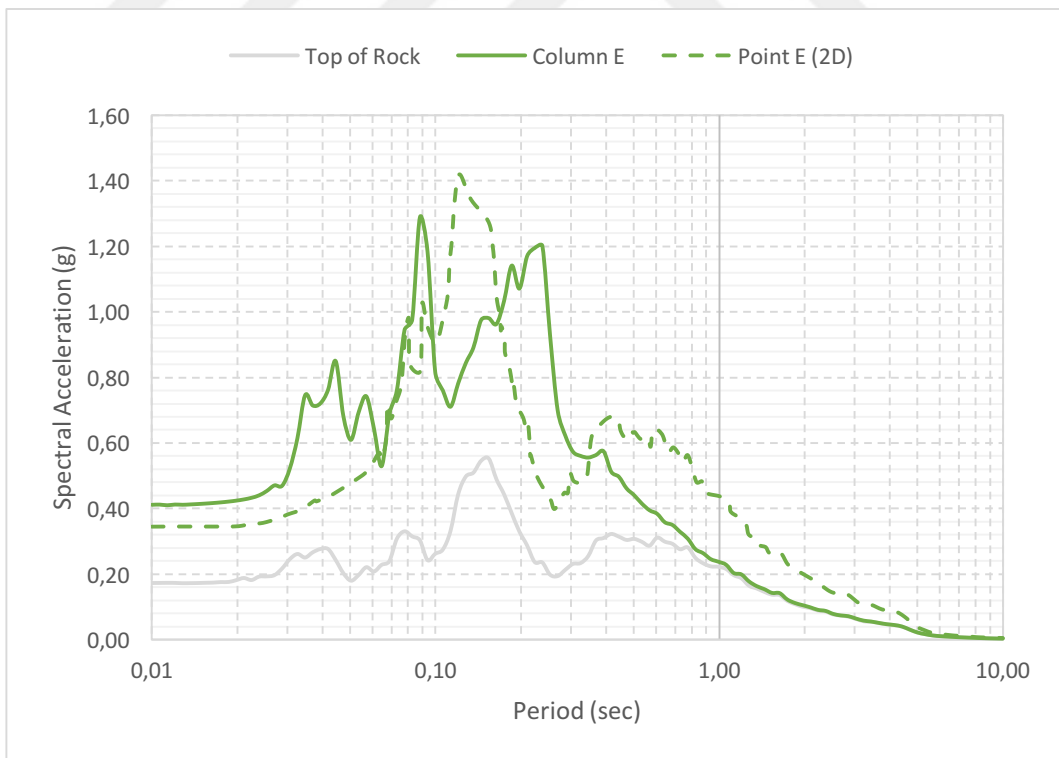


**Figure 5.6:** Comparison of the response of Column E with Plaxis 2D results at the same location

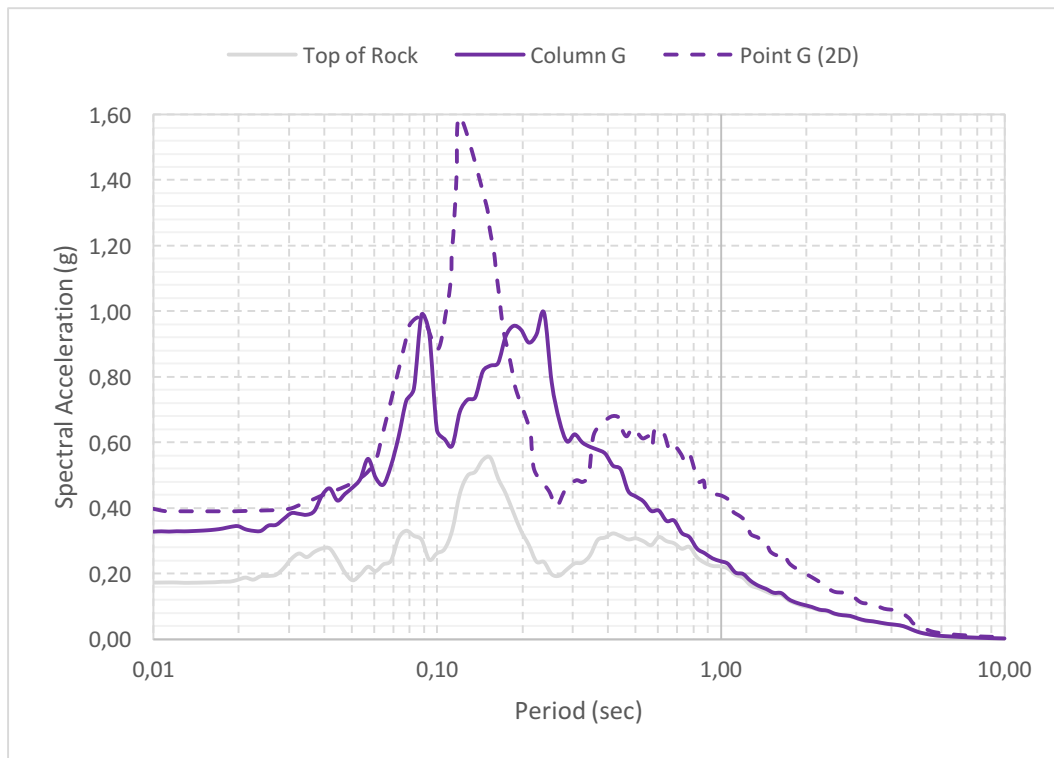


**Figure 5.7:** Comparison of the response of Column G with Plaxis 2D results at the same location

The site response analyses results of these four profiles show that peak ground accelerations are amplified from about 0.17 g on the top of rock, up to 0.41 g at the surface. The first and second predominant periods of all the input motions are around 0.09 s and 0.12 - 0.24 s for the surface records.

The highest peak spectral acceleration values for the surface records at the first predominant period are in the range of 0.82 - 1.42 g and at the second predominant period 0.99 - 1.59 g, respectively.

The predominant periods, peak spectral acceleration values corresponding to these periods and peak ground acceleration values of input rock and surface motions obtained from both one-dimensional and two-dimensional site response analysis results are shown as a tabulated form in Table 5.2.

**Table 5.2:** Predominant periods, PSA and PGA values of input rock and surface motions obtained in site response analyses of each soil profile

Soil Profile	Predominant Period (s)		PSA (g)		PGA (g)	Amplification (Surface PGA / Rock PGA)	Amplification (Surface PSA / Rock PSA)	
	T <sub>1</sub>	T <sub>2</sub>	@T <sub>1</sub>	@T <sub>2</sub>			@T <sub>1</sub>	@T <sub>2</sub>
Input rock	0.08	0.15	0.31	0.55	0.17	-	-	-
Point A	0.09	0.15	0.82	1.11	0.34	2.0	2.6	2.0
Col. A	0.09	0.22	1.14	1.24	0.34	2.0	3.7	2.3
Point C	0.09	0.15	1.00	1.20	0.38	2.2	3.2	2.2
Col. C	0.09	0.22	1.42	1.25	0.39	2.3	4.6	2.3
Point E	0.09	0.12	1.02	1.42	0.35	2.1	3.3	2.6
Col. E	0.09	0.24	1.29	1.20	0.41	2.4	4.2	2.2
Point G	0.09	0.12	0.98	1.59	0.40	2.4	3.2	2.9
Col. G	0.09	0.24	0.99	0.99	0.33	1.9	3.2	1.8

As seen on the Figure 5.4 – 5.7, 1D and 2D site response analyses results for the points A, C, E and G are compared individually. In the response spectra obtained from 1D equivalent linear analyses results, the motion is amplified at the first predominant periods, except point G. Besides, the second predominant periods for all points are shifted to a higher period in one-dimensional equivalent linear analyses. It is observed that in-depth-shear-wave-velocities change more heterogeneously at the columns E and G than the columns A and C.

At the points C, E and G, the response spectra of the motion obtained is amplified, while at the rest of the foundation, the response spectra are deamplified.

This effect would be better observed in SSI analysis of the super-structure together with the inclined layered soil profile.

Since the soil profile has deeply inclined layers, it introduces a considerably pronounced incoherency effect. Because of that, it is considered that this kinematic interaction deamplifies the free-field motion.

In site response analysis in DEEPSOIL the surface acceleration is most amplified nearly at the period of 0.23 s, whereas in PLAXIS analysis the amplification is at the periods of 0.12 - 0.15 s, which is the predominant period of the input rock motion.

At the predominant periods, peak spectral accelerations obtained by PLAXIS for soil columns E and G are higher than the results obtained by DEEPSOIL. However, in the same case, soil profiles A and C remains within the limits of the DEEPSOIL analysis results. The reasons of the differences between the two responses may be attributed to:

1. The different analysis methods: True nonlinear analysis in PLAXIS and equivalent linear analysis where nonlinear characteristics are implemented iteratively in DEEPSOIL.
2. The different boundary conditions in the two analysis: The compliant base boundary at the bottom of the soil profile and free field boundary at the sides of the model are used in PLAXIS, whereas the rigid boundary at the bottom is used in DEEPSOIL.

Finally, the effect of deeply inclined layered soil profile under the foundation on the site response is investigated by comparing the analyses performed in inclined layered soil and one-dimensional soil models. When the free-field site response analyses on BE profile and the inclined layered soil profile are compared, the effect of deeply inclined layering can be interpreted in terms of peak ground accelerations of the surface motions. The results of the site response analysis under the foundation indicated that the surface peak ground accelerations are 0.34 g (Table 4.5) in horizontal BE soil model and 0.34-0.40 g (Table 5.2) in inclined layer model.

Consequently, the response in the 2D inclined profile appeared to be less than the responses in the 1D profiles under the foundation. This outcome may be attributed to the greater effect of the kinematic interaction in the inclined layered soil profile owing to the emerging incoherency in the shear waves in the deeply inclined layering.

## **6. IMPLEMENTATION OF DYNAMIC SOIL-STRUCTURE INTERACTION ON A GENERIC NUCLEAR FACILITY DESIGN**

Soil conditions and seismicity are taken into considerations for a hypothetical site. The study is aimed to investigate seismic response of the generic nuclear reactor building. The dynamic seismic response calculations are performed considering soil-structure interaction (SSI) analyses. The design of a generic nuclear facility is investigated taking into account the soil-structure interaction effects.

The strain compatible soil profiles (degraded shear modulus and damping profiles) to be used in SSI analysis are computed in 1D equivalent linear site response analysis.

Maximum strain values for each soil layer are obtained as a result of the site response analysis. And consequently, strain compatible shear moduli and damping ratios of each layer, which are incorporated into the SSI analysis, are determined considering maximum strain values together with the strain dependent modulus degradation ( $G/G_{\max}$ ) and damping ratio curves.

Dynamic SSI analyses are performed on the assumption that the super-structure model and soil model beneath the foundation level respond linearly. In order to take inelastic behavior of the structure under seismic loading, based on the earthquake hazard level, section rigidities and damping ratios in the finite element model are adjusted as per ASCE 43-05 (ASCE, 2005). The soil nonlinearity is taken into consideration by using an equivalent linear model with dynamic high-strain properties of the soil. Dynamic soil-structure interaction analyses are performed in frequency domain using ACS SASSI software.

SASSI is one of the most commonly preferred computer programs using the substructuring method for the evaluation of the dynamic response of 2D and 3D foundation-structure systems. Finite element modeling is used in frequency domain. Soil is adopted as horizontally layered above a uniform halfspace. All of the node points of the base mat are interconnected with the under foundation media and transfer functions are calculated for each of them.

The model used in the soil-structure analyses is a combined model that contains the finite element model of the super-structure and the frequency dependent dynamic properties of the soil.

Strain compatible values are obtained from the each site response analysis for each soil layer. Afterwards, a 3D finite element model of the reactor building is developed using SAP 2000 software (Computers and Structures Inc., 2014). This 3D model contains only analytical information regarding the finite elements, nodes and material properties, and the model is exported as “.hou” file format supported by SASSI software. The imported file in SASSI is manually adapted and modified for the convenient use of ACS SASSI software (GP Technologies Inc., 2014).

In SASSI software, soil media is modelled as idealized horizontal layers with high strain soil properties. Soil layer plot interface is shown in Figure 6.1.

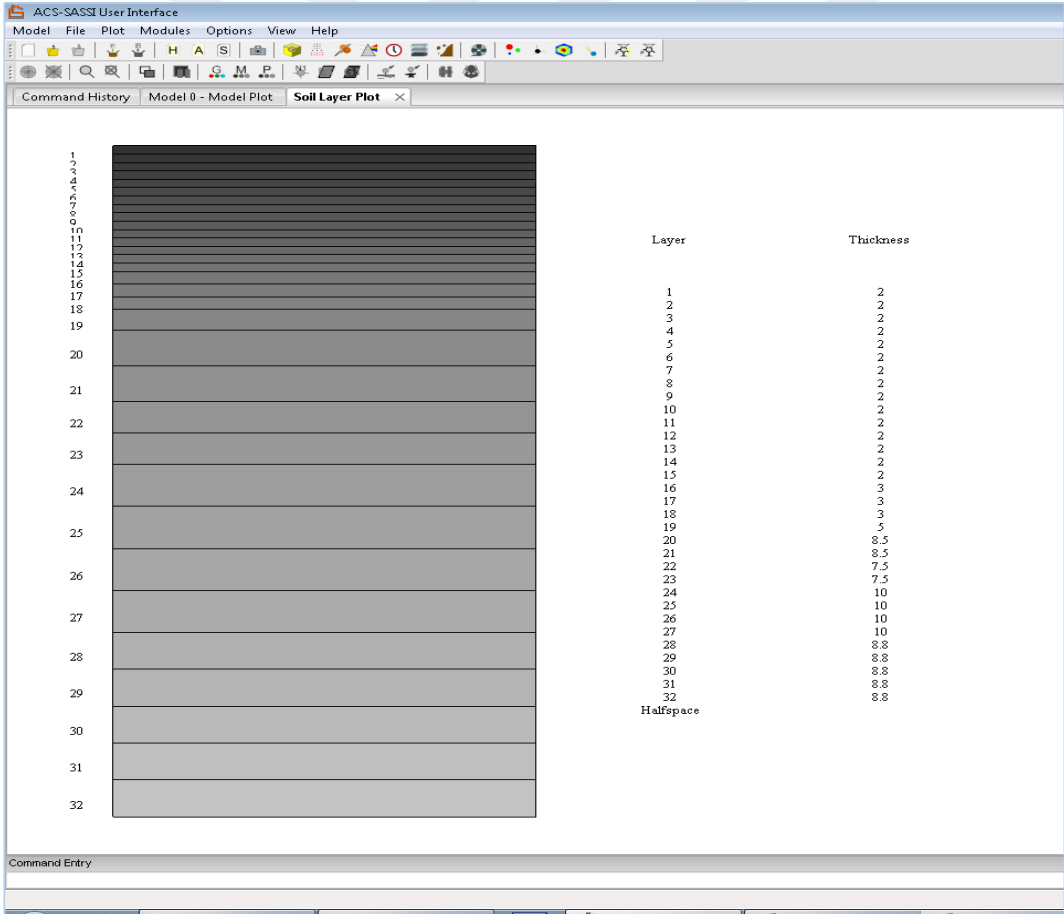


**Figure 6.1:** Soil layer plot interface in ACS SASSI

After the high strain soil properties, input motion and 3D model information is inserted into SASSI, analysis options such as embedded soil layers, control point layer,



boundary conditions, frequency steps, substructuring method, output options are defined using the analysis options interface as shown in Figure 6.2.

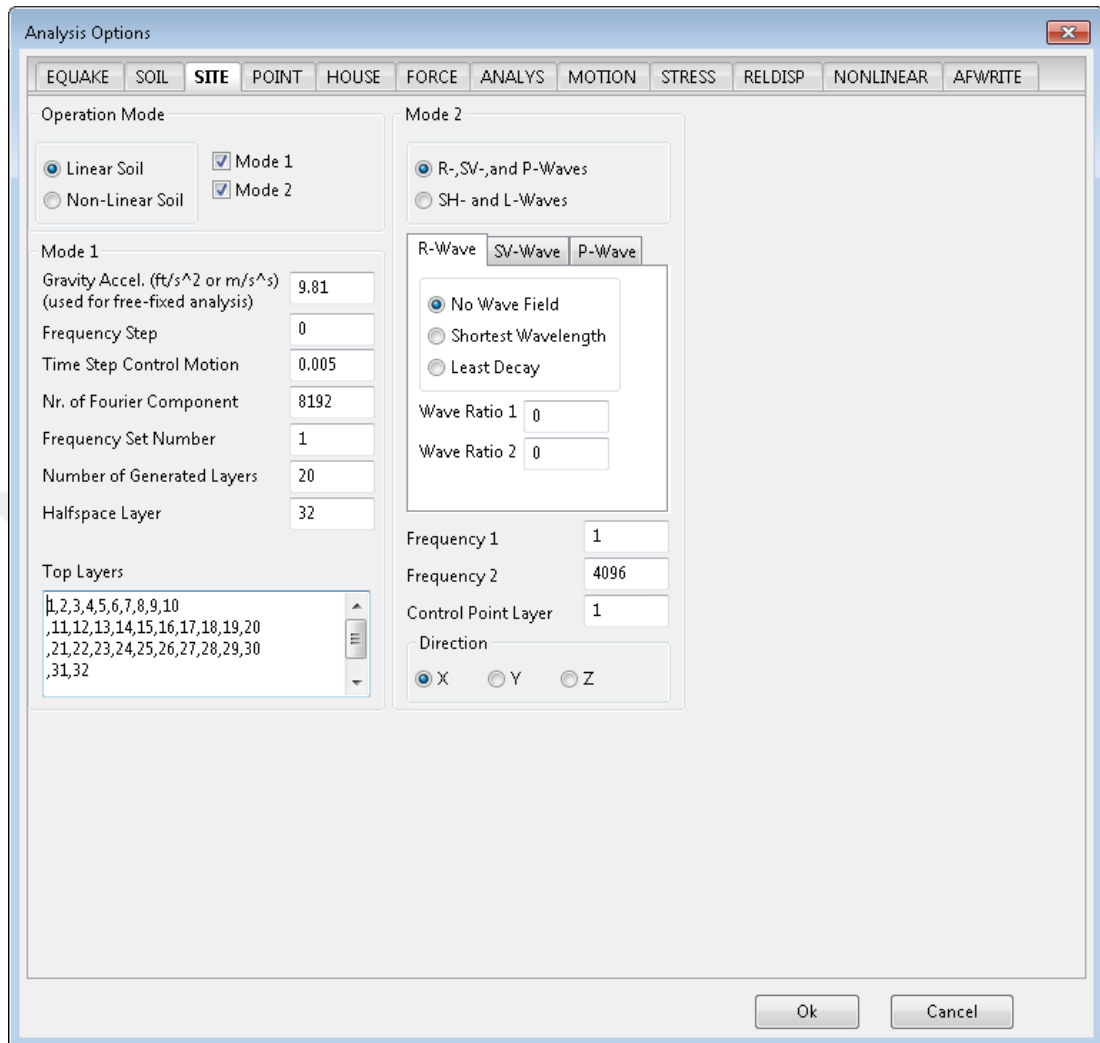


**Figure 6.2:** Analysis options interface in ACS SASSI

In line with these adjustments, analyses are carried out in frequency domain for the combined 3D SSI model taking into account the each soil profile.

### 6.1 Model of a Generic Nuclear Facility

The nuclear facility building model studied in this thesis was adapted from a generic VVER-type reactor building design developed by a designer company, namely Hidropress (Hidropress, 2011a, 2011b).

Reactor building consists of double protective reinforced concrete containment structure that houses normal operation and safety systems, electrical and mechanical

equipment and the reactor plant. Schematic view of the main building is presented in Figure 6.3.

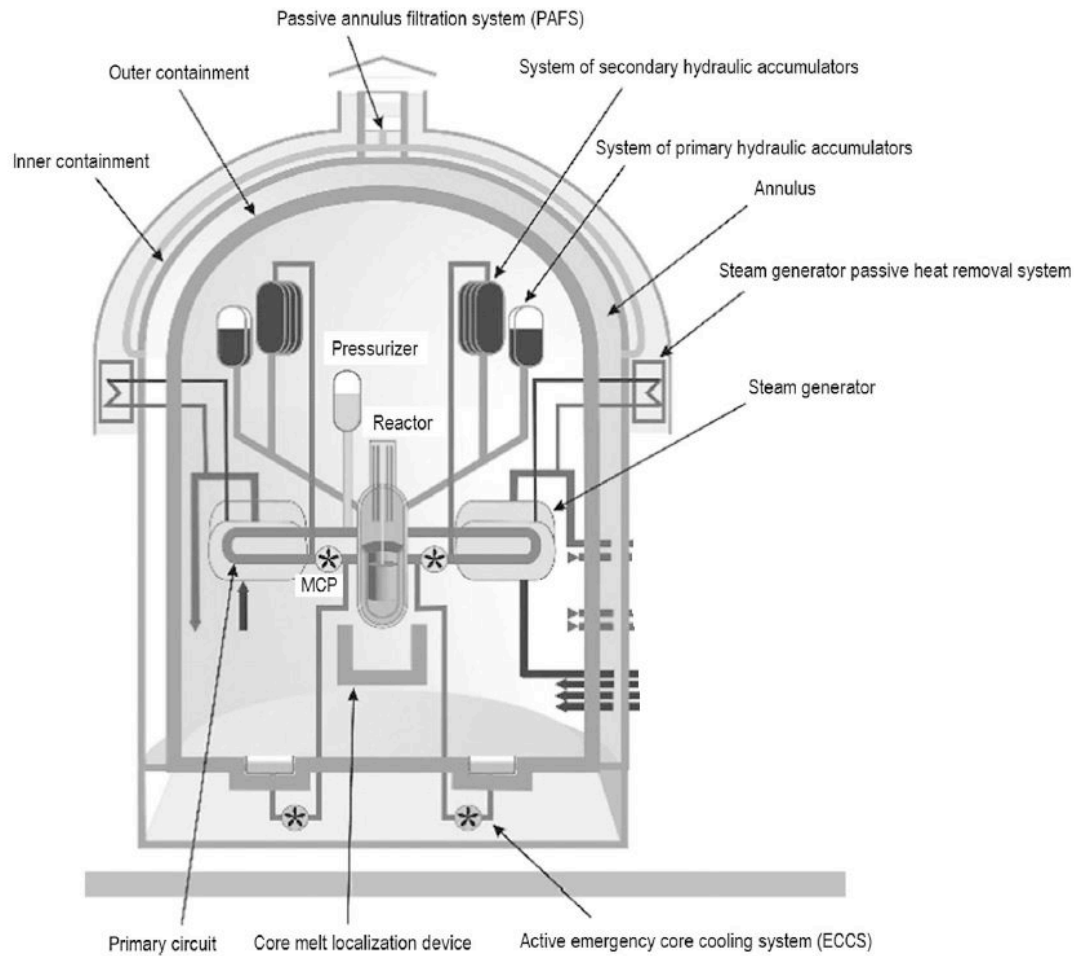


**Figure 6.3:** Schematic view of a VVER design (adapted from (Asmolov et al., 2017))

### 6.1.1 Facility description

The containment is a component of the accident localization system and consists of two reinforced concrete cylindrical structure with a hemispherical dome. Internal containment structure is designed for internal pressure and temperature released in case of an emergency, and outer containment structure protecting from external impacts such as explosion and aircraft crash. There is an annular space between the containment structures where the safety system cable channels are located. In this annular space, leakage material is collected in case of an accident. The reactor is located at the center of the internal containment structure in the accident localization area. Containment internal houses a spent fuel pool and main components such as

steam generators, reactor coolant pumps, main coolant pipelines and pressurizer (Gidropress, 2011a).

The inner containment structure is made of prestressed reinforced concrete and outer containment structure is reinforced concrete, overlapped with hemispherical dome. Outer containment has an internal diameter of 50.8 m. The outer containment structure thickness is 1500 mm in the locations that are not closed with annex building. Outer containment structure is designed to withstand the loads from external impacts such as external shock wave, aircraft crash, extreme wind, tornado and seismic impact.

The annular space between inner and outer containment structures is 2.2 m considering requirements for maintenance of the prestressing system of inner containment, equipment available in the annulus and in order to inspect the surface the containment structure. Structural dimensions are mainly as follows:

- Internal diameter of the inner containment is 44.0 m,
- Internal diameter of the outer containment is 50.8 m,
- Height of the cylindrical part is 38.5 m,
- Height of the inner containment structure with dome is 61.7 m,
- Height of the outer containment structure with dome is 65.4 m,
- Inner containment wall thickness is 1.2 m,
- Outer containment wall thickness is 1.5 m,

The containment provides three tight locks. Main lock for the transportation of fuel and the large equipment with entrance to maintenance elevation of the reactor hall is at the elevation of +31.700 m. Operational lock for personnel and small cargoes to pass is at the elevation level +28.250 m. Emergency lock is at the elevation of +21.280 m (Gidropress, 2011a).

### **6.1.2 Structural model and its dynamic properties**

The model used in the soil-structure analyses is a combined model that contains the finite element model of the super-structure and the frequency dependent dynamic properties of the soil. Analytical 3D finite element model of the reactor building is initially developed using SAP 2000 software (Computers and Structures Inc., 2014) and then transferred to the ACS SASSI software (GP Technologies Inc., 2014).

SSI analyses of the reactor building for ten soil profiles and one earthquake level using ACS SASSI software. SSI analysis is performed in frequency domain dynamic response calculation using SASSI software. Response spectra are obtained for 75 frequencies defined in ASCE 4-98 (ASCE, 2000), U.S NRC Regulator Guide 1.122 (U.S. NRC, 1978) and SRP 3.7.1 (U.S. NRC, 2007b).

The methodology of soil-structure interaction analyses is consistent with ASCE 4-98 (ASCE, 2000) and ASCE 43-05 (ASCE, 2005). Soil-structure interaction is considered in the linear dynamic analyses and they are performed in the frequency domain. SSI analyses are performed with SASSI finite element analysis software, which is the System for Analysis of Soil-Structure Interaction, a computer code for performing finite element analyses of soil-structure interaction during seismic ground motions. It is first developed at the University of California, Berkeley in 1981 (Lysmer et al., 1981). SASSI software is a substructuring program that uses the complex frequency response method and finite element technique to solve a wide range of dynamic soil-structure interaction problems. SASSI software is widely used within the global nuclear industry to analyze the effect of seismic ground motions on structures.

In this study, SSI analyses are performed with a commercial version of the SASSI, ACS SASSI finite element analysis software (GP Technologies Inc., 2014). SSI analyses are performed considering a surface mounted model with no excavated soil. Thus, all of the interaction nodes are selected at the foundation bottom level. Finite element model of the reactor building is developed in SAP 2000 software (Computers and Structures Inc., 2014) and converted to ACS SASSI format for the SSI analyses.

Reactor Building consists of reinforced concrete shear walls and large columns. All of these systems are modelled using SAP 2000 software with thick shell elements as shown in Figure 6.4.

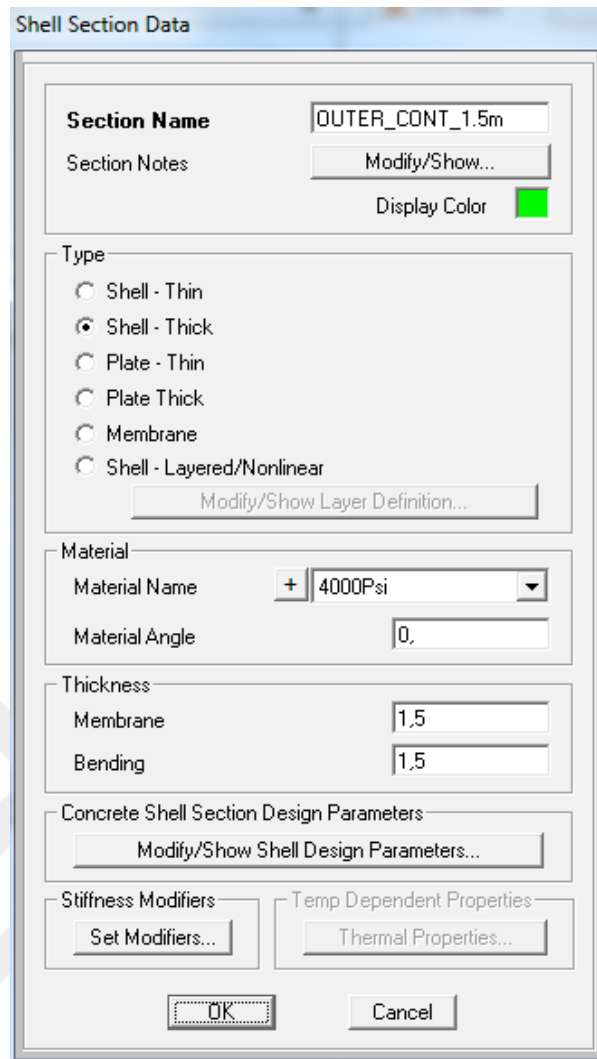


**Figure 6.4:** Element section type and thickness interface in SAP 2000

In the SAP 2000 model mass, shell and beam elements are utilized. Heavy equipments are modelled with mass elements. Shear walls, slabs and large columns are modelled with thick shell elements and rigid links are modelled with beam elements. Walls and slabs are modelled on their centerline. The model consists of 6272 nodes and 9058 finite elements. The 3D model of the structure is shown in Figure 6.5.

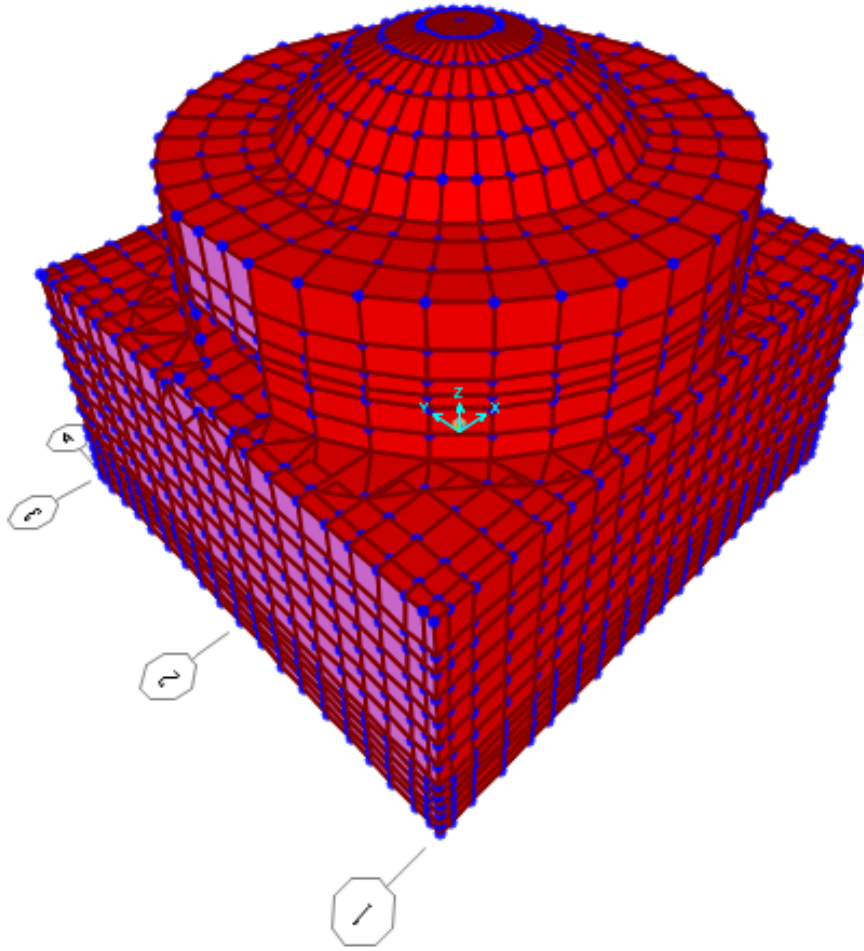


**Figure 6.5:** 3D model of the reactor building

Walls and slabs are modeled on their centerline. Rigid links are used to link equipment mass elements to the model. The reactor building is composed of three separate structures (containment internal, inner containment and outer containment) together with the adjacent structures resting on the same foundation as seen on Figure 6.6.

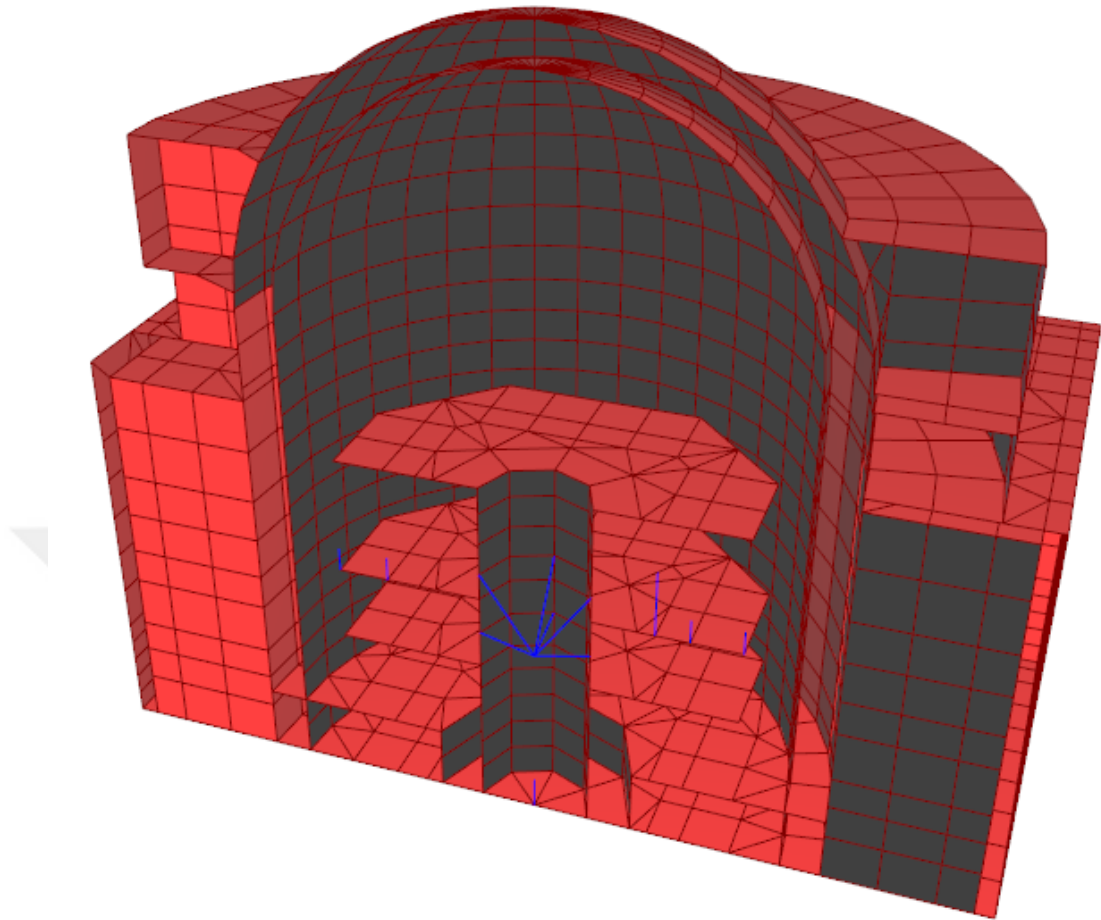


**Figure 6.6:** 3D view of reactor building with the inner and outer containment structure

SSI analysis performed in this study is a linear elastic dynamic structural analysis, and therefore, per ASCE 43-05 (ASCE, 2005) based on the earthquake hazard levels section rigidities and damping ratios in the finite element model are adjusted.

High intensity input ground motions may reduce the stiffness of shear walls due to cracking. For linear elastic solution this stiffness reduction is modeled with effective stiffnesses. Element stiffnesses are modified according to ASCE 43-05. In lieu with this standard, Young's modulus of all materials is halved. Effective stiffness of reinforced concrete members are shown in Table 6.1 as adapted from this standard (ASCE, 2005).

**Table 6.1:** Effective stiffness of reinforced concrete members (ASCE, 2005)

Member	Flexural Rigidity	Shear Rigidity	Axial Rigidity
Beams—Nonprestressed	$0.5 E_c I_g$	$G_c A_w$	
Beams—Prestressed	$E_c I_g$	$G_c A_w$	
Columns in compression	$0.7 E_c I_g$	$G_c A_w$	$E_c A_g$
Columns in tension	$0.5 E_c I_g$	$G_c A_w$	$E_s A_s$
Walls and diaphragms—Uncracked	$E_c I_g$	$G_c A_w$	$E_c A_g$
Walls and diaphragms—Cracked	$(f_b < f_{cr})$ $0.5 E_c I_g$	$(V < V_c)$ $0.5 G_c A_w$	$E_c A_g$
	$(f_b > f_{cr})$	$(V > V_c)$	

*Notes:*

- $A_g$  = Gross area of the concrete section
- $A_s$  = Gross area of the reinforcing steel
- $A_w$  = Web area
- $E_c$  = Concrete compressive modulus, from ACI-349  $57,000(f'_{c'})^{1/2}$
- $E_s$  = Steel modulus
- $f_b$  = Bending stress
- $f_{cr}$  = Cracking stress
- $G_c$  = Concrete shear modulus =  $0.4 E_c$
- $I_g$  = Gross moment of inertia
- $V$  = Wall shear
- $V_c$  = Nominal concrete shear capacity

For the same purposes mentioned above, damping ratios are taken into account based on the earthquake hazard levels in lieu with ASCE 43-05 as shown in Table 6.2.

**Table 6.2:** Specified damping values for dynamic analysis (ASCE, 2005)

Type of Component	Damping (% of Critical)		
	Response Level 1	Response Level 2	Response Level 3
Welded and friction-bolted metal structures	2	4	7
Bearing-bolted metal structures	4	7	10
Prestressed concrete structures (without complete loss of prestress)	2	5	7
Reinforced concrete structures	4	7	10
Reinforced masonry shear walls	4	7	10
Piping	5	5	5
Distribution systems:			
• Cable trays 50% or more full and in-structure response spectrum Zero Period Acceleration of 0.25 g or greater	5	10	15
• For other cable trays, cable trays with rigid fireproofing and conduits	5	7	7
Massive, low-stressed mechanical components (pumps, compressors, fans, motors, etc.)	2	3	—*
Light welded instrument racks	2	3	—*
Electrical cabinets and other equipment	3	4	5**
Liquid containing metal tanks:			
• Impulsive mode	2	3	4
• Sloshing mode	0.5	0.5	0.5

*Notes:*

- \* Should not be stressed to Response Level 3. Use damping for Response Level 2.
- \*\* May be used for anchorage and structural failure modes that are accompanied by at least some inelastic response. Response Level 1 damping values shall be used for functional failure modes such as relay chatter or relative displacement issues that may occur at a low cabinet stress level.



Coefficients for these adjustments are obtained from ASCE 43-05 (ASCE, 2005). In consequence of using Safe Shutdown Earthquake level, damping ratios are taken as 7% and 5% respectively for reinforced concrete and prestressed concrete members.

## **6.2 Soil Model**

Totally, as described in Chapter 4, ten 1D equivalent linear site response analyses are performed using 1994 Northridge Earthquake horizontal time history. In addition to seven soil profiles, Best-estimate (BE), Lower-bound (LB), Upper-bound (UB) profiles with the coefficient of variation ( $C_v$ ) values are taken into account for the site response analyses. Ten separate site response analyses are carried out for all 10 different soil profiles idealized in 32 layers. Each soil profile is taken as 160 m deep within the scope of SSI analyses.

The corresponding strain-compatible shear moduli and damping ratios are determined from the  $G/G_{\max}$  vs. strain and damping ratio vs. strain input curves. Typical output plots for BE, LB and UB profiles are shown in Figure 6.7.

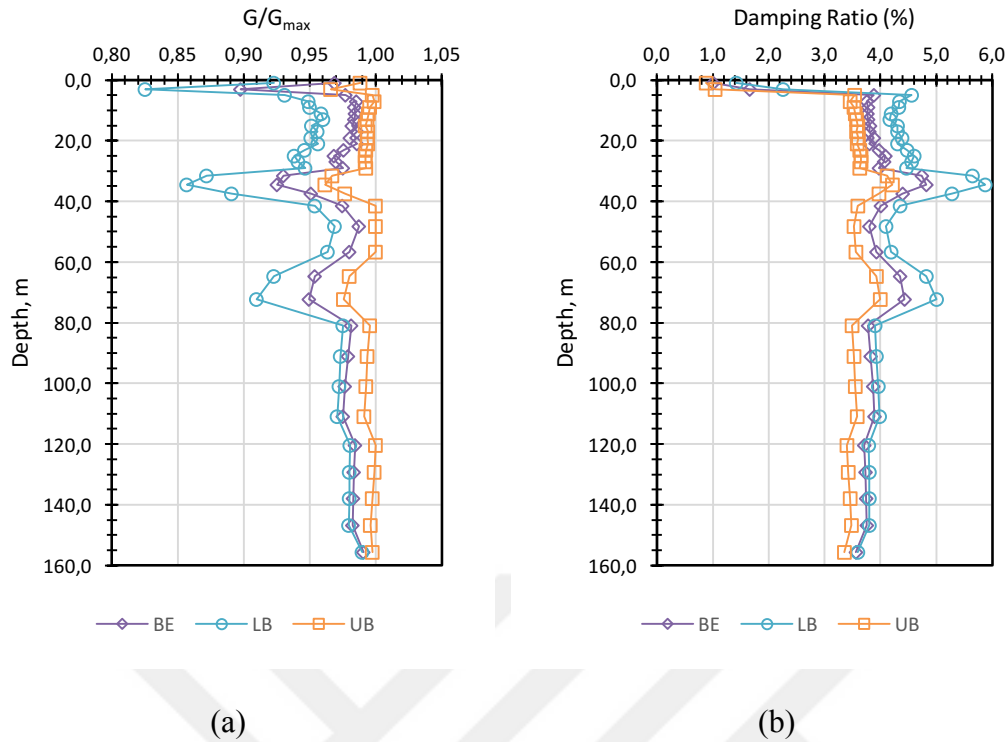
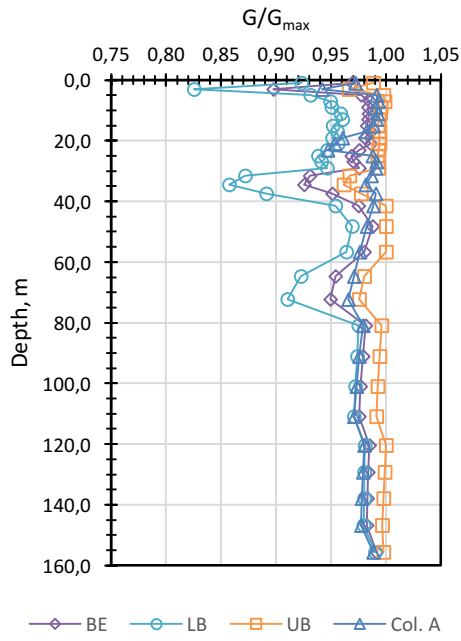


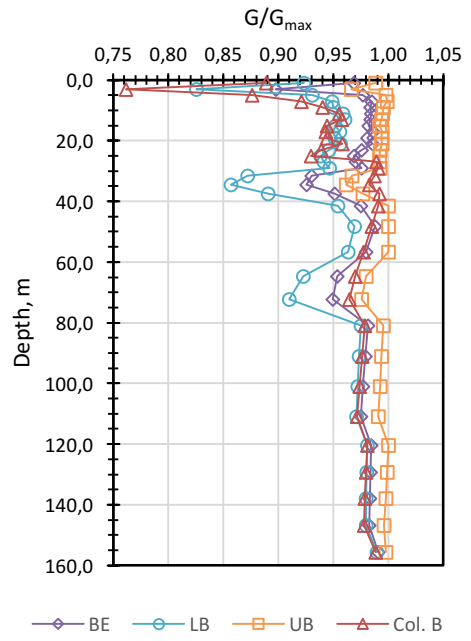
**Figure 6.7:** (a) The variation of strain-compatible  $G/G_{max}$ , (b) damping ratio with depth for BE, LB and UB profiles

Low effective strains are achieved in stiff soil layers with high shear moduli, hence corresponding  $G/G_{max}$  values are obtained above 0.95, demonstrating almost linear behavior. In layers, where higher effective strains are observed, generally at lower depths,  $G/G_{max}$  values reduce down to as low as about 80%. The site response in UB profile is almost linear since the strain-compatible shear moduli achieved are almost above 95% of  $G_{max}$  values at all depths. In BE profile, the shear modulus degradations are down to 90% in less stiff layers. The site response behavior of the LB profile is more nonlinear compared to the other profiles (BE and UB), where the  $G/G_{max}$  values reduce down to 80%. Likewise, as it is seen in the same figure, the damping ratios at deeper and/or stiffer layers are almost the minimum damping ratios, whereas at depths with higher effective strains, damping ratios increased up to about 6%.

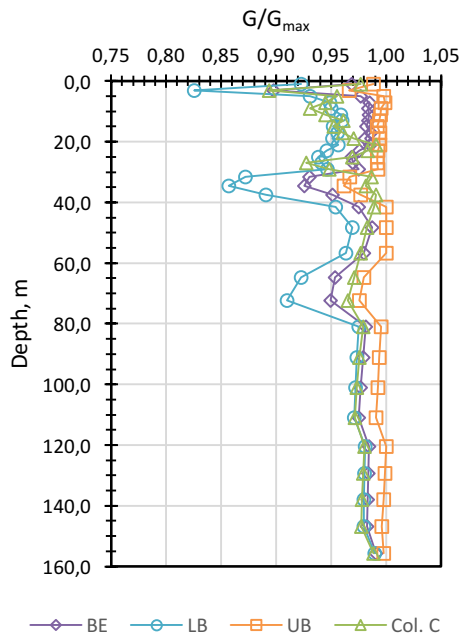
Moreover, the comparison of strain-compatible  $G/G_{max}$  and damping ratios of Col. A – Col. G with BE, LB and UB profiles are depicted in Figure 6.8 and Figure 6.9, respectively.



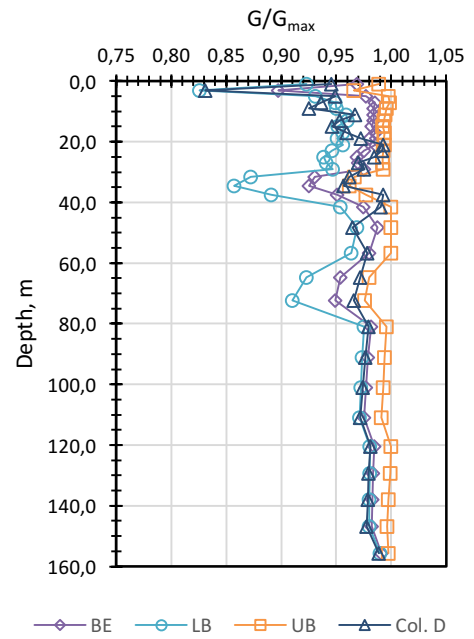
(a)



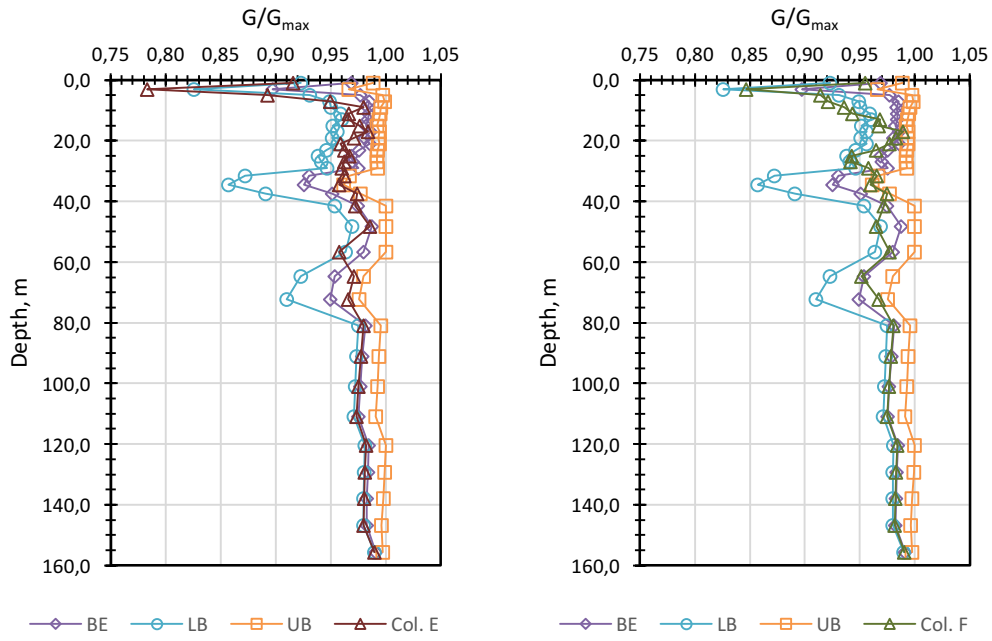
(b)



(c)

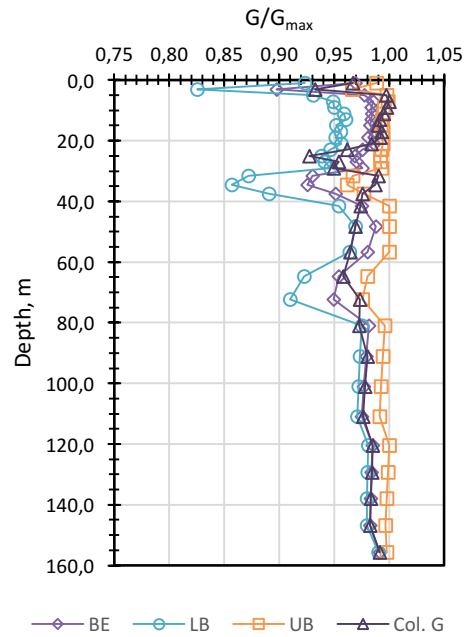


(d)



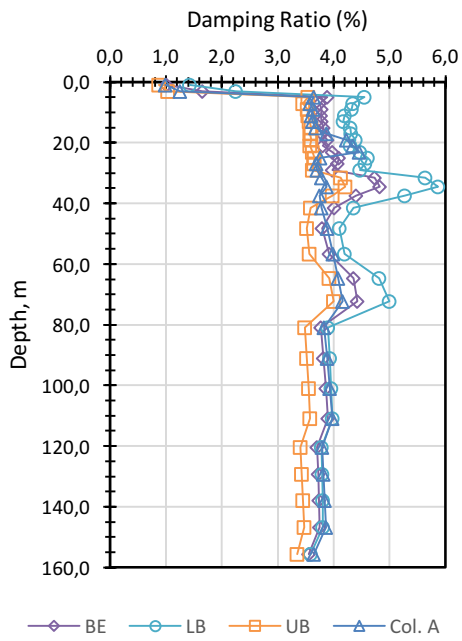
(e)

(f)

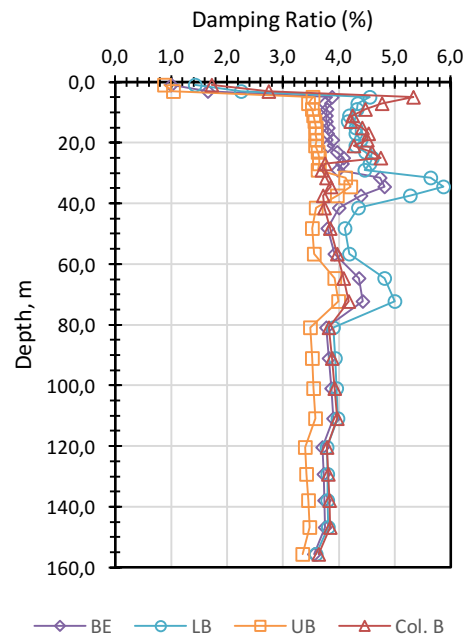


(g)

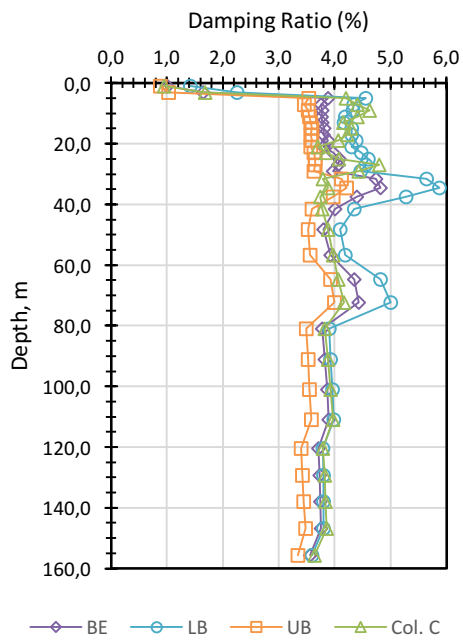
**Figure 6.8:** The comparison of strain-compatible  $G/G_{max}$  of Col. A – Col. G with BE, LB and UB profiles



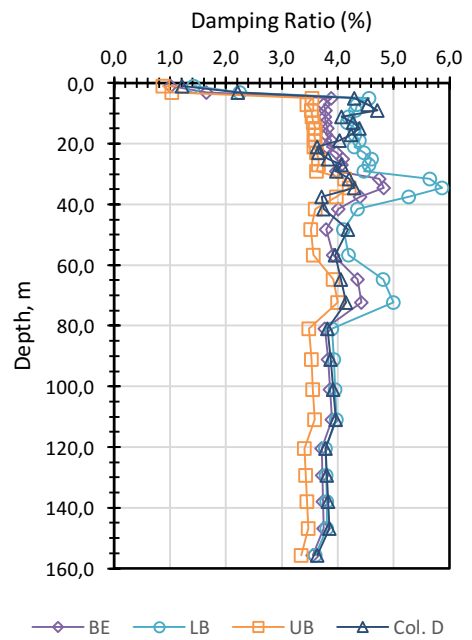
(a)



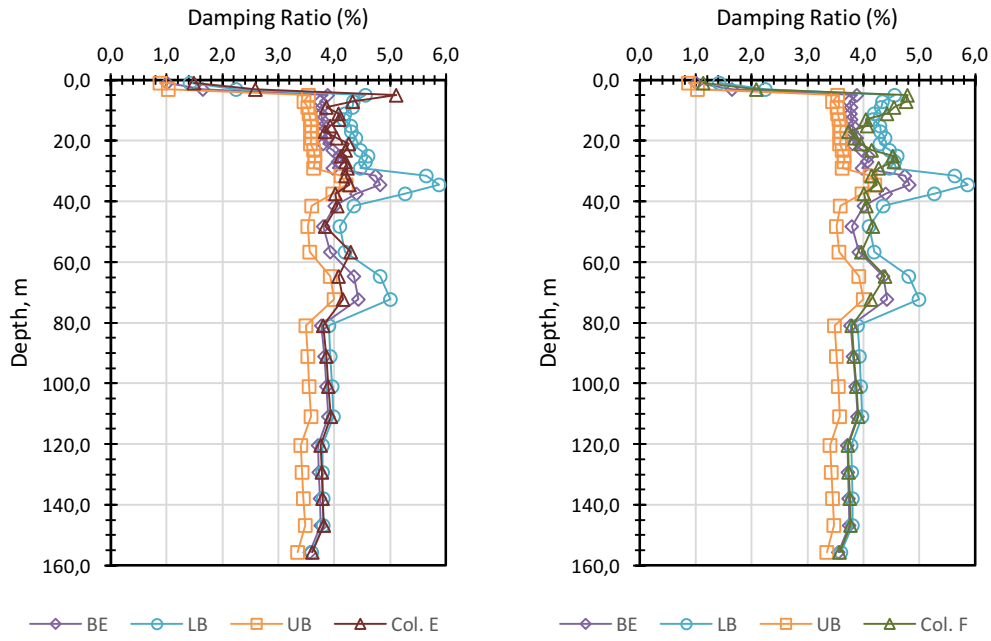
(b)



(c)

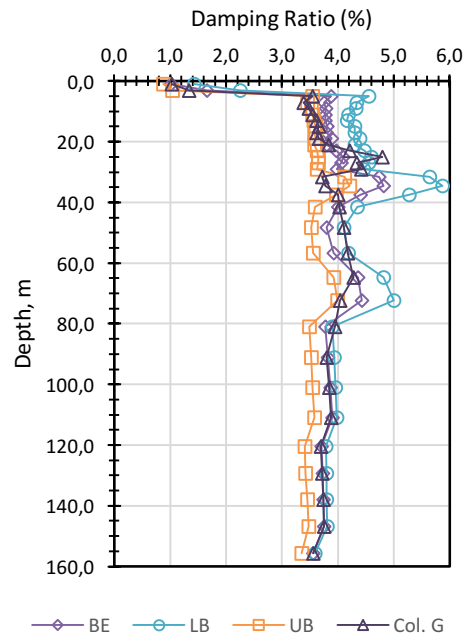


(d)



(e)

(f)

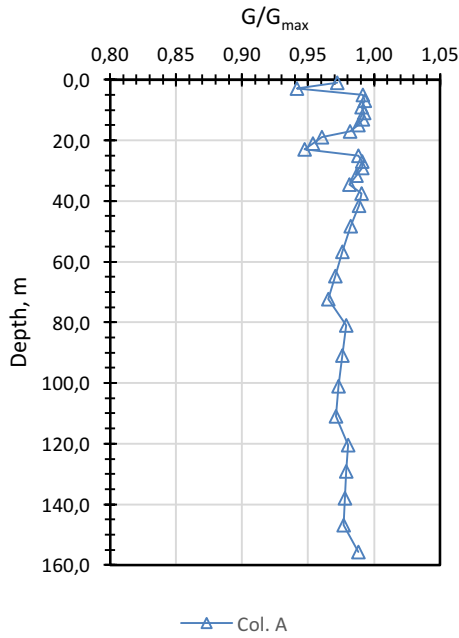


(g)

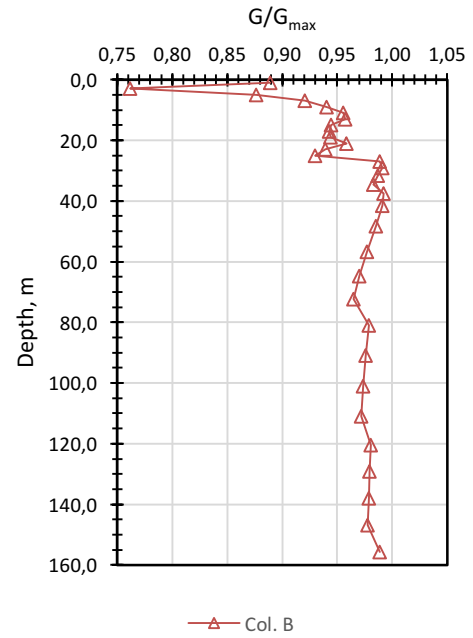
**Figure 6.9:** The comparison of strain-compatible damping ratios of Col. A – Col. G with BE, LB and UB profiles

As seen in Figure 6.10, the site response in Column A and G are almost linear since the strain-compatible shear moduli achieved are almost above 93% of  $G_{max}$  values at

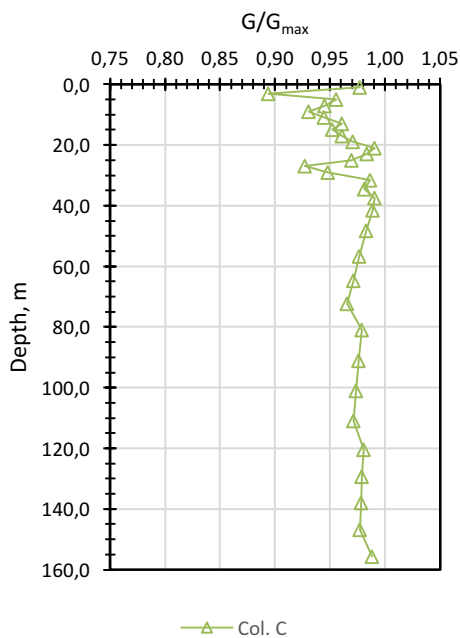
all depths. On the other hand, especially in Column B and Column E  $G/G_{max}$  values reduces down to 0.76~0.78. This may be due to the nonlinear behavior arising from the in-depth variation of soil layer properties.



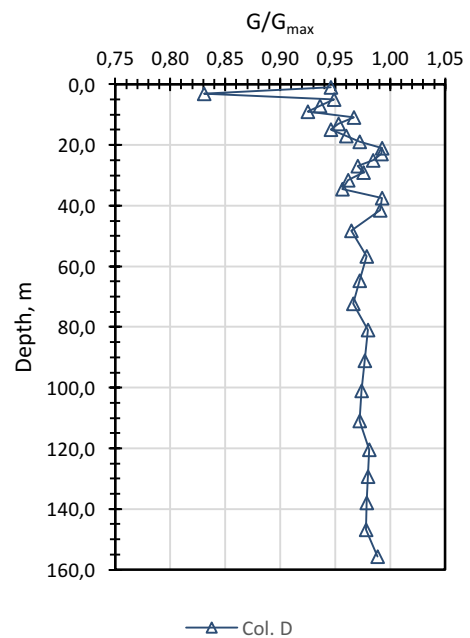
(a)



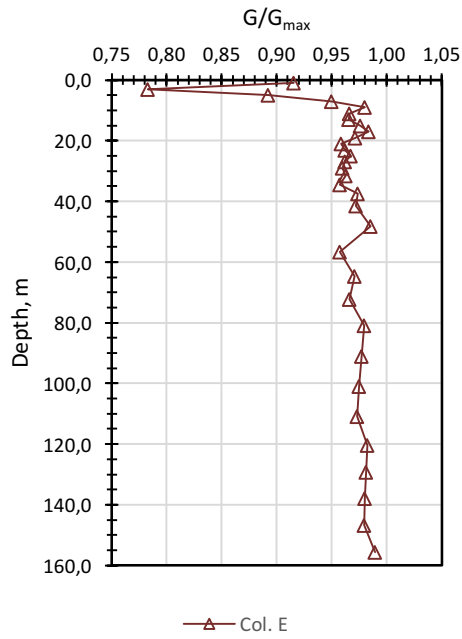
(b)



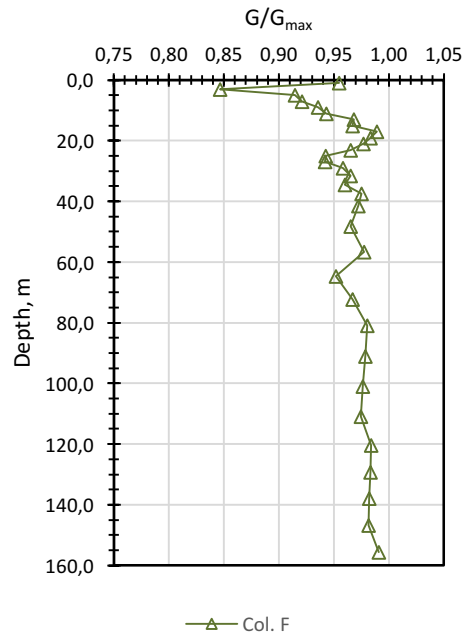
(c)



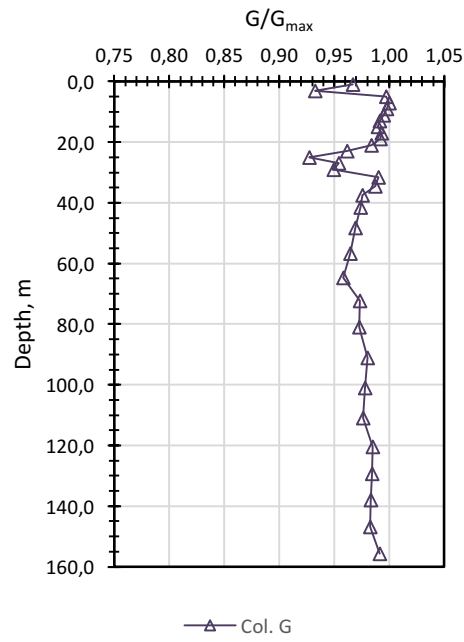
(d)



(e)

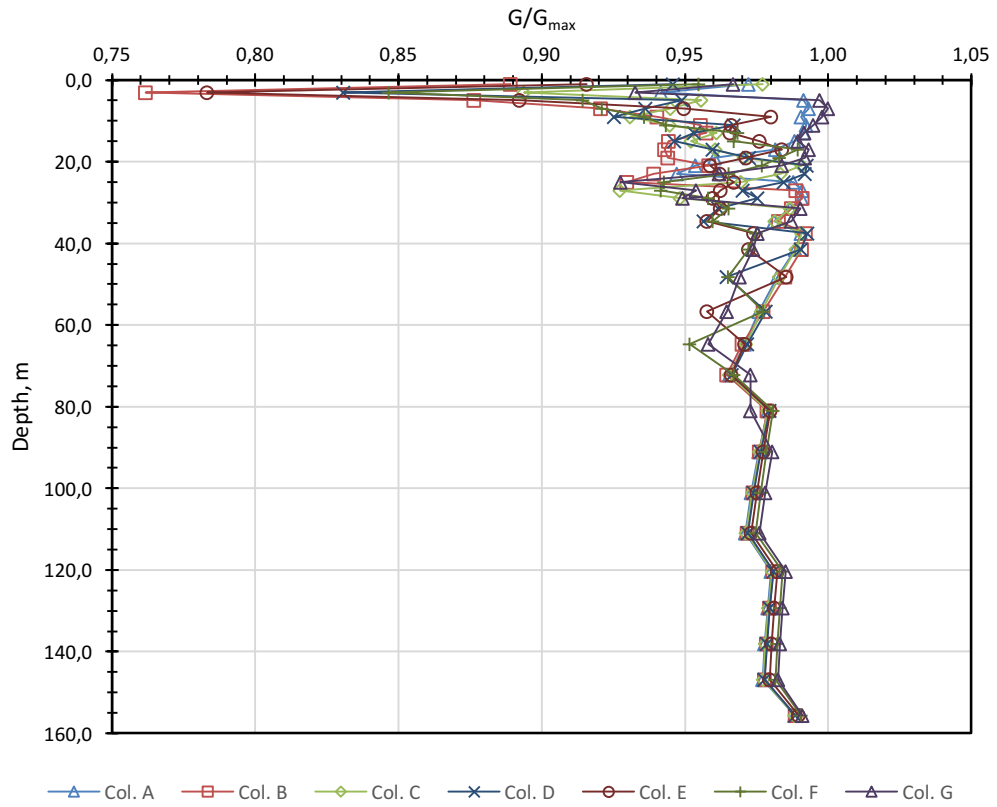


(f)



(g)

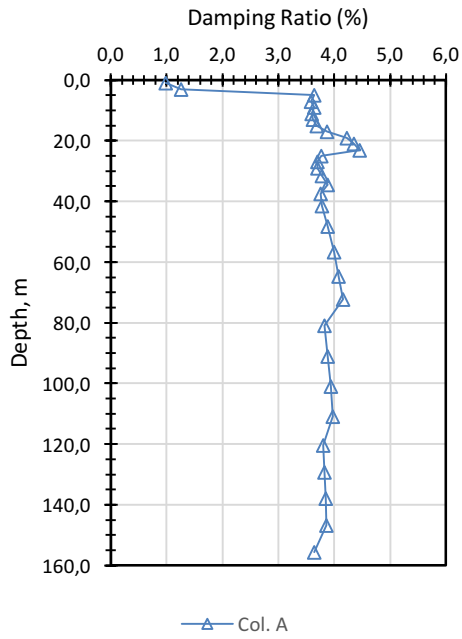




(h)

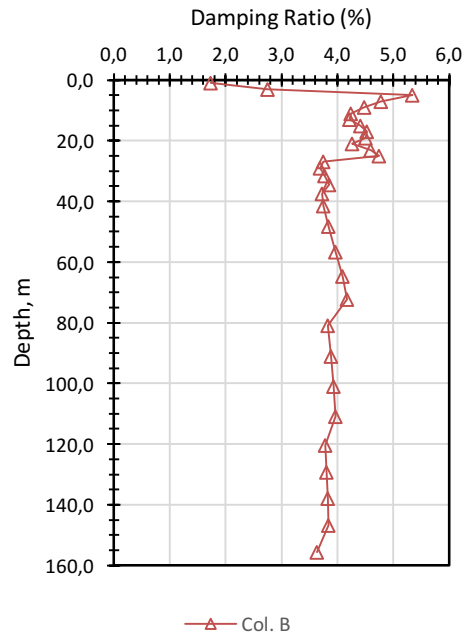
**Figure 6.10:** The variation of strain-compatible  $G/G_{max}$  with depth for Col. A – Col. G profiles

Besides, as it is shown in Figure 6.11, the damping ratios at deeper and/or stiffer layers are almost the minimum damping ratios, whereas at depths with higher effective strains, damping ratios increased up to about 5.4%.



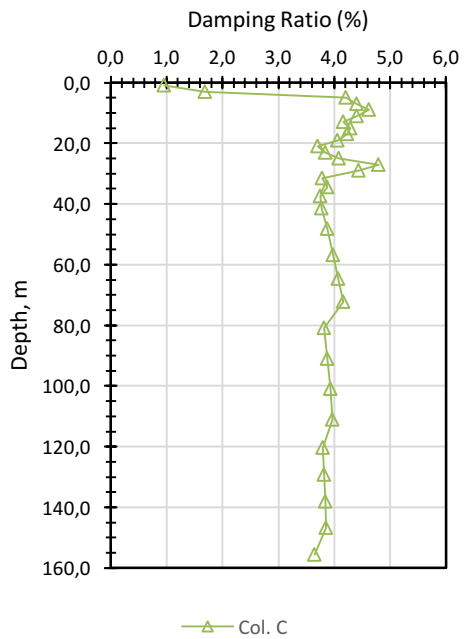
—△ Col. A

(a)



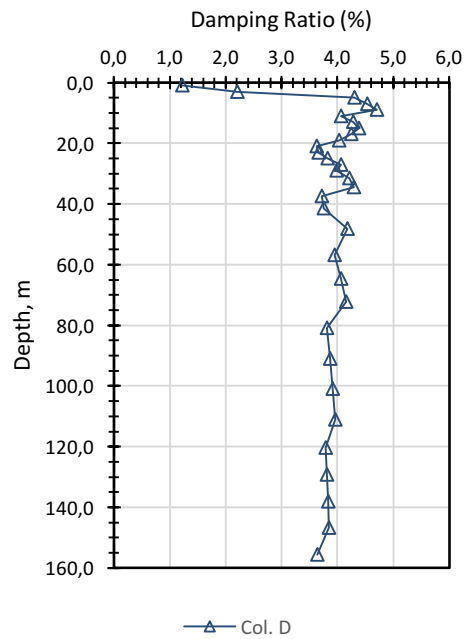
—△ Col. B

(b)



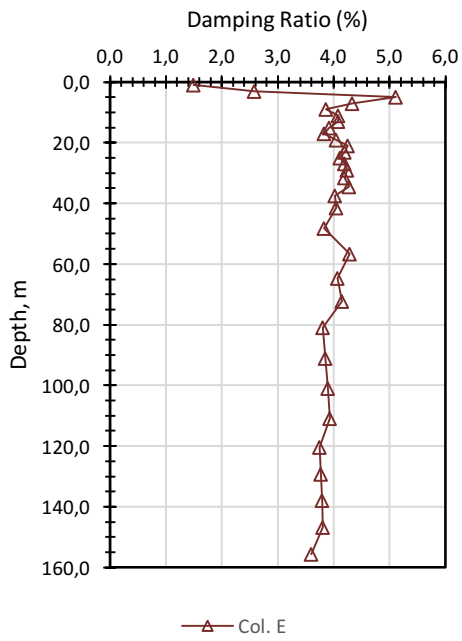
—△ Col. C

(c)

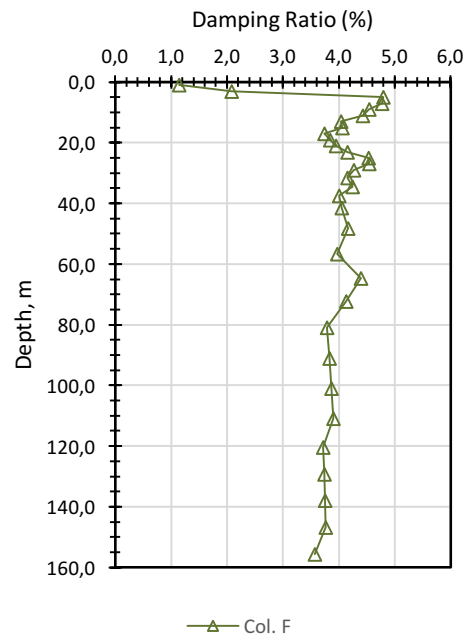


—△ Col. D

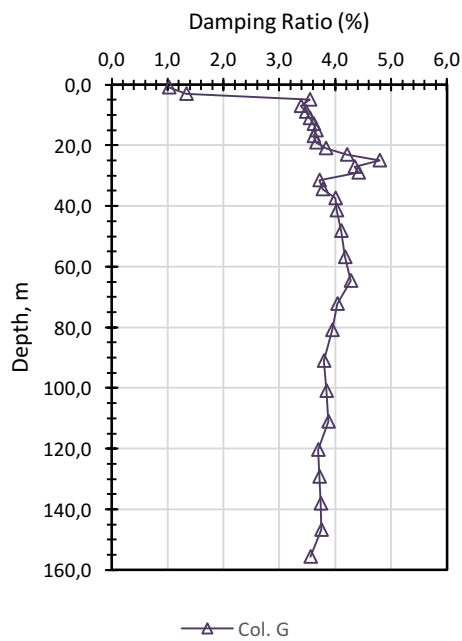
(d)



(e)



(f)



(g)

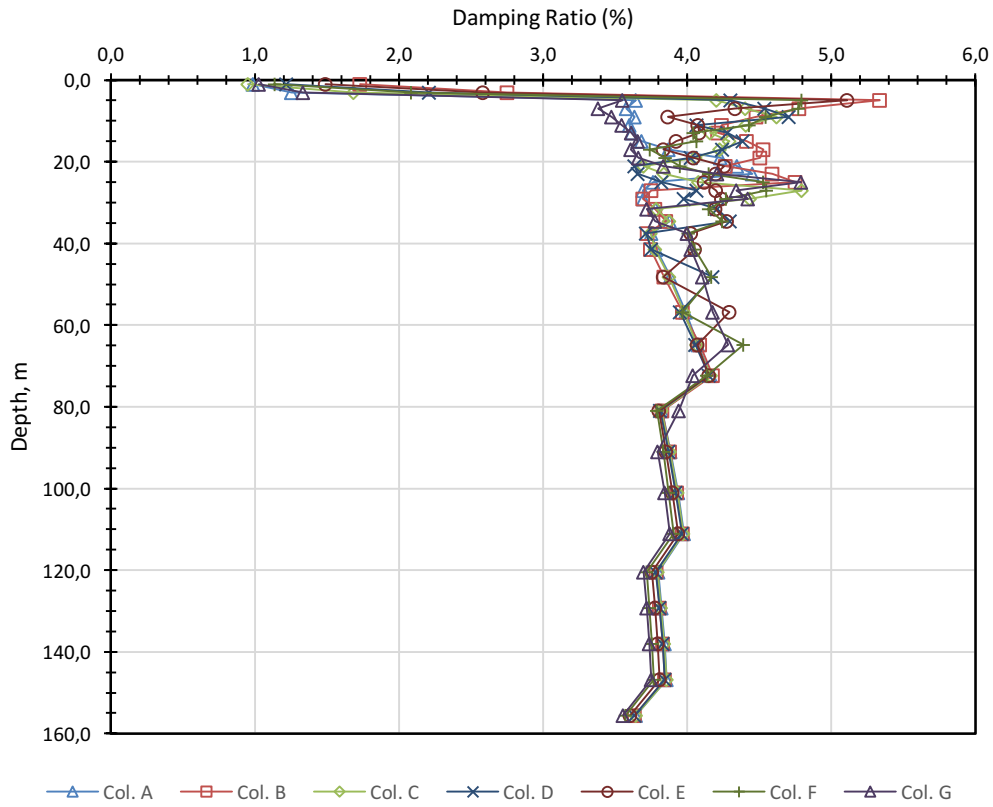


**Figure 6.11:** The variation of strain-compatible damping ratio with depth for Col. A – Col. G profiles

Additionally, the variation of  $G_{\max}$  (small-strain) values with depth for Col. A – Col. G profiles are depicted in Figure 6.12.

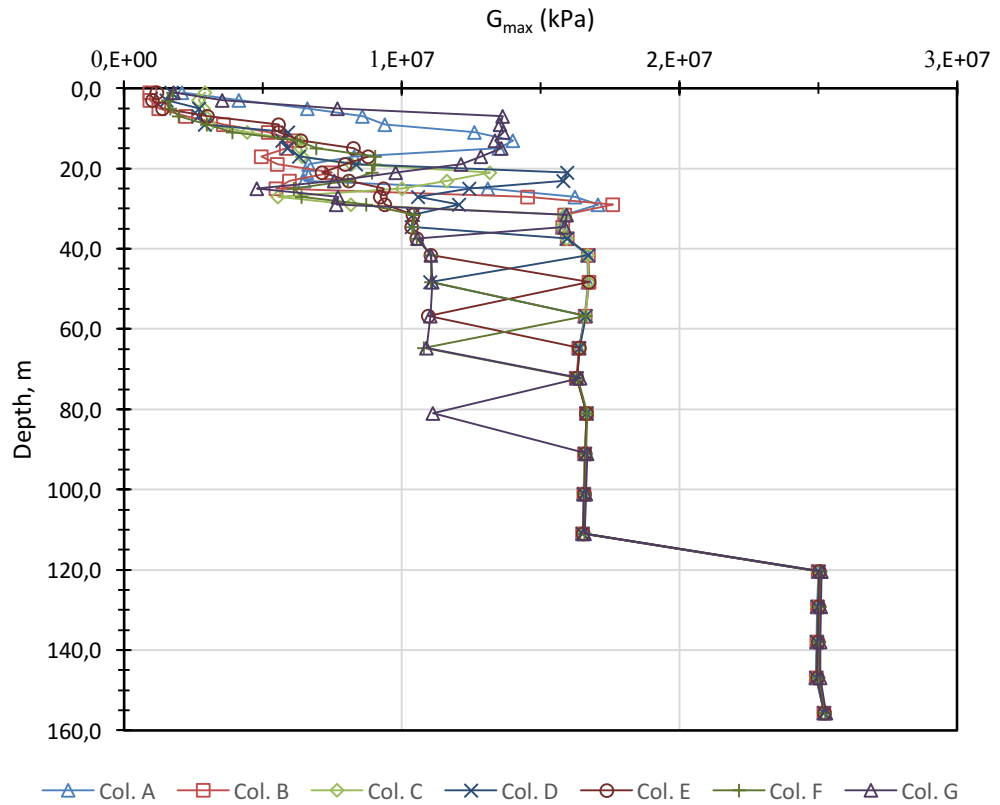
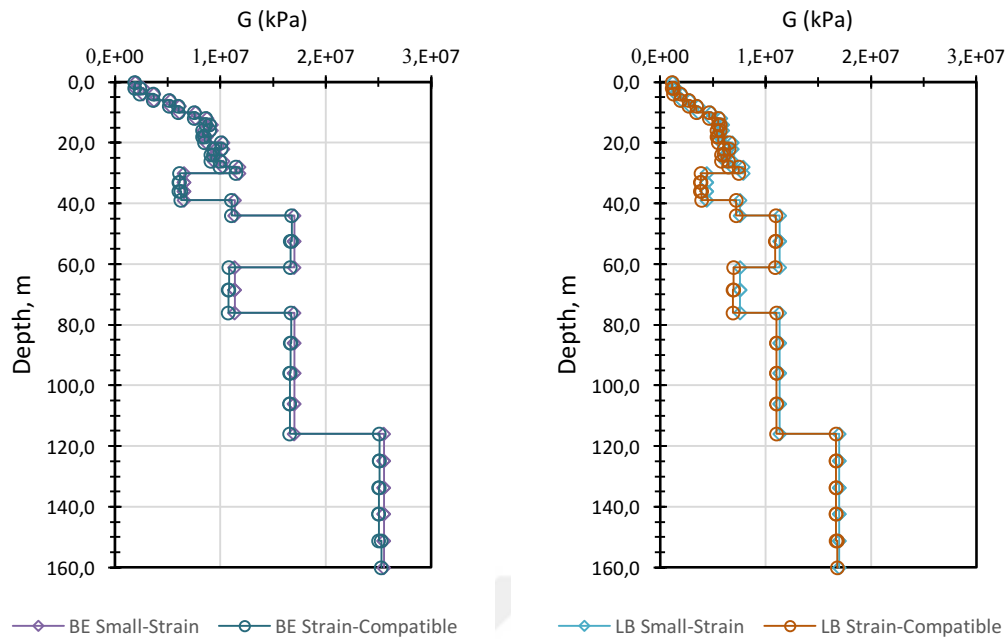


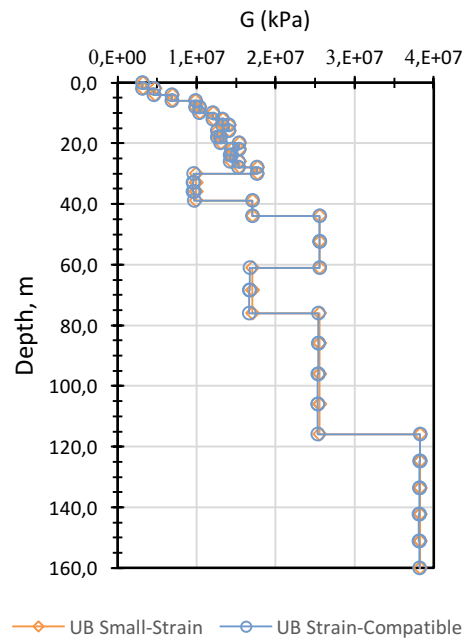
**Figure 6.12:** The variation of  $G_{max}$  values with depth for Col. A – Col. G profiles

As input for soil-structure interaction analysis of the building, the strain-compatible shear modulus depth and damping ratio depth profiles of the foundation soil are computed from each ten one-dimensional equivalent linear site response analyses. In substructure soil model in SASSI analysis, dynamic high-strain properties of these soil profiles which are shown in Figure 6.13 and Figure 6.14 are used.



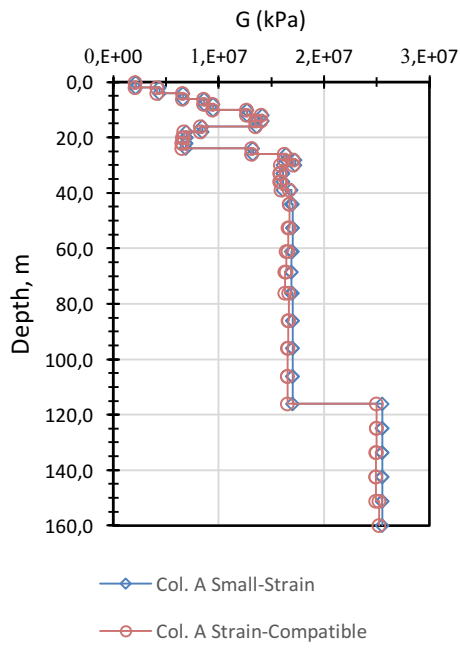
(a)

(b)

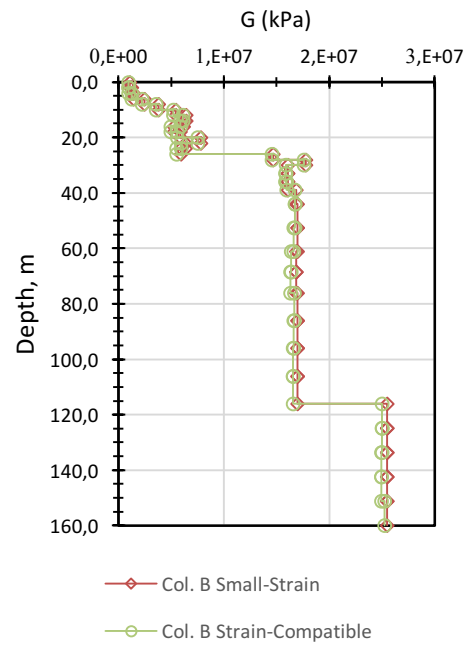


(c)

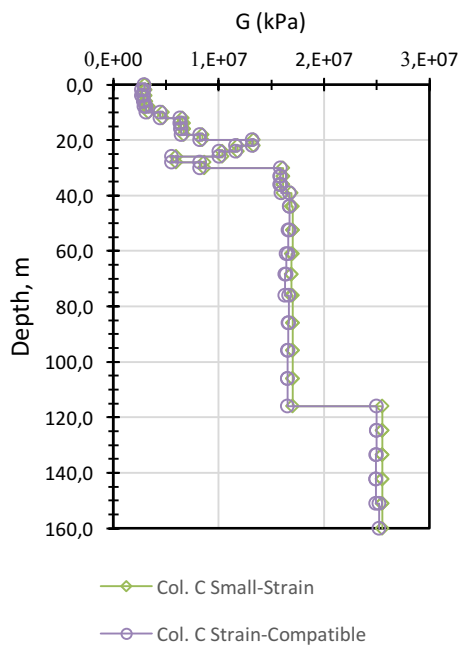
**Figure 6.13:** The variation of small-strain and average strain-compatible shear moduli ( $G$ ) with depth for (a) BE, (b) LB and (c) UB profiles



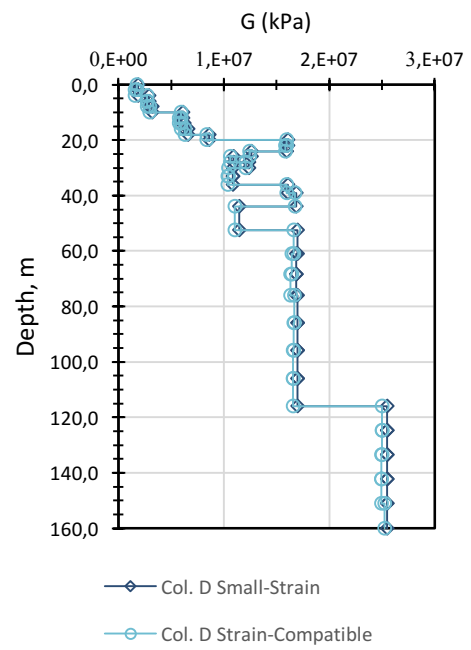
(a)



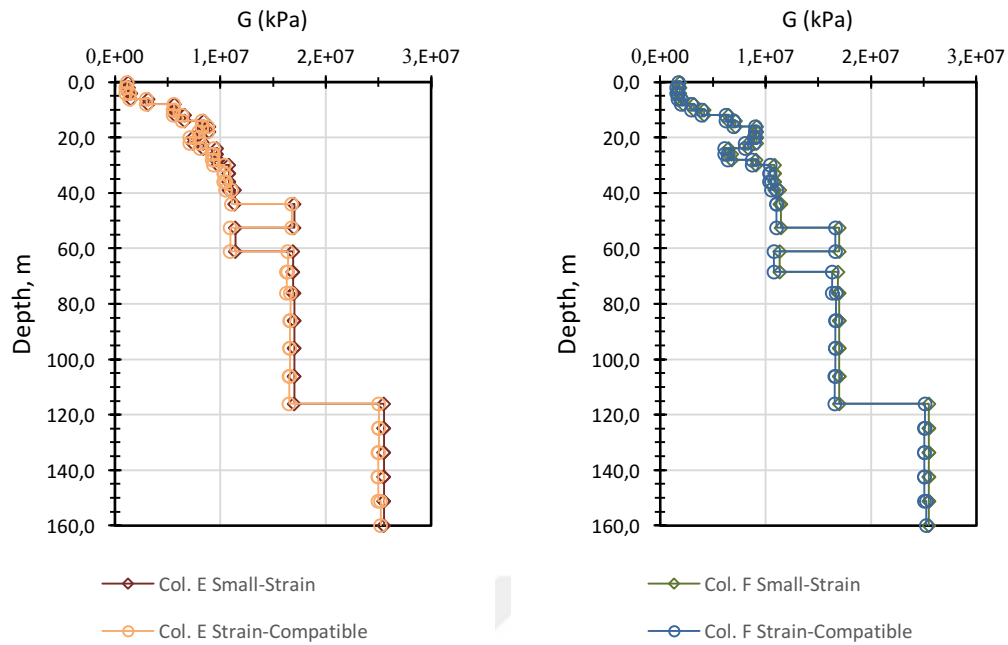
(b)



(c)

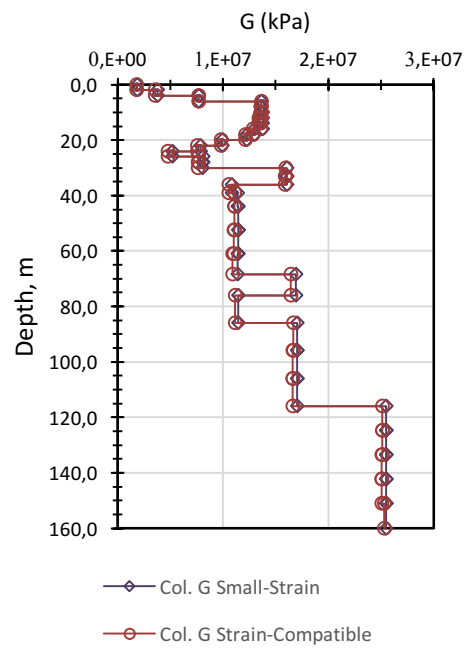


(d)



(e)

(f)



(g)

**Figure 6.14:** The variation of small-strain and average strain-compatible shear moduli ( $G$ ) with depth for Col. A - Col. G profiles



### 6.3 Input Ground Motion

In compatible with the design spectra depicted in Figure 6.15, ground motion Northridge 1994 is used in the site response analyses. In the site response analyses, foundation input time histories sets are obtained from 1D seismic site response analyses.

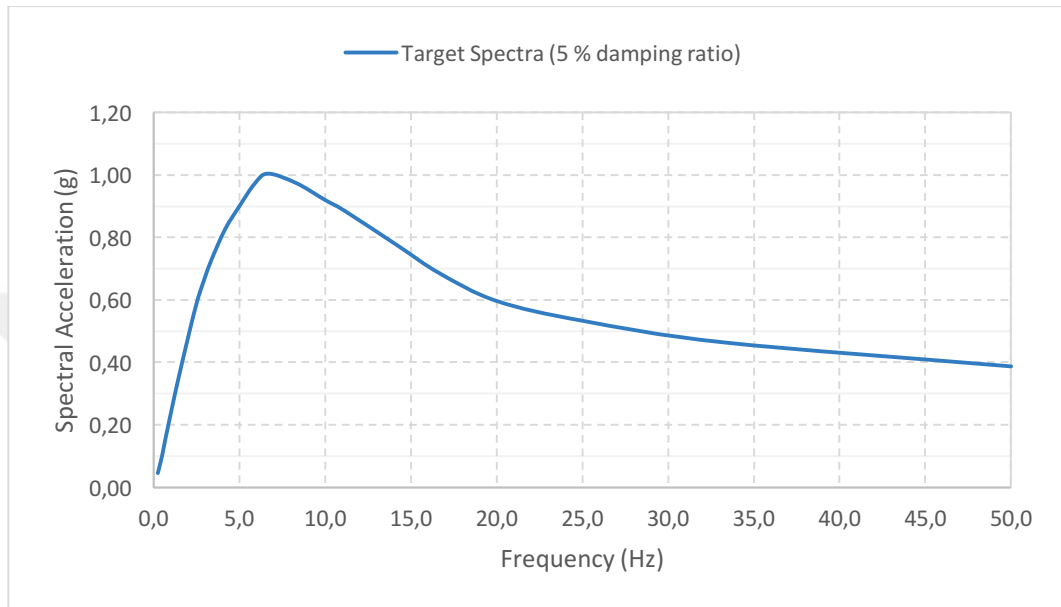


**Figure 6.15:** Horizontal design target spectra

These foundation input motion time history sets are used for the SSI analyses. In order to generate ground motion time histories data based on the acceptance in ASCE 43-05 (ASCE, 2005), spectral matching method are applied using ACS SASSI software. Station and seismic event information of the seed ground motion used in the spectral matching application is presented in Table 4.4. Foundation input ground motion for 10 different soil-structure analysis obtained from 10 soil profiles are presented in Figure 6.16 – 6.25.

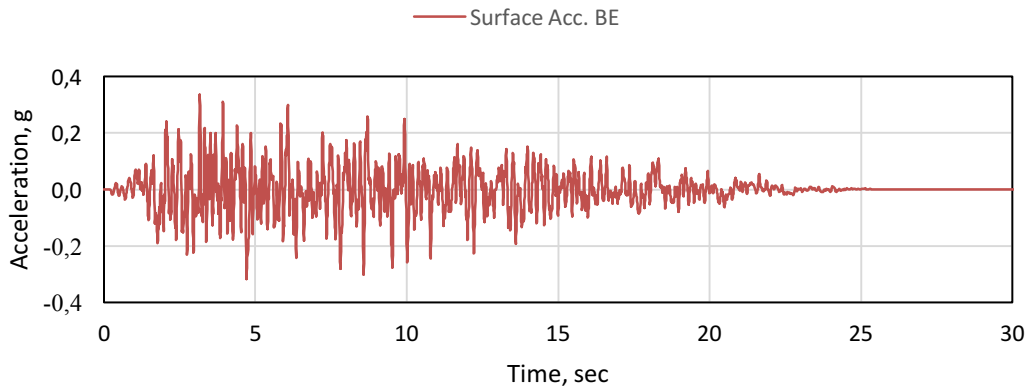


**Figure 6.16:** Foundation input motion obtained from best-estimate soil profile

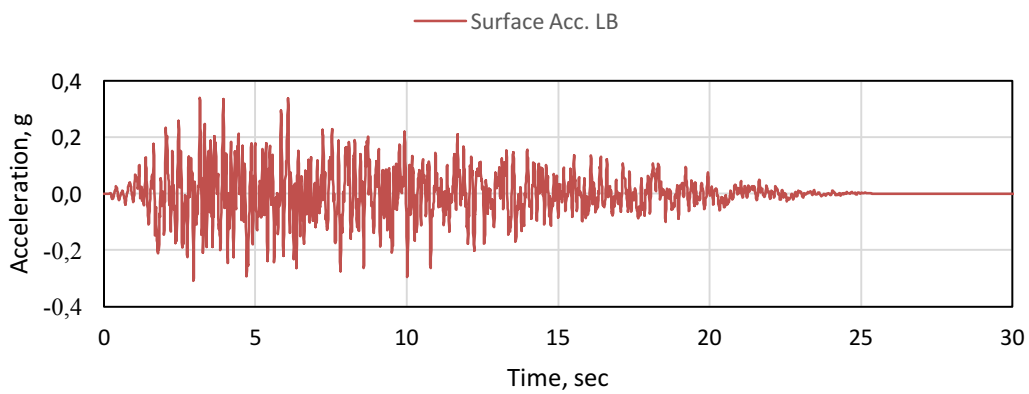


**Figure 6.17:** Foundation input motion obtained from lower-bound soil profile

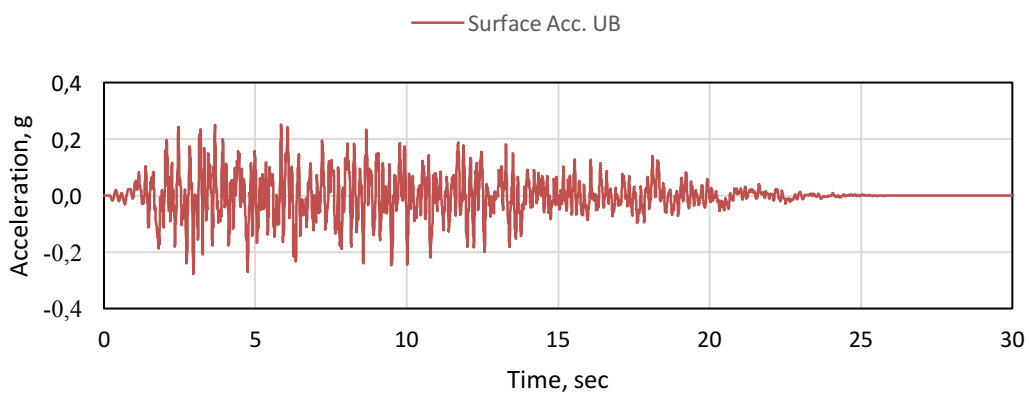


**Figure 6.18:** Foundation input motion obtained from upper-bound soil profile

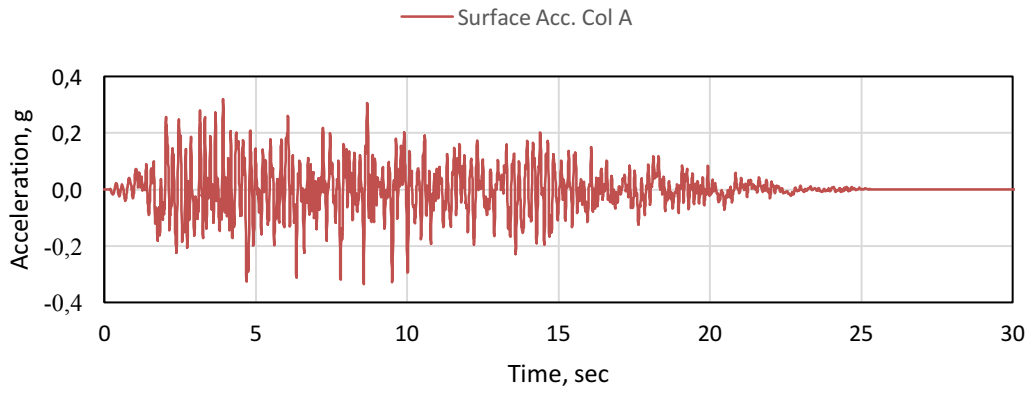


**Figure 6.19:** Foundation input motion obtained from Col A soil profile

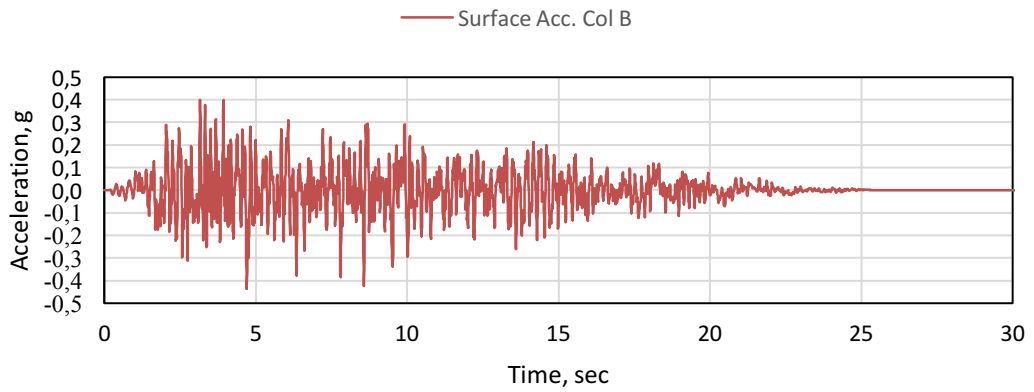


**Figure 6.20:** Foundation input motion obtained from Col B soil profile

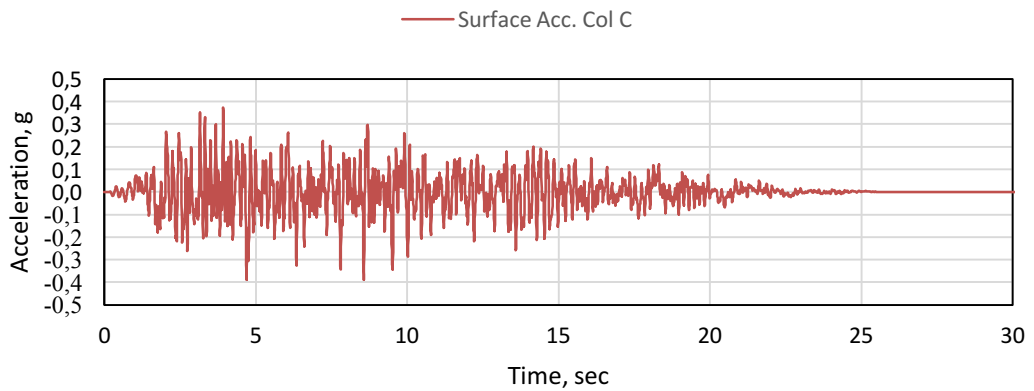


**Figure 6.21:** Foundation input motion obtained from Col C soil profile

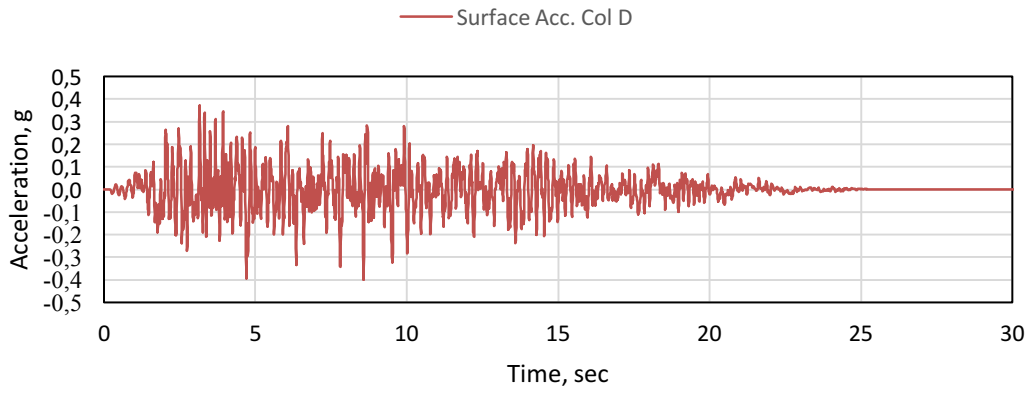


**Figure 6.22:** Foundation input motion obtained from Col D soil profile

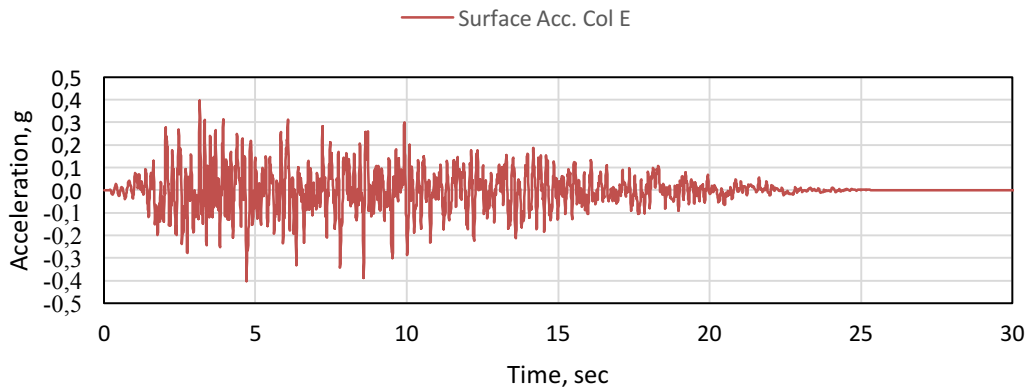


**Figure 6.23:** Foundation input motion obtained from Col E soil profile

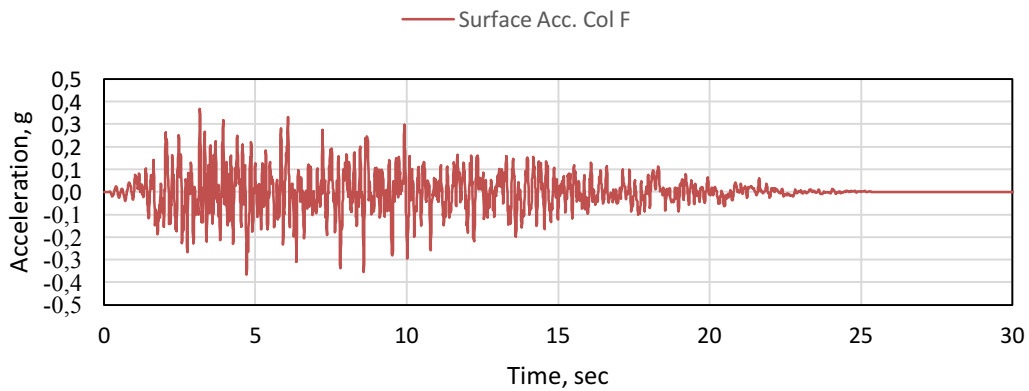


**Figure 6.24:** Foundation input motion obtained from Col F soil profile

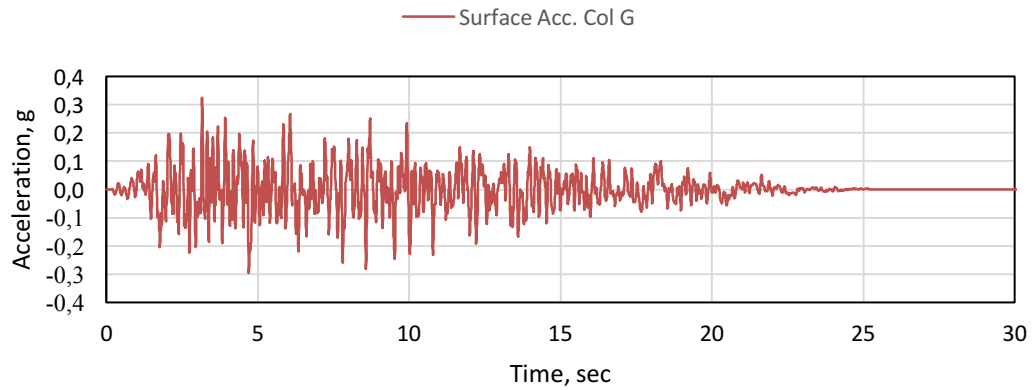


**Figure 6.25:** Foundation input motion obtained from Col G soil profile

In order to demonstrate the local seismic response of the reactor building, in-structure response spectra (ISRS) are generated for the earthquake level based upon the modified record seismicity of the hypothetical site.

#### **6.4 Transfer Functions and In-Structure Response Spectra**

According to the site response analysis results, transfer functions and the in-structure response spectra (ISRS) are calculated at different elevations and locations where critical equipment is located. For in-structure response spectra generation, considering critical equipment locations, 6 regions are selected. The in-structure response spectra plots are generated for 2% damping. In Table 6.3, locations of the calculated in-structure response spectra are shown.

**Table 6.3:** Calculated ISRS Locations

<b>ISRS Region</b>	<b>Structure</b>	<b>Location</b>
1	Outer containment (foundation plate)	Foundation plate from outer walls to annulus
2	Foundation plate	Foundation plate center
3	Foundation plate	Foundation plate upper right
4	Containment internal	Elevation +26.3 m
5	Inner containment	Zenith. Elevation +61.7 m
6	Outer containment	Zenith. Elevation +65.4 m

One of most critical step in the frequency domain dynamic analysis is that the frequency dependent transfer functions of the SSI model are calculated. These functions are mapping the input motion at the control location to the response at the degree-of-freedoms. In the SASSI software, the transfer functions are obtained by curve fitting to SSI analysis results at selected frequencies. In order to obtain accurate transfer functions it's suggested that solutions are obtained at least 75 frequencies that are listed in Standard Review Plan (SRP) 3.7.1 (U.S. NRC, 2007b).

Transfer functions show the dynamic input output relation of control point and other nodes in the system. Dynamic response of the reactor building is obtained by multiplying transfer functions and ground motion time histories in frequency domain. Therefore, calculation of the transfer functions is critical for obtaining an accurate estimate of dynamic behavior of the reactor building.

Computing transfer function data points at each frequency point is not efficient, as it requires very high computational power. On the other hand, curve fitting techniques such as interpolation functions yield accurate results even with much smaller frequency lists. The SSI analysis of reactor building was performed using transfer functions that were developed in ACS SASSI (GP Technologies Inc., 2014) using 75 frequencies provided in SRP 3.7.1 (U.S. NRC, 2007b). Transfer function data points

are initially calculated at 75 standard frequencies as well as at the fundamental frequencies of the super-structure. These data points in transfer functions were interpolated using SASSI interpolation algorithms. Initial data points in transfer functions are interpolated using the second interpolation algorithm option of SASSI, which is dense overlapping windows scheme. From the output of this interpolation additional frequencies were selected based on peaks and the shape of the transfer function at multiple structural nodes.

In-structure response spectra are used for the seismic response calculation and the risk assessment of critical equipment in the reactor building. In SASSI analyses, dynamic response of the reactor building was calculated for each 10 soil condition considering the foundation input motion obtained using each 10 soil profile. These in-structure response spectra are compared for the locations presented in Table 6.3. The ISRS shown in Figure 6.26 – 6.31 are obtained from SASSI results.

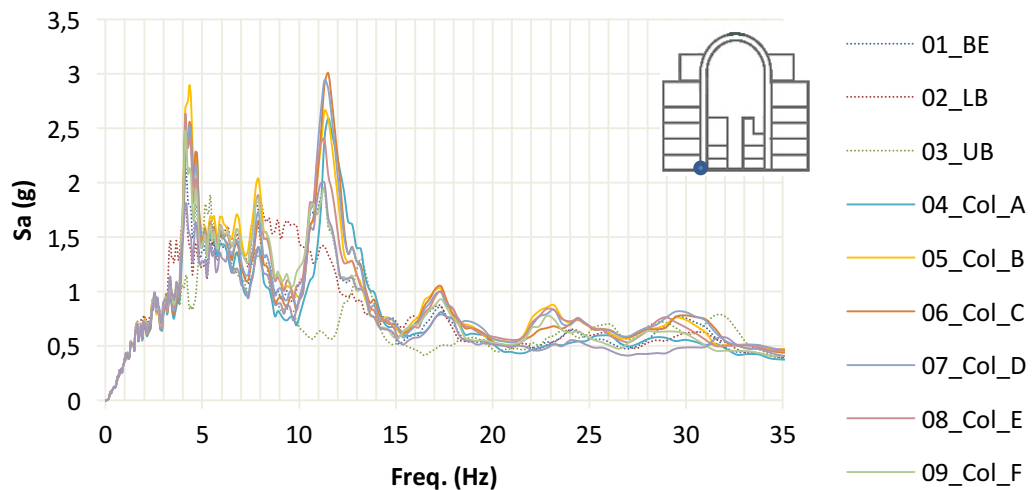


**Figure 6.26:** Comparison of ISRS at Region 1 for each soil profile

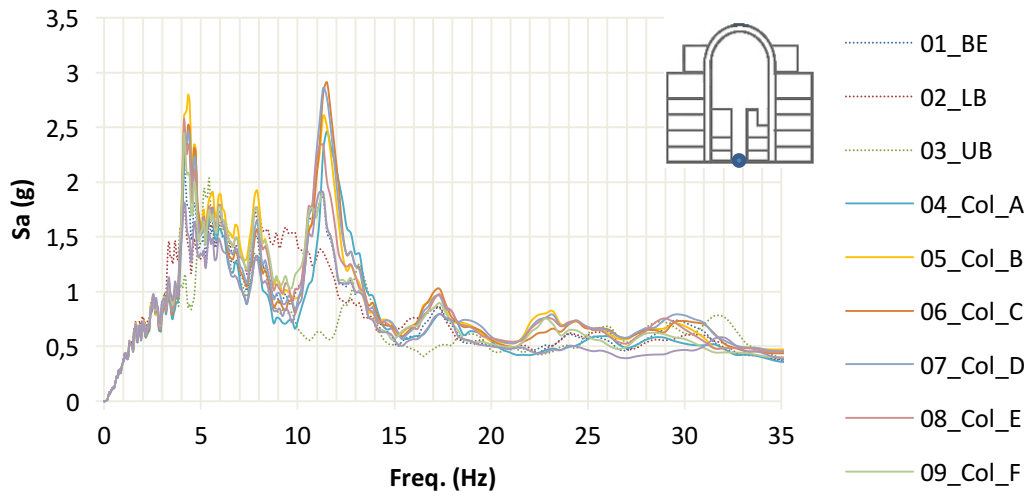


**Figure 6.27:** Comparison of ISRS at Region 2 for each soil profile

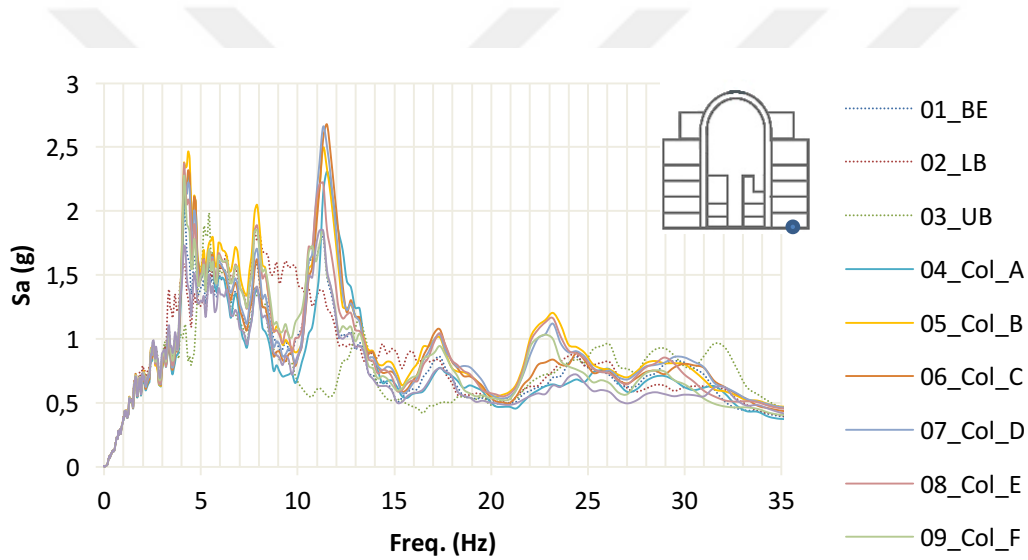


**Figure 6.28:** Comparison of ISRS at Region 3 for each soil profile



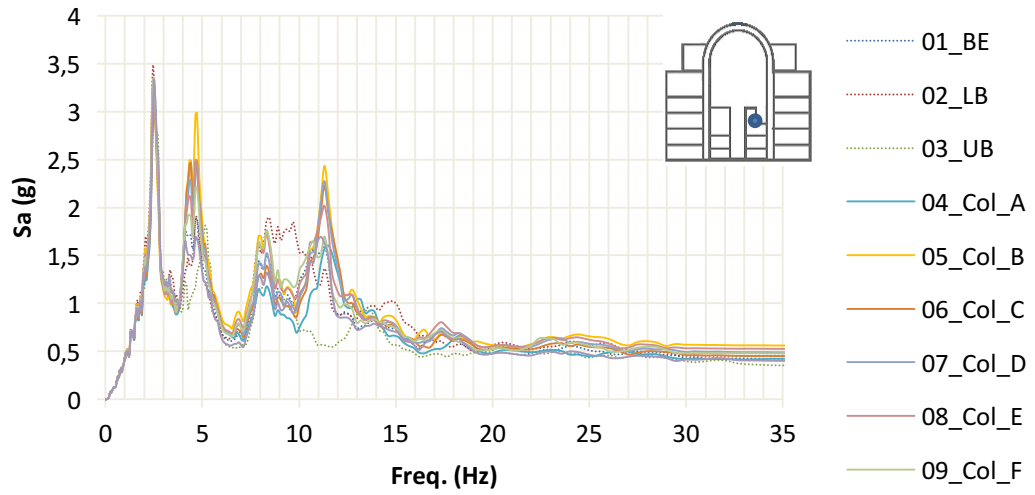


**Figure 6.29:** Comparison of ISRS at Region 4 for each soil profile

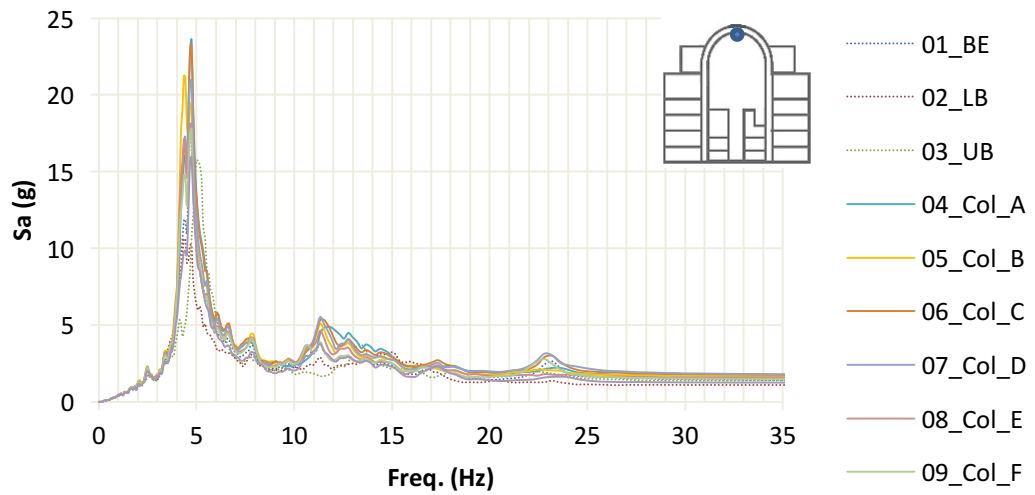


**Figure 6.30:** Comparison of ISRS at Region 5 for each soil profile

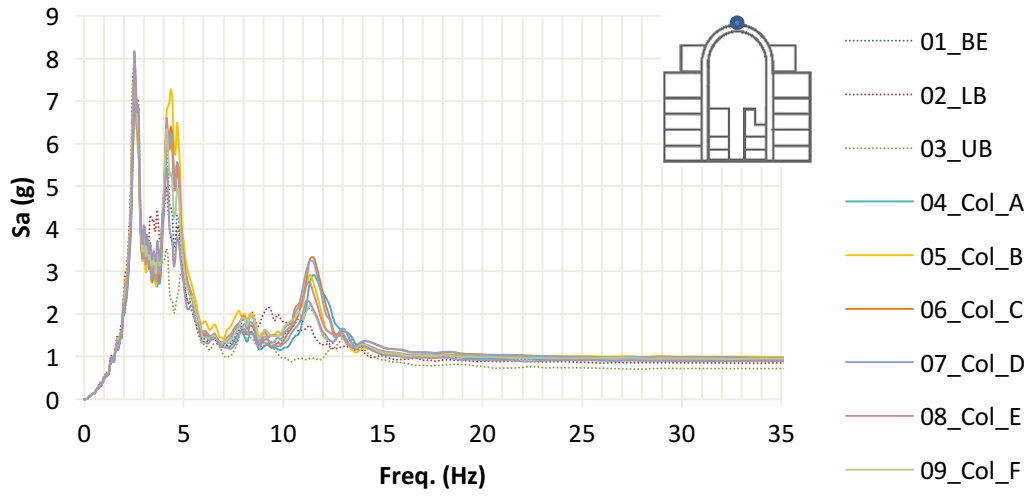


**Figure 6.31:** Comparison of ISRS at Region 6 for each soil profile

## **7. RESULTS AND DISCUSSIONS**

In this thesis, the influence of soil heterogeneity throughout the subsurface of nuclear reactor building with containment structure, which is identified as the most important structure in nuclear power plant designs, is studied.

During an earthquake, the properties of soil media affects the dynamic response of the structure. These dynamic effects transferred from the soil to the structure and vice versa, is named as soil-structure interaction (SSI).

Within this context, site parameters and their variations in lateral and vertical directions are taken into account to investigate site heterogeneity effects and their transfer to the super-structure. Strain dependent modulus degradation and damping curves are used to take into account the nonlinearity in the equivalent linear soil response analyses performed using DEEPSOIL software for 10 different soil profiles. Accordingly, soil model with dynamic high-strain properties and foundation input motion that are incorporated into the soil-structure interaction analyses performed using ACS SASSI software based on the International Atomic Energy Agency (IAEA) safety guides and U.S. standards and guidelines.

The results are given as graphs that includes in-structure-response-spectra considering the effects of each soil profile in certain points of super-structure, and those graphs are compared. Hence, the dynamic seismic response of the structure originating from the soil parameters and their influence on the outputs of the soil-structure interaction analyses are discussed.

### **7.1 Effects of Soil Geometry**

The influences of site heterogeneity due to the deeply inclined layering on the dynamic responses of the foundation and super-structure are investigated.

The effect of deeply inclined layering at the site on the foundation input motion is investigated through equivalent linear site response analyses in free-field. One-dimensional analysis method has been chosen in the scope of the thesis and the fact

that these 1D and 2D have differences considering free-field foundation input motions resulting from site response analyses. However, insignificant deviations are observed within the context of in-structure response spectra, particularly at the foundation.

Based on the site response analyses performed in free field on the 2D inclined layered soil model under earthquake motion, it is concluded that the peak ground accelerations are not varying noticeably along the width of the foundation, nevertheless the peak spectral accelerations are considerably changing from the north to the south of the foundation.

The importance of the analysis depth in site response analysis when input motion is applied at the bedrock is not discussed.

## **7.2 Effects of Soil Parameters Variation**

According to the shear wave velocity variations with depth, the  $V_s$  profiles on the most south and the most north sections of the site significantly differ from the  $V_s$  profiles on the middle sections. This deviation is contributed to the deep slope layering of the rock over each other in north-south direction. This layering scheme repeats itself on the east-west direction.

According to ASCE 4-98 (ASCE, 2000), small-strain values, best estimate (BE), upper bound (UB) and lower bound (LB) soil profiles should be taken into account for uncertainties in the SSI analysis and soil properties.

As discussed previously, ten different soil profiles, including BE, LB and UB, are considered in these soil-structure interaction analyses. The wide variation in thickness of each unit or layer in the ten soil profiles are thought to be sufficient to allow qualitative assessment of the potential influence of soil parameter variation on the dynamic response of the structure.

Generally, it is seen that the soil parameter change is more at the first 10 - 15 metres depth. Besides, it is concluded that in-depth variation of the soil layers impedances, especially in Column B, have significant effects on the dynamic structural response.

### **7.3 Comparison of In-Structure Response Spectra**

In the low frequency regions of the in-structure response spectra (ISRS) plots, largest horizontal peaks are observed at 3-4 Hz range. This is compatible with the horizontal natural frequency of the reactor building. Low frequency regions in the ISRS plots demonstrate fundamental global behavior of the structure.

This also suggests that very stiff rock layers under the reactor building do not change the SSI behavior of the reactor building significantly at low frequencies.

Generally, in this generic reactor design, the main components of the reactor are located in the containment internal part, especially on the +26.3 m elevation (Gidropress, 2011a). This location represents Region 4 in Table 6.3. The results of the each soil profile's ISRS indicate that site heterogeneity is not likely influential for brittle components such as relays and ceramic insulators at high frequency motions above about 20 Hz. However, it is seen that the site heterogeneity has significant effects between the frequencies of 10–12 Hz. It may influence the components in this natural frequency interval.

According to the ISRS plots, it can be concluded that the site heterogeneity has significant influence on the dynamic response of foundation. However, this effect diminishes at the higher elevations on the super-structure.

### **7.4 Future Recommendations**

In this thesis, the soil effects on a nuclear power plant structure has been studied through one-dimensional equivalent linear site response analyses and frequency domain SASSI methodology, which is industry standard.

The utilization of these equivalent linear codes to calculate the responses of both soil and structure might be insufficient for heterogeneous subsurface soil media. Time-domain finite element programs such as LS-DYNA will be more capable to analyze in such soil conditions. However, assumptions and boundary conditions should be carefully defined.

Probabilistic soil-structure interaction analysis methods using Monte Carlo simulation and Latin Hypercube simulation can be utilized to determined the site properties. A

minimum of 30 site response calculations when using Latin Hypercube and 200 calculations when using Monte Carlo simulation is suggested to reduce uncertainties.

The results of this study show that site heterogeneity may be influential for some certain locations in the containment structure. As for the proposals, a fragility assessment would be useful for those type of components considering site heterogeneity in the future works.



## 8. SUMMARY AND CONCLUSIONS

Heterogeneous configuration of subsurface soil media under a dynamic effect such as an earthquake may be influential on the behavior of structures. Dynamic response of a reactor building, which is deemed as the most critical structure in a nuclear power plant facility, is investigated taking into account the site heterogeneity.

A variety of scenarios including different soil columns, assumptions and boundary conditions are considered in the site response analyses and accordingly soil-structure interaction calculations. Within this scope, in order to take into account the soil nonlinearity, strain dependent modulus degradation and damping curves are incorporated into the equivalent linear site response analyses. Furthermore, high-strain dynamic soil characteristics, with a variation of soil uncertainties according to ASCE 4-98 standard, as a result of site response analyses, are used as input for the soil-structure interaction analyses. Henceforth, site heterogeneity effects and their transfer to the super-structure are discussed.

Within this framework, this study has led to following conclusions:

- It is seen that in-depth impedance change of the soil layers considerably influence the dynamic response of the structure.
- The heterogeneity of soil profile especially in 2D has significant effect on the dynamic response of the foundation. However, this effect diminishes at the higher elevations on the super-structure.
- The surface responses are amplified due to rocky and stiff formations with low damping characteristics and low modulus degradation. Moreover, the amplifications are quite high since the predominant periods of the NPP structure and the subsurface media coincide at certain frequencies.
- At low frequencies, it is construed that very stiff rock layers under the reactor building do not change the dynamic interaction behavior of the reactor building significantly.

- The results of 1D and 2D site response analyses have differences by means of free-field foundation input motions. This may be based upon the different analysis methods such as direct nonlinear analysis and equivalent linear analysis where nonlinear characteristics are considered iteratively. In addition to that, differences may be arisen from the different boundary conditions of the two analysis, while the compliant base boundary at the bottom of the soil profile and free field boundary at the sides of the model are used in 2D analysis, whereas the rigid boundary at the bottom is used in 1D equivalent linear analysis. Also, the results show that the heterogeneity in 2D soil profile could not be accurately modelled by 1D analyses.
- It is inferred that peak ground accelerations do not prominently change across the foundation. Nevertheless, the peak spectral accelerations are variable along with the north-south direction of the foundation.
- Uncertainties (BE (best estimate), UB (upper bound) and LB (lower bound)) that should be taken into account as per ASCE 4-98 are considered in soil-structure interaction analyses. Additionally, the dynamic response of 7 different one-dimensional soil columns are calculated whether BE, UB and LB represent the foundation soil media that shows heterogeneous features. Hence, it is concluded that BE, UB and LB are insufficient under these circumstances.
- As for the proposal, a probabilistic approach utilizing Monte Carlo or Latin Hypercube simulation should be used that allows more accurate results to determine the site properties.



## REFERENCES

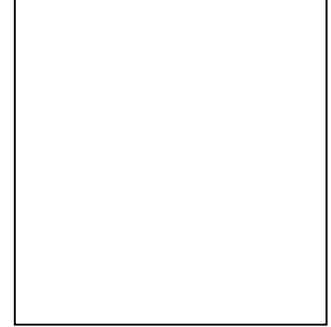
- ASCE. (2000). *Seismic Analysis of Safety-Related Nuclear Structures and Commentary ASCE/SEI 4-98*. USA.
- ASCE. (2005). *Seismic Design Criteria for Structures, Systems, and Components in Nuclear Facilities ASCE/SEI 43-05*.
- ASCE. (2013). *Minimum Design Loads for Buildings and Other Structures ASCE/SEI 07-10* (ASCE/SEI 0). <https://doi.org/10.1061/9780784404454>
- ASCE. (2017). *Seismic Analysis of Safety-Related Nuclear Structures ASCE/SEI 4-16*.
- Asmolov, V. G., Gusev, I. N., Kazanskiy, V. R., Povarov, V. P., & Statsura, D. B. (2017). New generation first-of-the kind unit – VVER-1200 design features. *Nuclear Energy and Technology*, 3(4), 260–269. <https://doi.org/10.1016/j.nucet.2017.10.003>
- Bayat, E., & Alver, O. (2018). *Personal Communication*.
- Bhaumik, L., & Raychowdhury, P. (2013). Seismic response analysis of a nuclear reactor structure considering nonlinear soil-structure interaction. *Nuclear Engineering and Design*, 265, 1078–1090. <https://doi.org/10.1016/j.nucengdes.2013.09.037>
- Bolisetti, C. (2015). Site response, soil-structure interaction and structure-soil-structure interaction for performance assessment of buildings and nuclear structures. *ProQuest Dissertations and Theses*, (Cmmi), 446.
- Bolisetti, C., Whittaker, A. S., Mason, H. B., Almufti, I., & Willford, M. (2014). Equivalent linear and nonlinear site response analysis for design and risk assessment of safety-related nuclear structures. *Nuclear Engineering and Design*, 275, 107–121. <https://doi.org/10.1016/j.nucengdes.2014.04.033>
- Brinkgreve, R. B. J., Broere, W., & Waterman, D. (2006). *Plaxis 2D Manual - Version 8*.
- Computers and Structures Inc. (2014). *SAP 2000*.
- Dassault Systemes. (2005). *Computer Program ABAQUS - Finite Element Analysis Software*. Providence, Rhode Island: Dassault Systemes.
- Eisenhower, S. (2003). Atoms for Peace Plus Fifty. *IAEA Bulletin*, 45/2(December), 5–6.
- EPRI. (1993). *Guidelines for determining design basis ground motions EPRI TR-102293* (Vol. 1–5). Palo Alto, California.
- Evans, J. J. B., & Keogh, P. M. (1987). The influence of non-linearity and foundation behaviour on containment integrity. *Nuclear Engineering and Design*, 104(3), 357–364. [https://doi.org/10.1016/0029-5493\(87\)90214-7](https://doi.org/10.1016/0029-5493(87)90214-7)
- Gazetas, G. (1991). Foundation Vibrations. In *Foundation Engineering Handbook* (H.

- Fang). Norwell, Massachusetts: Kluwer Academic Publishers.
- Gidropress. (2011a). *Status report 107 - VVER-1200 (V-392M). 1200*. Retrieved from [https://aris.iaea.org/PDF/VVER-1200\(V-392M\).pdf](https://aris.iaea.org/PDF/VVER-1200(V-392M).pdf)
- Gidropress. (2011b). *Status report 107 - VVER-1200 (V-392M), https://aris.iaea.org/PDF/VVER-1200(V-392M).pdf. 1200*. Retrieved from [https://aris.iaea.org/PDF/VVER-1200\(V-392M\).pdf](https://aris.iaea.org/PDF/VVER-1200(V-392M).pdf)
- Gidropress. (2011c). *Status report 93 - VVER-1000 (V-466B)*.
- GP Technologies Inc. (2014). *ACS SASSI*.
- Gu, Z. (2018). History review of nuclear reactor safety. *Annals of Nuclear Energy*, 120, 682–690. <https://doi.org/10.1016/j.anucene.2018.06.023>
- Hardy, C. (1999). *Atomic rise and fall: the Australian Atomic Energy Commission, 1953-1987*. Retrieved from <http://www.worldcat.org/title/atomic-rise-and-fall-the-australian-atomic-energy-commission-1953-1987/oclc/44594224>
- Hashash, Y. M. A., Musgrove, M. I., Harmon, J. A., Groholski, D., Phillips, C. A., & Park, D. (2016). *DEEPSOIL V6.1, User Manual*. Urbana, IL: Board of Trustees of University of Illinois at Urbana-Champaign.
- Housner, G. W. (1957). Interaction of Building and Ground during an Earthquake. *Bulletin of the Seismological Society of America*, 47(3), 179–186.
- IAEA. (2003). *Seismic Design and Qualification for Nuclear Power Plants NS-G-1.6*. Vienna, Austria.
- IAEA. (2004). *Geotechnical Aspects of Site Evaluation and Foundations for Nuclear Power Plants NS-G-3.6*.
- IAEA. (2006). Fundamental Safety Principles SF-1. In *Safety Standards for protecting people and the environment. Fundamental Safety Principles*. (Vol. 2). Retrieved from <http://www-ns.iaea.org/standards/documents/default.asp?sub=100>
- IAEA. (2007). Terminology Used in Nuclear Safety and Radiation Protection. In *IAEA Safety Glossary*. Vienna, Austria.
- IAEA. (2010). *Seismic Hazards in Site Evaluation for Nuclear Installations SSG-9*.
- Idriss and Seed, H. B., I. M. (1967). *Response of Horizontal Soil Layers During Earthquakes*. Berkeley, California: Soil Mechanics and Bituminous Materials Research Laboratory, University of California.
- INSAG. (1996). *Defence in Depth in Nuclear Safety INSAG-10*. Retrieved from [http://www-pub.iaea.org/MTCD/publications/PDF/Pub1013e\\_web.pdf](http://www-pub.iaea.org/MTCD/publications/PDF/Pub1013e_web.pdf)
- Kausel, E. (2010). Early history of soil-structure interaction. *Soil Dynamics and Earthquake Engineering*, 30(9), 822–832. <https://doi.org/10.1016/j.soildyn.2009.11.001>
- Kramer, S. L. (1996). *Geotechnical Earthquake Engineering*. Upper Saddle River, New Jersey: Prentice Hall.
- LSTC. (2009). *LS DYNA Keyword User's Manual - Release 971*. Livermore, California: Livermore Software Technology Corporation.
- Luco and Westman, R.A., J. E. (1971). *Dynamic response of circular footings*. Journal of the Engineering. Mechanics Division, ASCE, 97 (EM5), 1381-1395.

- Luco and Westman, R.A., J. E. (1972). *Dynamic response of rigid footing bonded to an elastic half-space*. Journal of Applied Mechanics, 39 (2) 527-534.
- Lysmer Tabatabaie-Raissi, M., Tajirian, F., Vahdani, S., & Ostadan, F, J. (1981). *SASSI: A System for Analysis of Soil-Structure Interaction*. Berkeley, California.
- Lysmer F. Ostandan, and C.C. Chin., J. (1999). *SASSI 2000-A System for Analysis of Soil-Structure Interaction, User's Manual*. Berkeley, California: University of California, Berkeley.
- Mazzoni McKenna, F., Scott, M. H., and Fenves, G. L., S. (2009). *Computer Program OpenSees: Open System for Earthquake Engineering Simulation*. Berkeley, California: Pacific Earthquake Research Center (PEER, University of California).
- McGuire Silva, W. J and Constantino, C. J., R. K. (2001). *Technical basis for revision of regulatory guidance of design ground motions: hazard- and risk- consistent ground motion spectra guidelines*.
- Merrit, R., & Housner, G. W. (1954). Effect of the Foundation Compliance on Earthquake Stresses in Multi-Story Buildings. *Bulletin of the Seismological Society of America*, 44(4), 551–569.
- NIST. (2012). *Soil-Structure Interaction for Building Structures NIST GCR 12-917-21*. 292. <https://doi.org/12-917-21>
- Nuclear Energy Agency. (2009). Nuclear Energy Outlook 2008. In *Nuclear Energy Outlook 2008*. <https://doi.org/10.1787/9789264054110-en>
- Ostadan, F. (2006). *SASSI2000: A System for Analysis of Soil Structure Interaction - Theoretical Manual*. Berkeley, California: University of California, Berkeley.
- Saxena, N., & Paul, D. K. (2012). Effects of embedment including slip and separation on seismic SSI response of a nuclear reactor building. *Nuclear Engineering and Design*, 247, 23–33. <https://doi.org/10.1016/j.nucengdes.2012.02.010>
- Saxena, N., Paul, D. K., & Kumar, R. (2011). Effects of slip and separation on seismic SSI response of nuclear reactor building. *Nuclear Engineering and Design*, 241(1), 12–17. <https://doi.org/10.1016/j.nucengdes.2010.10.011>
- Schnabel Lysmer, J., and Seed, H. B., P. B. (1972). *Computer Program SHAKE2000: A Computer Program for the Earthquake Ground Response Analysis for Horizontally Layered Sites*. Berkeley, California: Earthquake Engineering Research Center, University of California.
- Schnabel Lysmer, J., and Seed, H. B., P. B. (2009). *Computer Program SHAKE2000: A Computer Program for the 1D Analysis of Geotechnical Earthquake Engineering Problems*. Berkeley, California: University of California.
- U.S. NRC. (1978). *Development of Floor Design Response Spectra for Seismic Design of Floor-Supported Equipment or Components RG 1.122*.
- U.S. NRC. (2007). *A performance-based approach to define the site-specific earthquake ground motion RG 1.208*.
- U.S. NRC. (2007b). *Standard Review Plan 3.7.1 Seismic Design Parameters*. (March), 1–8.
- U.S. NRC. (2007c). *Standard Review Plan 3.7.2 Seismic System Analysis*. (March), 1–8.

- U.S. NRC. (2014). *Design Response Spectra for Seismic Design of Nuclear Power Plants RG 1.60*.
- U.S. NRC. (2014b). *Earthquake Engineering Criteria for Nuclear Power Plants Appendix S to 10 CFR Part 50* (pp. 9–11). pp. 9–11.
- Url-1. (n.d.). Retrieved December 17, 2018, from <https://www.ucsusa.org/clean-energy/energy-water-use/water-energy-electricity-nuclear>
- Url-2. (n.d.). Retrieved January 15, 2019, from <https://www.iaea.org/pris/>
- Url-3. (n.d.). Retrieved December 20, 2018, from <http://www.energyglobalnews.com/1954-obninsk-nuclear-plant-produces-worlds-first-commercial-electricity/>
- Url-4. (n.d.). Retrieved December 19, 2018, from [https://www.wired.com/science/discoveries/news/2007/06/dayintech\\_0627](https://www.wired.com/science/discoveries/news/2007/06/dayintech_0627)
- Vegge, T., Sethna, J. P., Cheong, S. A., Jacobsen, K. W., Myers, C. R., & Ralph, D. C. (2001). Calculation of quantum tunneling for a spatially extended defect: The dislocation kink in copper has a low effective mass. *Physical Review Letters*, 86(8), 1546–1549. <https://doi.org/10.1103/PhysRevLett.86.1546>
- Veletsos A.S., and W. Y. T. (1971). *Lateral and Rocking Vibration of Footings*. Journal of Soil Mechanics Foundation Division (ASCE).
- Venancio-Filho, F., De Barros, F. C. P., Almeida, M. C. F., & Ferreira, W. G. (1997). Soil-structure interaction analysis of NPP containments: Substructure and frequency domain methods. *Nuclear Engineering and Design*, 174(2), 165–176. [https://doi.org/10.1016/S0029-5493\(97\)00076-9](https://doi.org/10.1016/S0029-5493(97)00076-9)
- Vucetic, M., & Dobry, R. (1991). shear strain for the first cycle of unidirectional cyclic shear loading . The relation consists of the initial loading curve OD , the unloading branch of the loop DEC , and the reloading branch CFD . The loop in Fig . 1 ( a ) is somewhat idealized in th. *Journal of Geotechnical Engineering*, 117(1), 89–107.
- Winkler, E. (1867). *Die Lehre von der Elastizitaet und Festigkeit mit besonderer Ruecksicht auf ihre Anwendung in der Technik : fuer polytechnische Schulen, Bauakademien, Ingenieure, Maschinenbauer, Architecten, etc. 1. 1*. Prag: Dominicius.
- Wolf, J. P. (1985). *Dynamic soil-structure interaction*.
- Wolf, J. P. (1988). *Soil-structure-interaction analysis in time domain*.
- Wong and Luco, J.E., H. L. (1970). *Soil-Structure Interaction: A Linear Continuum Mechanics Approach (CLASSI)*. Los Angeles: Department of Civil Engineering, University of Southern California.
- Zentner, I. (2010). Numerical computation of fragility curves for NPP equipment. *Nuclear Engineering and Design*, 240(6), 1614–1621. <https://doi.org/10.1016/j.nucengdes.2010.02.030>

## CURRICULUM VITAE



**Name Surname** : Berke SAYIN  
**Place and Date of Birth** : Eskişehir – 01.01.1987  
**E-Mail** : berkesayin@gmail.com

### EDUCATION

- **B.Sc.** : 2009, Istanbul University, Civil Engineering

### PROFESSIONAL EXPERIENCE AND REWARDS:

- 2009-2010 Na-Lidco Construction Libya / Technical Office Engineer
- 2010-... Turkish Atomic Energy Authority / Civil Engineer

### PUBLICATIONS, PRESENTATIONS AND PATENTS ON THE THESIS:

- -

### OTHER PUBLICATIONS, PRESENTATIONS AND PATENTS:

- **Sayın B.**, Uçak B., Güner B., İşcan B.: *Comparison of the Country Approaches In Regulation and Application on Aircraft Crash in Nuclear Power Plants, Structural Analysis*. October, 2016, Kuşadası, Aydın, Turkey.
- Güner B., İşcan B., **Sayın B.**, Uçak B.: *Lessons Learned from Fukushima Regarding Structural Design and External Events*. October, 2016, Kuşadası, Aydın, Turkey.